

Enabling Numerical Modeling of Extreme-Intensity Laser Produced Hot Dense Plasma

Ionization degree of silicon



Ionization wave inside a glass target
driven by relativistic electrons

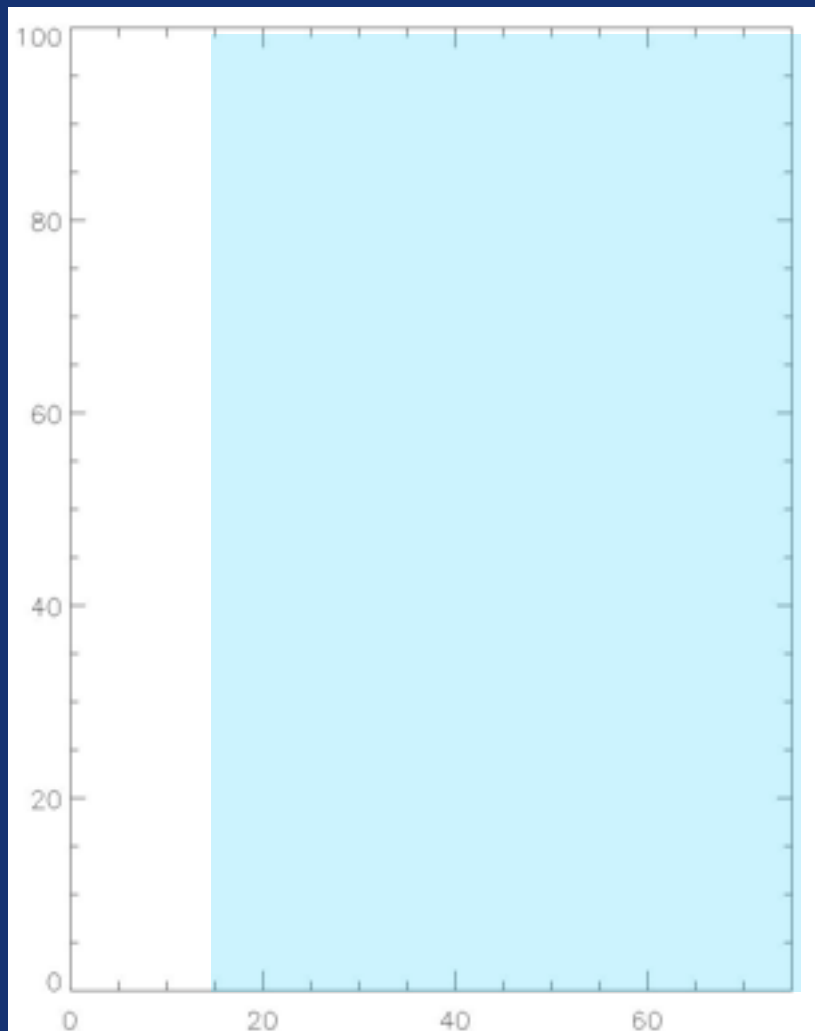
Yasuhiko Sentoku

*Department of Physics
University of Nevada, Reno*

01/07/2011@Edinburgh, UK

Enabling Numerical Modeling of Extreme-Intensity Laser Produced Hot Dense Plasma

Ionization degree of silicon



Ionization wave inside a glass target
driven by relativistic electrons

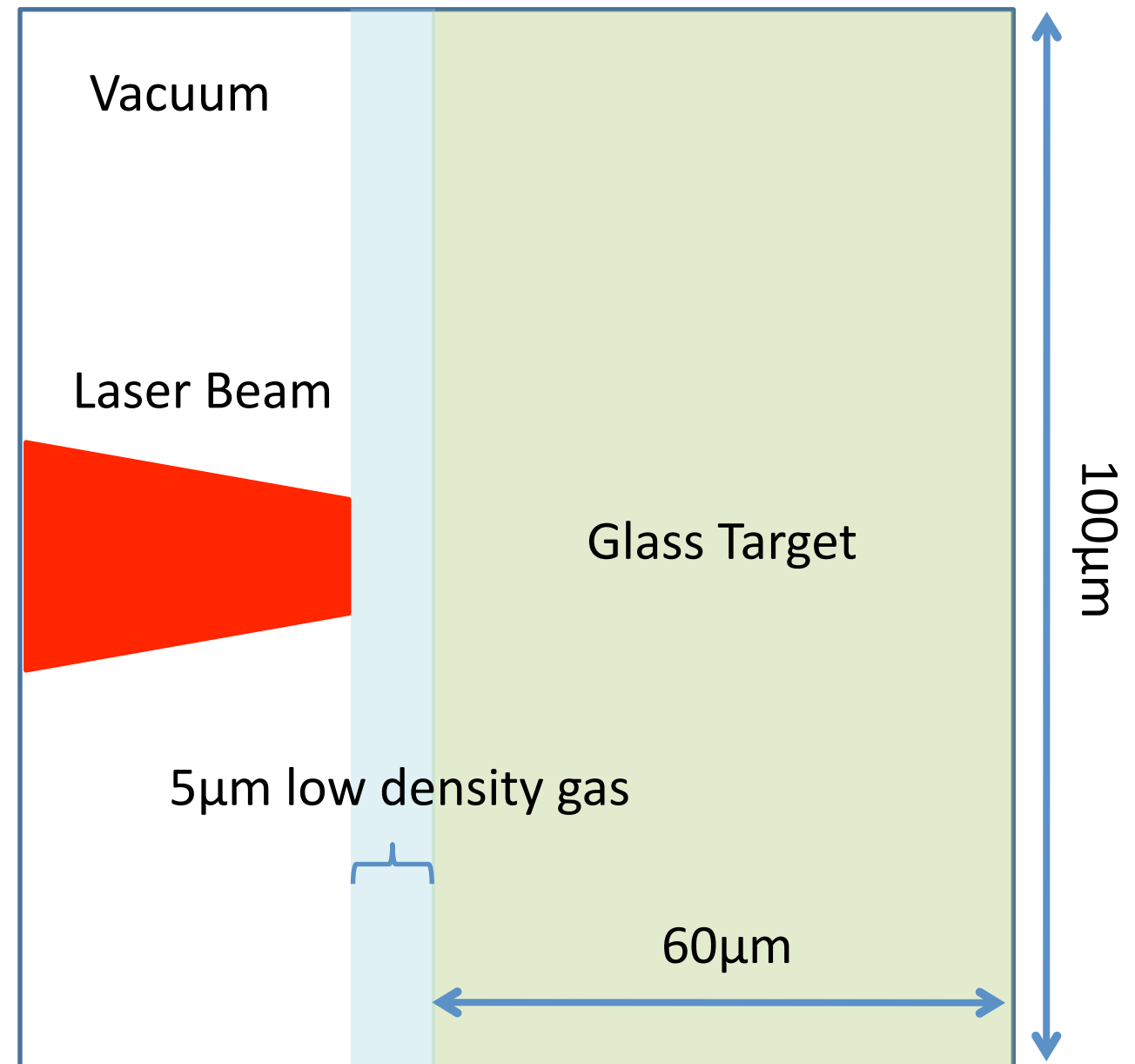
Yasuhiko Sentoku

*Department of Physics
University of Nevada, Reno*

01/07/2011@Edinburgh, UK

2D Simulation Parameters

- Target
 - 60x100 μm thick solid density SiO_2
 - $N_e = 690n_c$
 - $N_{\text{si}} = 23n_c$
 - $N_{\text{O}_2} = 46n_c$
 - 5 μm low density gas precursor
- Laser
 - Intensity: $5 \times 10^{18} \text{W}/\text{cm}^2$
 - 500fs pulse length
 - 15 μm focal spot
- Code Parameters:
 - Thomas-Fermi and Saha ionization models included
 - Binary collisions included
 - 686 million particles inserted
 - 3000x4000 grids
 - Absorbing boundary condition
 - 100 CPU used
 - 1 ps total simulation duration



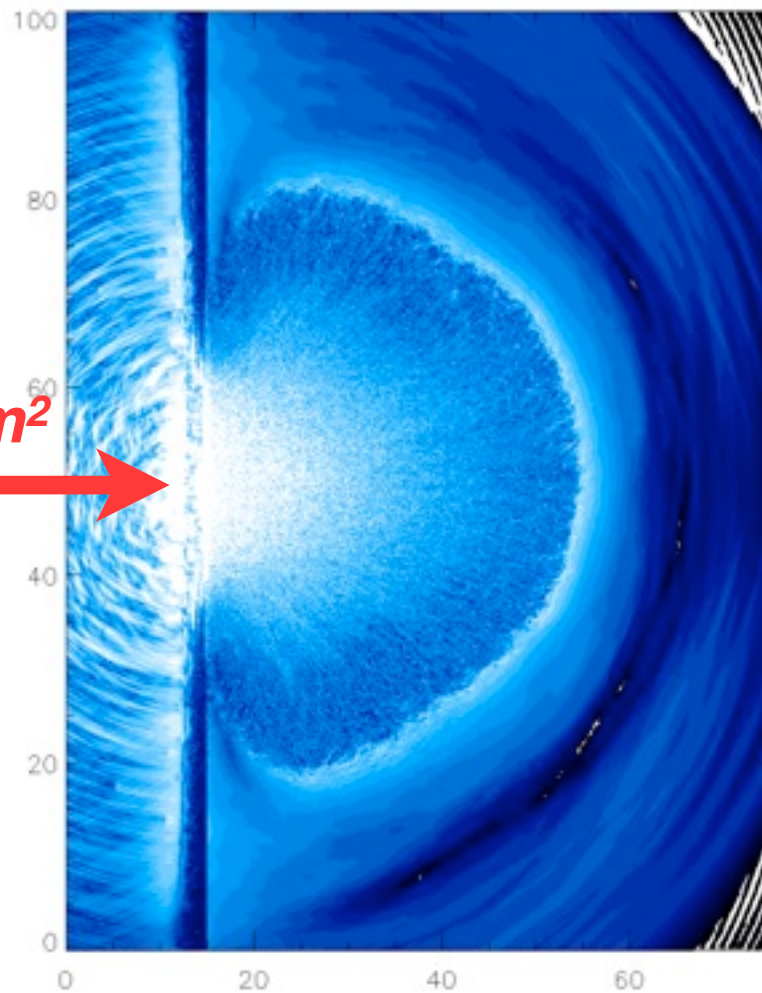
Simulation box geometry

Hot electron transport in insulator target

Ionization wave in silica driven by relativistic laser pulse

Electric Field $|E|$

Laser
 $I=10^{18} \text{ W/cm}^2$

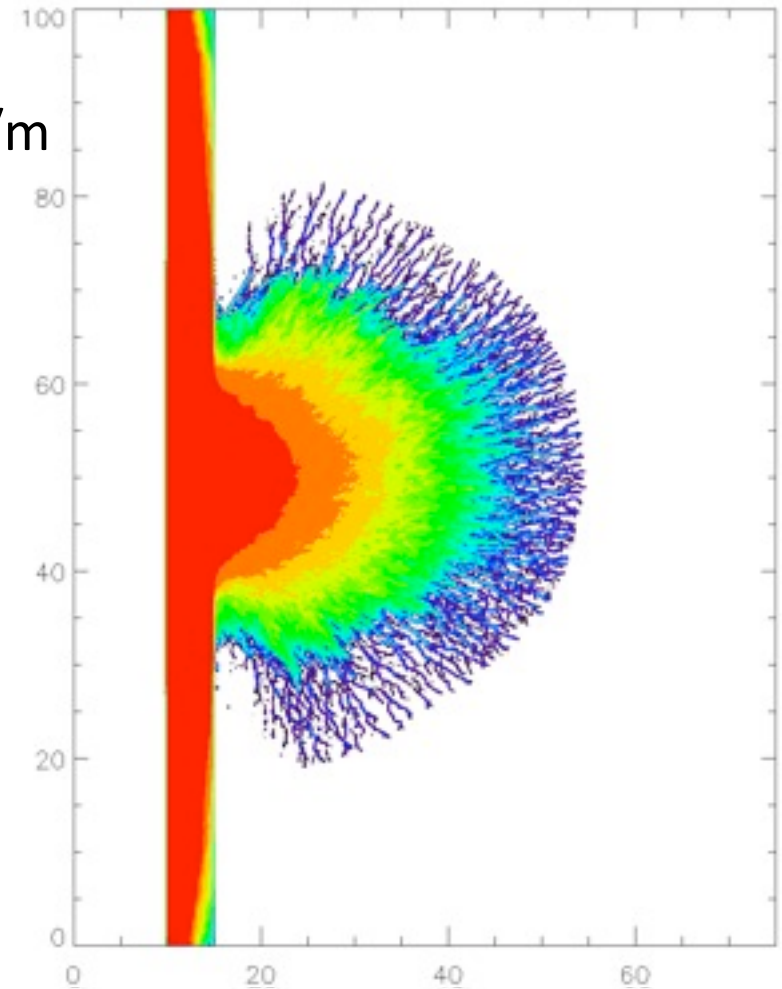


Ionization of Silicon

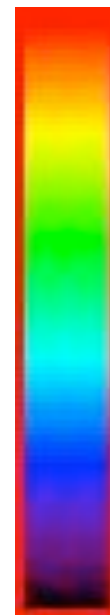
$3 \times 10^{11} \text{ V/m}$



3×10^8



14.0

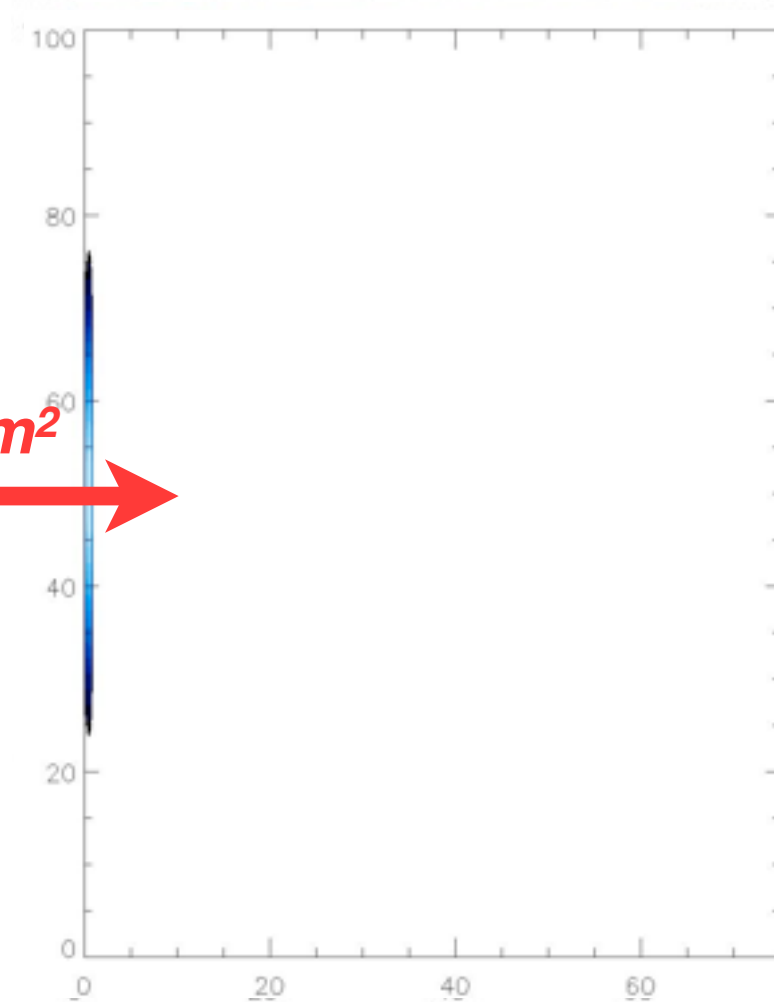


0.14

Hot electron transport in insulator target

Ionization wave in silica driven by relativistic laser pulse

Electric Field $|E|$

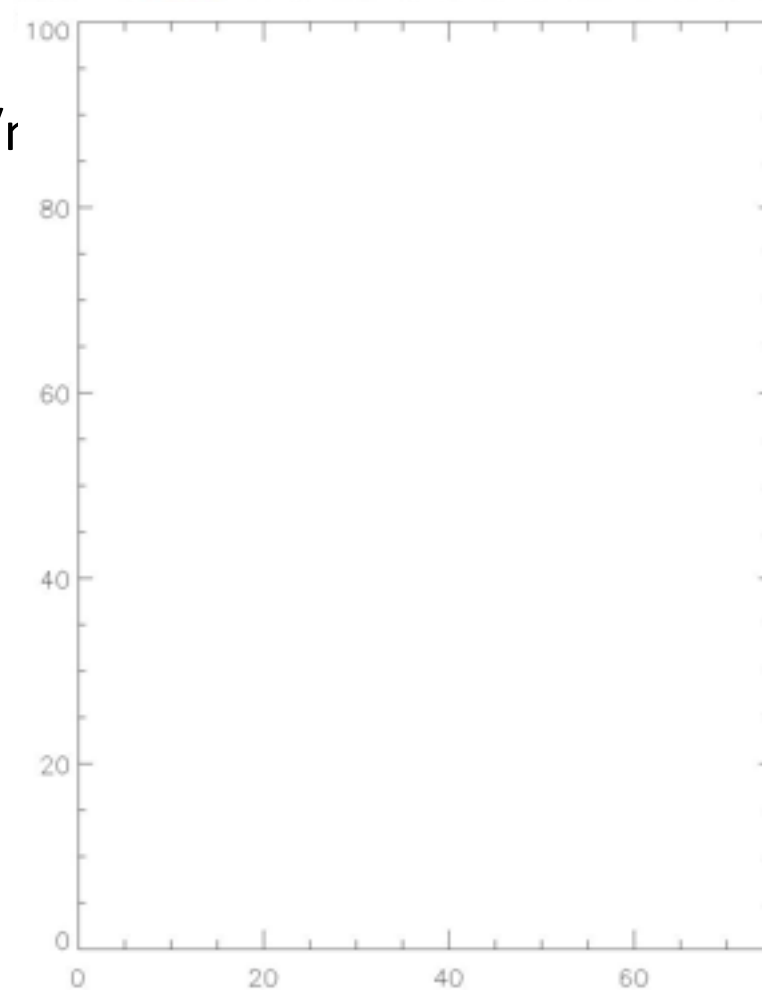


Ionization of Silicon

$3 \times 10^{11} \text{ V/r}$



3×10^8



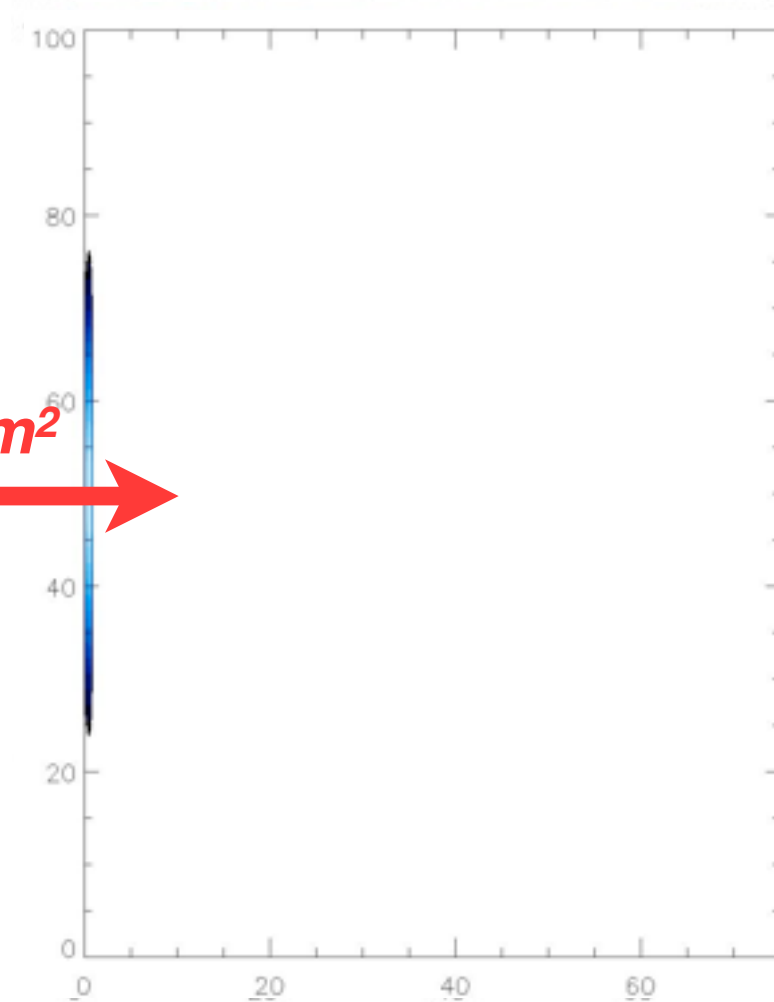
14.0

0.14

Hot electron transport in insulator target

Ionization wave in silica driven by relativistic laser pulse

Electric Field $|E|$

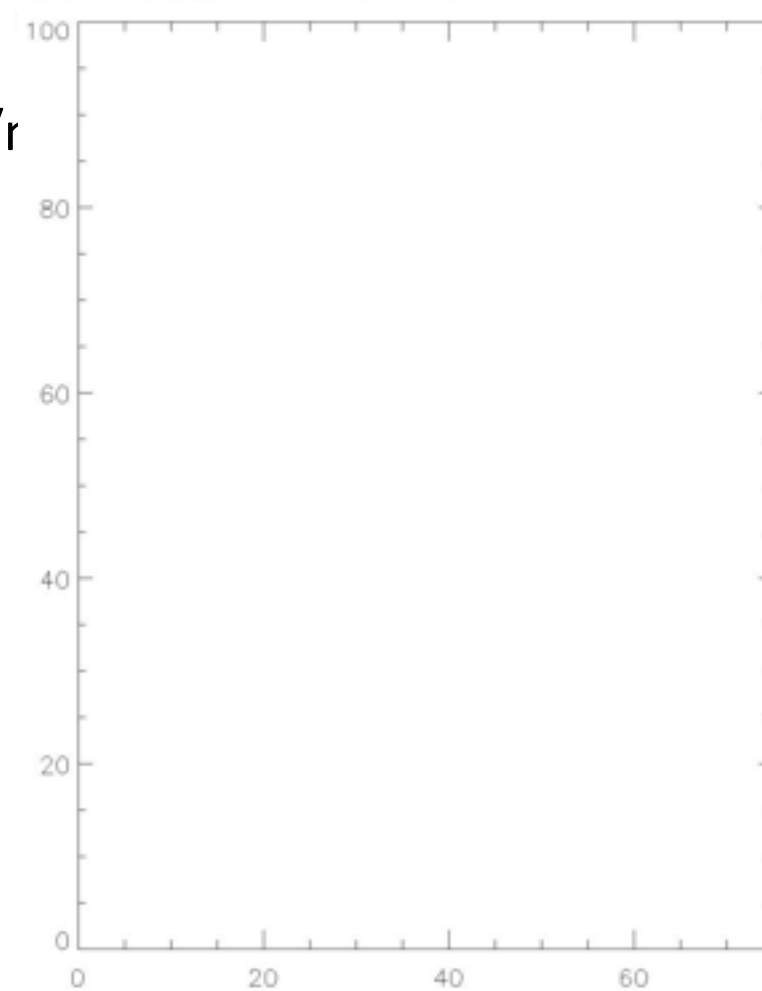


Ionization of Silicon

$3 \times 10^{11} \text{ V/r}$



3×10^8



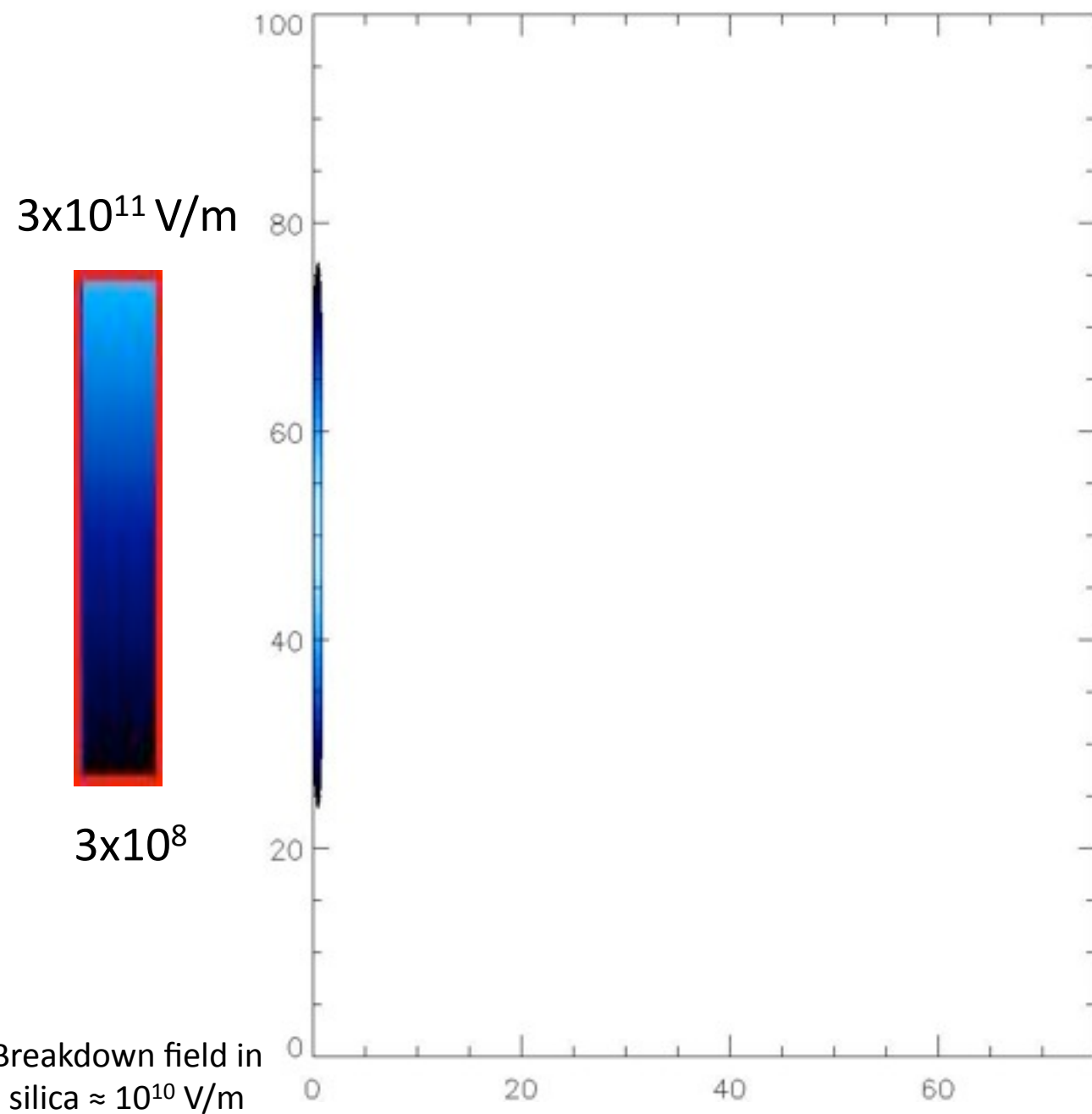
14.0

0.14

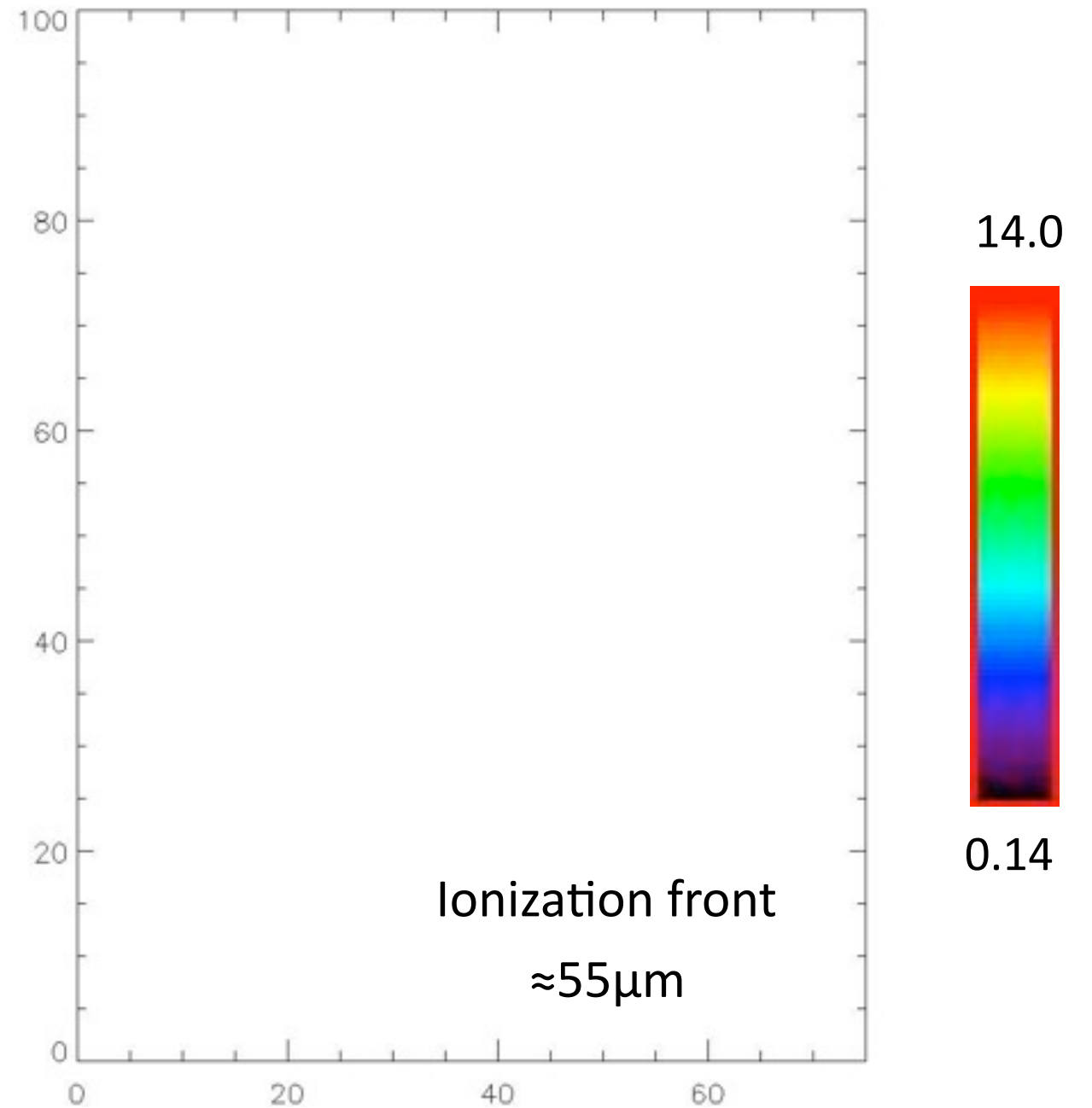


Fast Electron Beam Preceding Ionization Front

Sheath Field |E|

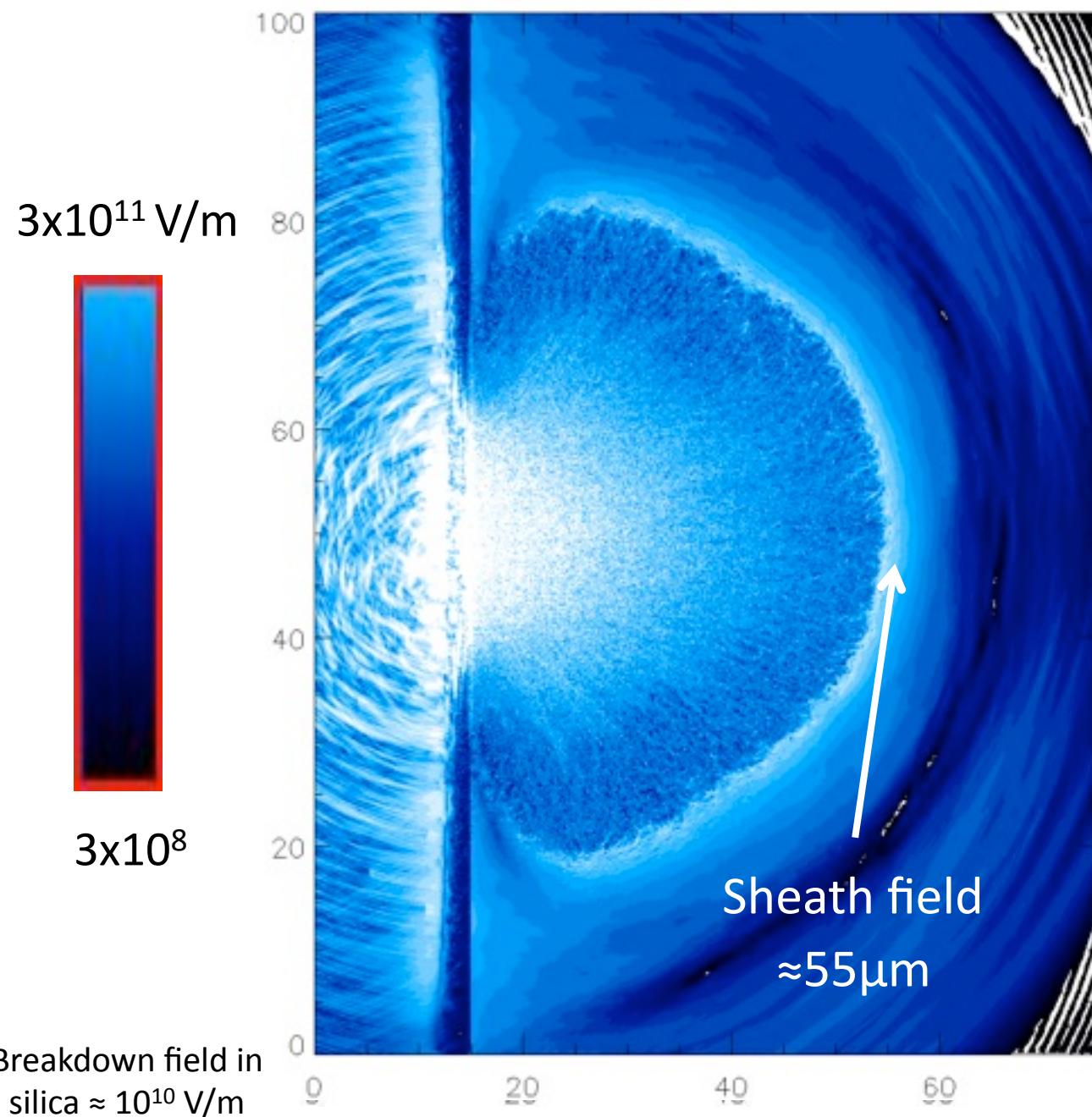


Ionization of Silicon

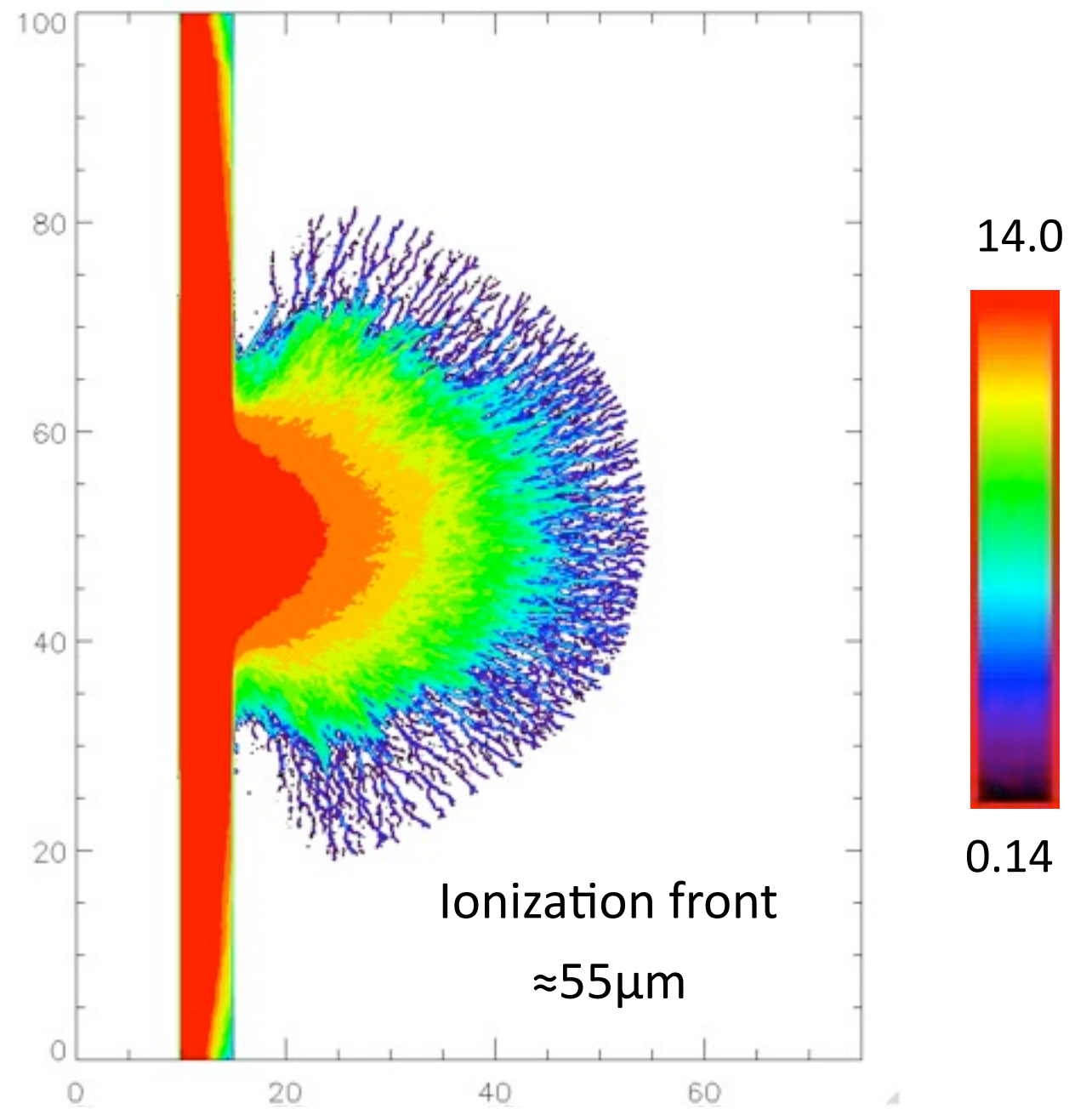


Fast Electron Beam Preceding Ionization Front

Sheath Field $|E|$

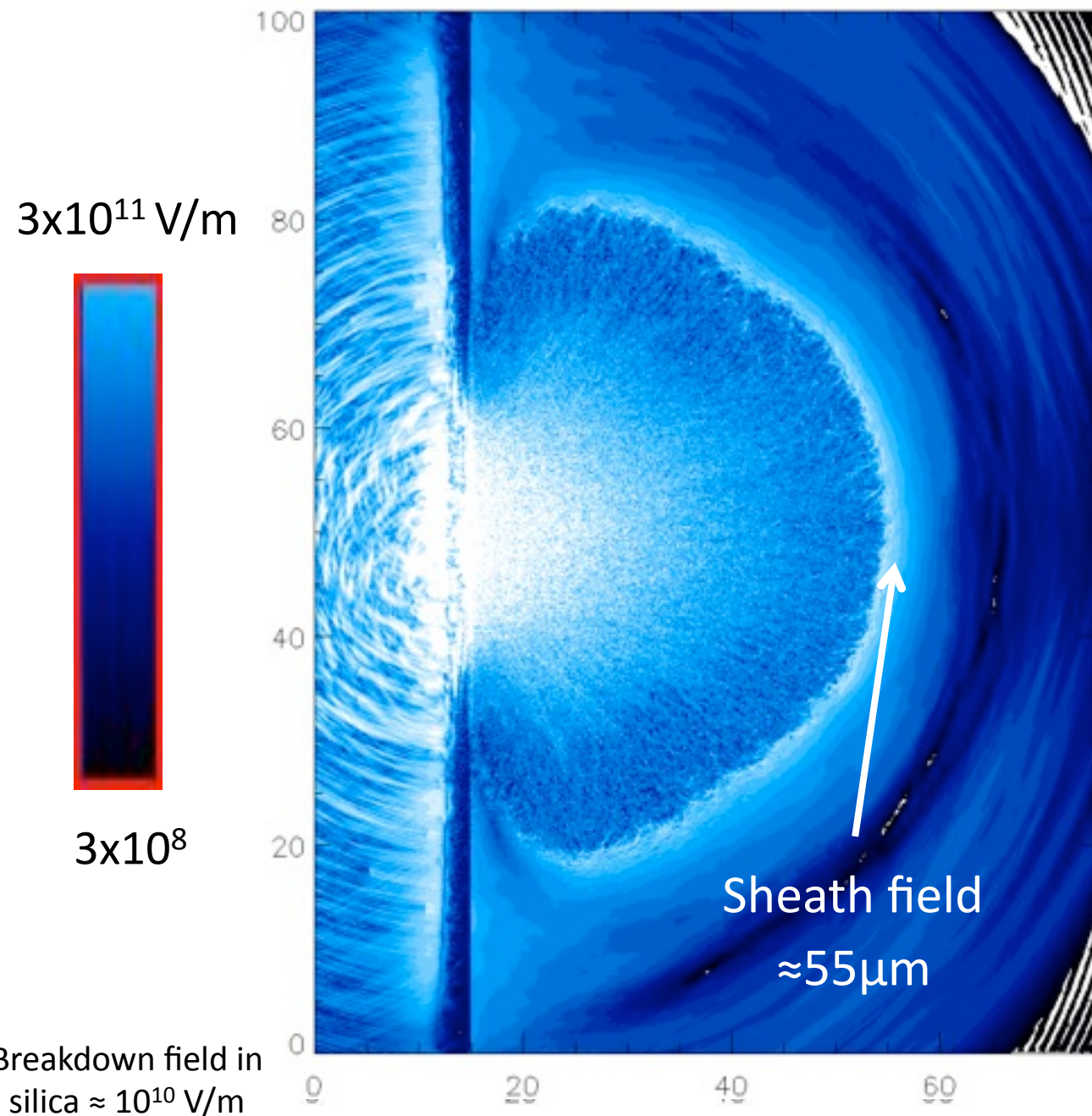


Ionization of Silicon

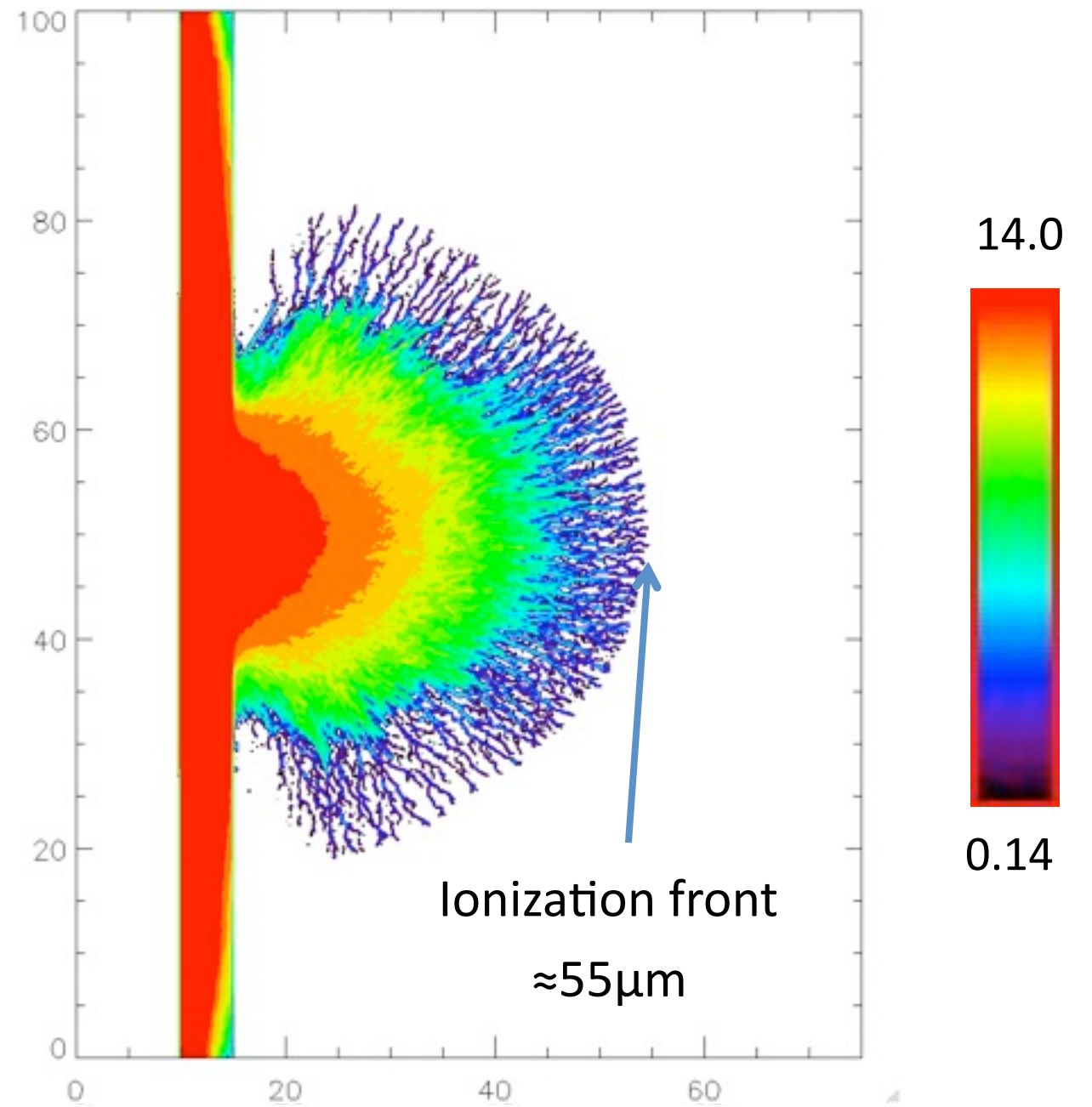


Fast Electron Beam Preceding Ionization Front

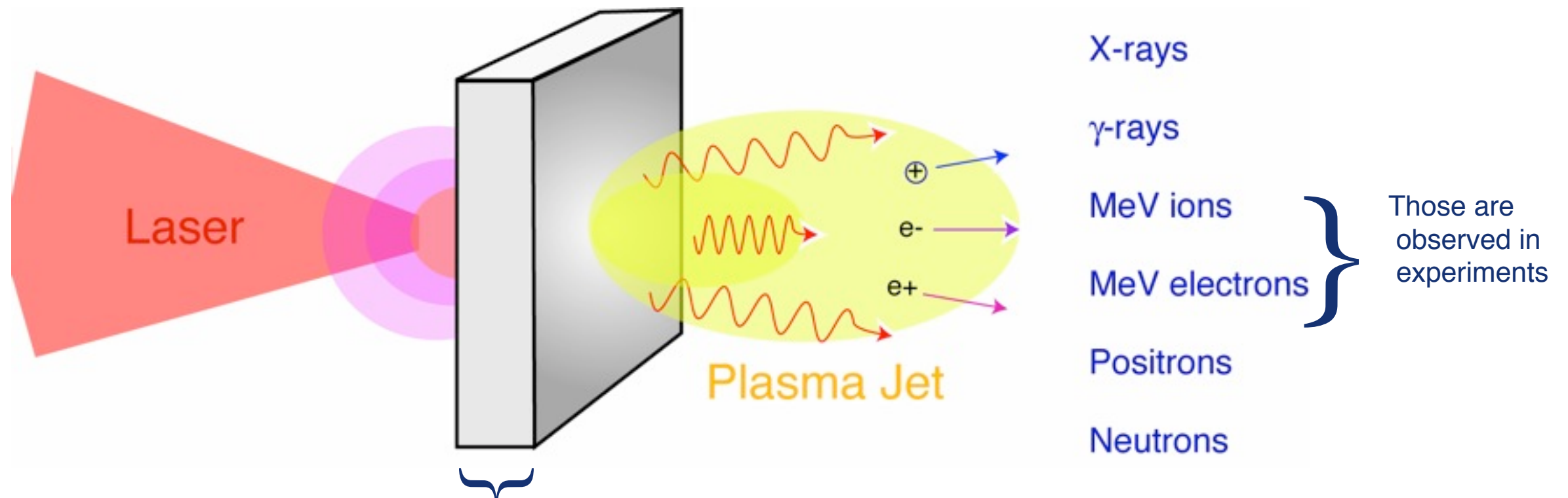
Sheath Field $|E|$



Ionization of Silicon



What physics is necessary in simulation to study HEDP in ultra-intense LPI?

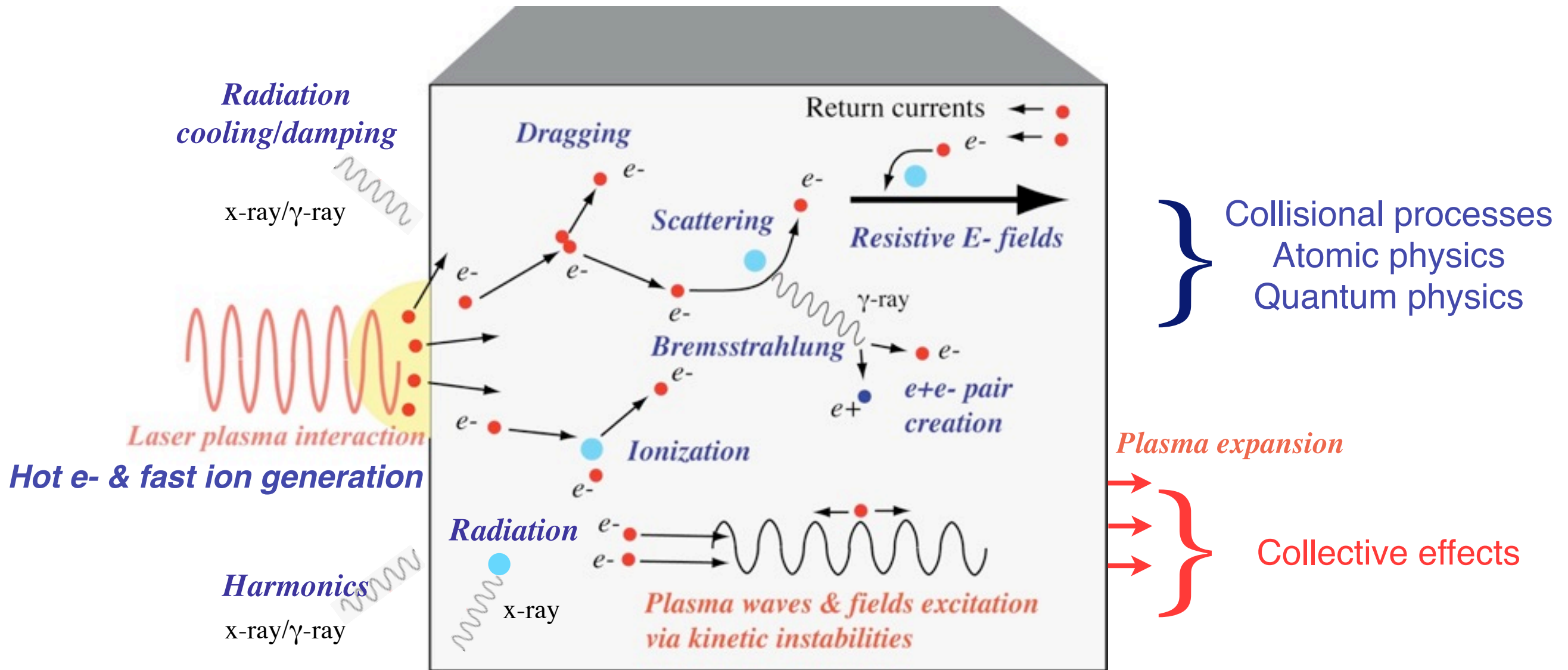


Everything happens in less than a picosecond (10^{-12} s).
(Information is very limited in experiments...)

Summary: Physics in ultra-fast heated solid target



Plasma discharge
Kinetic instabilities and wave excitations
Collisional energy transport and target heating



The physics in the laser isochoric heating is complicated. The collective effects and the collisional effects are competing inside the target.

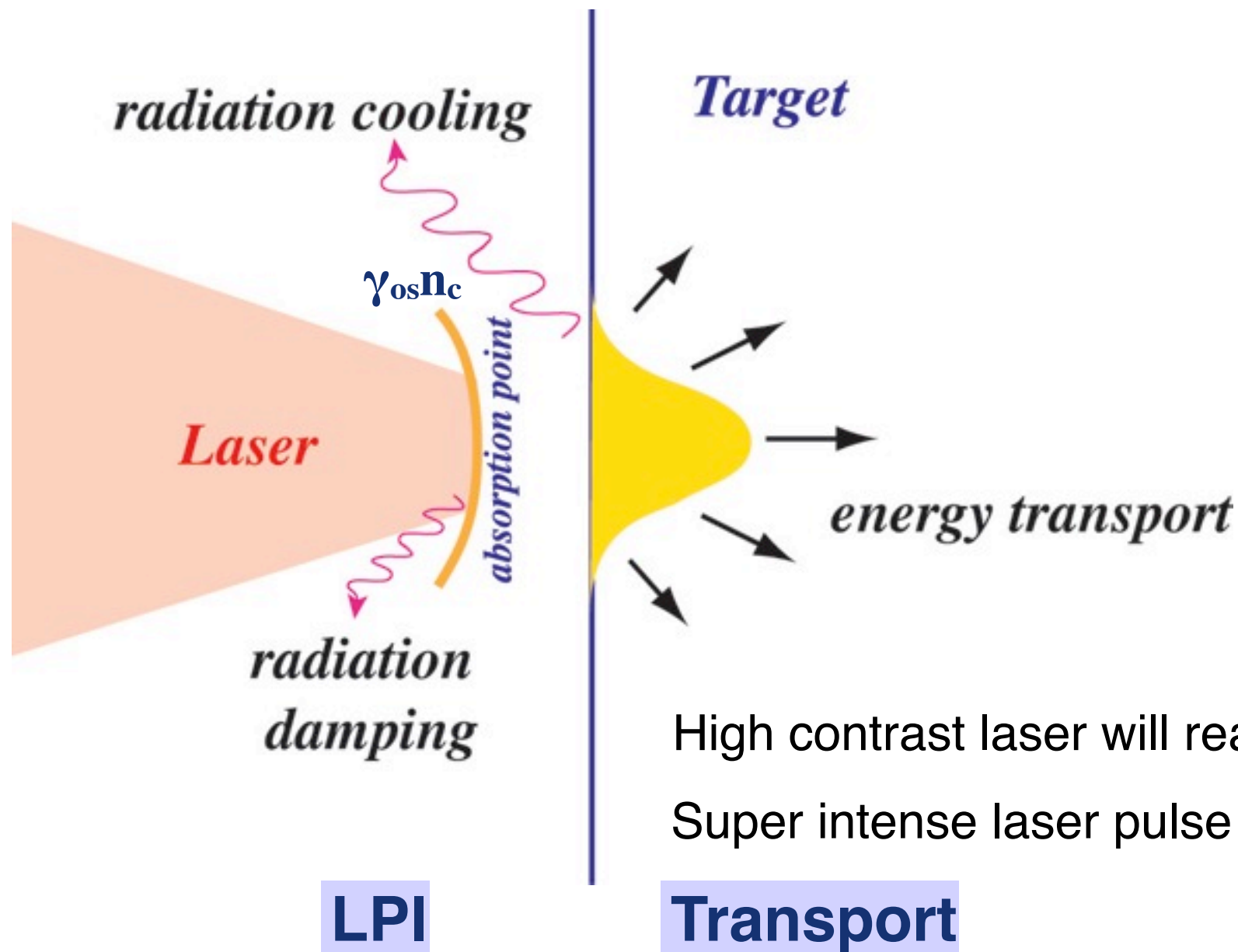
We need a kinetic simulation code with the atomic physics models.

What model will be capable of simulating ultra-intense laser produced HEP plasmas?



Laser intensity will be $> 10^{22}$ W/cm².

$$\gamma_{os} = [1 + (1 + \eta)a^2/2]^{1/2} > 100$$

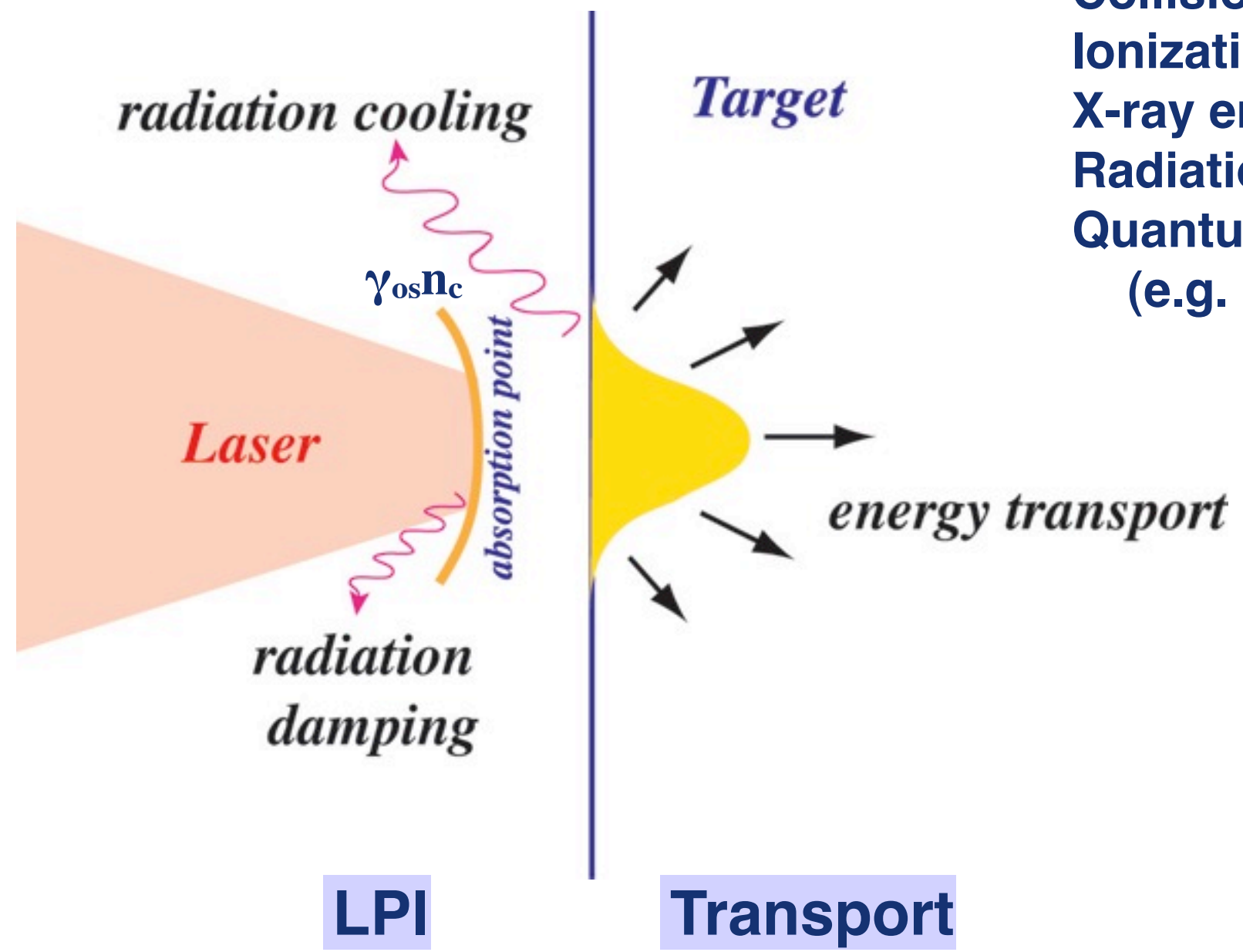


High contrast laser will realize the direct interaction.
Super intense laser pulse will directly interact on the target.

LPI - target region will not be able to be separated. We need to solve both regions self-consistently.

Transport region: atomic physics

- Collision (Coulomb, Elastic)
- Ionization (Field, Collisional)
- X-ray emission (Free, Bounded)
- Radiation transport
- Quantum physics
(e.g. pair creation)



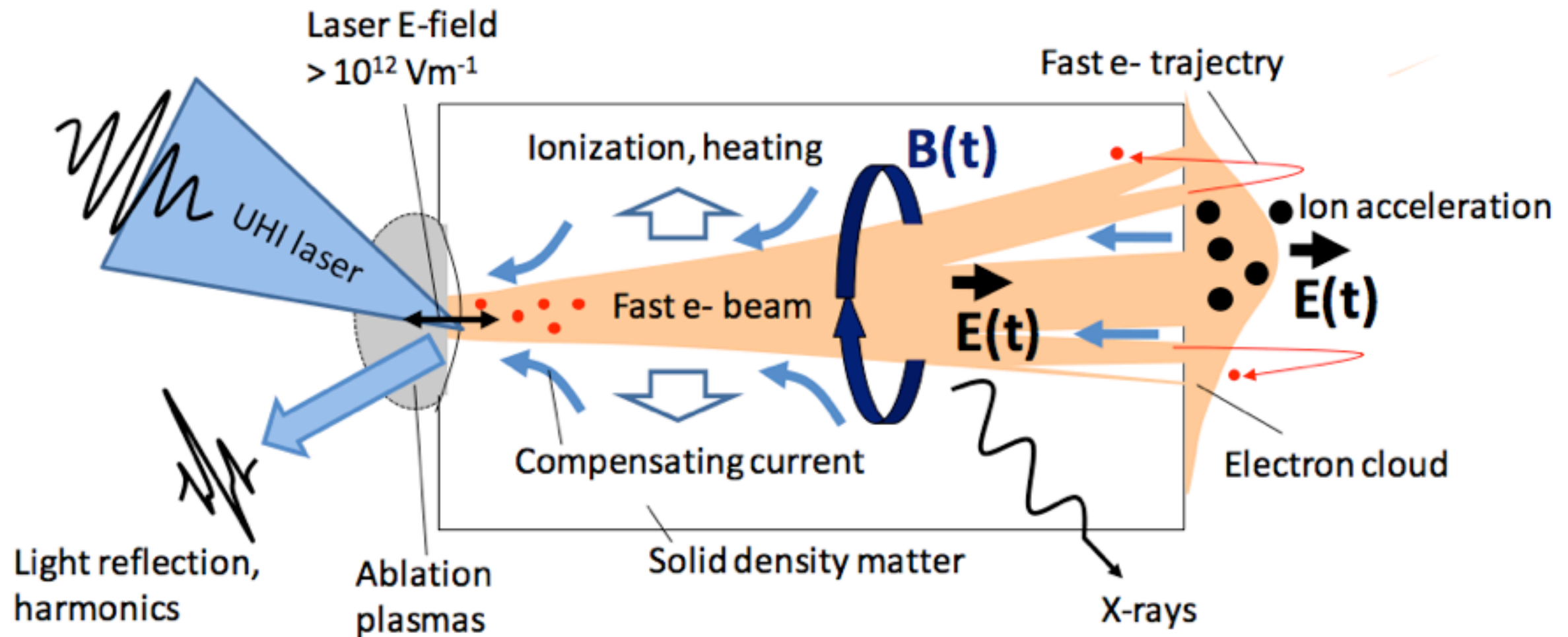
LPI

Transport

Energy transport depends on resistive magnetic fields inside solid



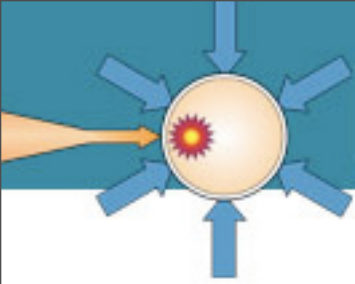
Illustration by M. Nakatsutsumi, LULI



Resistive magnetic fields depend on how resistivity evolves during the interaction.

Correct resistivity and dynamic ionization are crucial in the modeling.

Resistive magnetic field $\sim 10 - 100 \text{ MG}$.

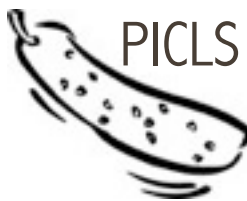


Challenges in computational modeling of HEDLP by LPI



- Model requires to resolve extremely large density scales plasmas. (e.g. $10^{19} \sim 10^{26} \text{ cm}^{-3}$ for Fast Ignition)
- Model requires the Coulomb collision to simulate the energy transport and heating in HEDLP. (i.e. resistive effects, scattering)
- Model requires the dynamics ionization processes since the plasma electron density and the resistivity depend on the charge state inside the target. (e.g. ultra-fast heated thin metal target by LPI)
- Model should have a strict energy conservation to avoid the numerical heating/numerical ionization in HEDLP.

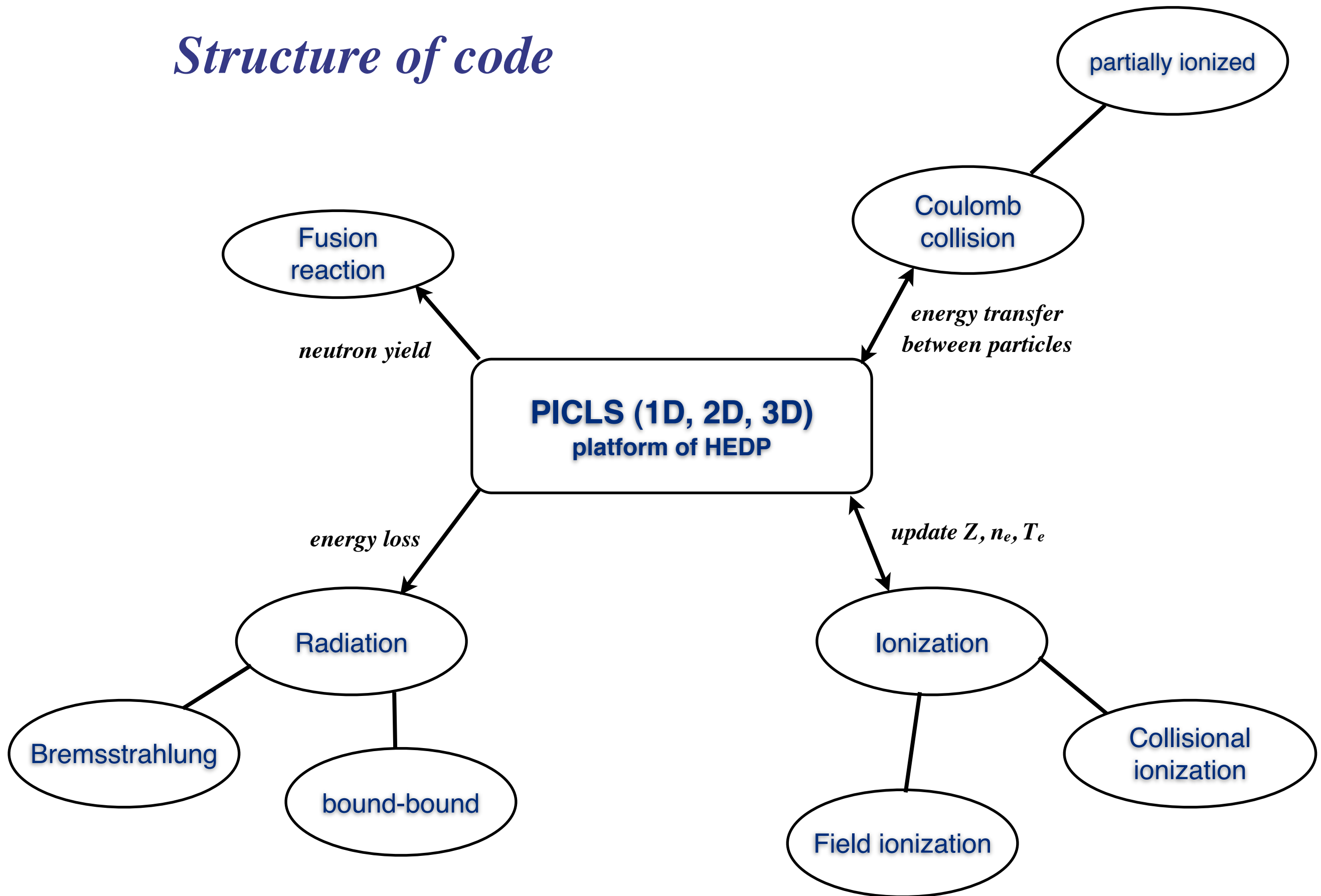
PICLS is a particle-in-cell simulation code, which is designed to solve the above issues, featuring the binary collisions among charged particles and the ionization processes.



Y. Sentoku, and A. J. Kemp, "Numerical methods for particle simulations at extreme densities and temperatures", J. Comput. Phys. 227, 6846 (2008)

PICLS development had been supported by FSC (DE-FC02-04ER54789), DOE/OFES (DE-FG02-05ER54837), NTF/UNR (DOE/NSAA, DE-FC52-06NA27616).

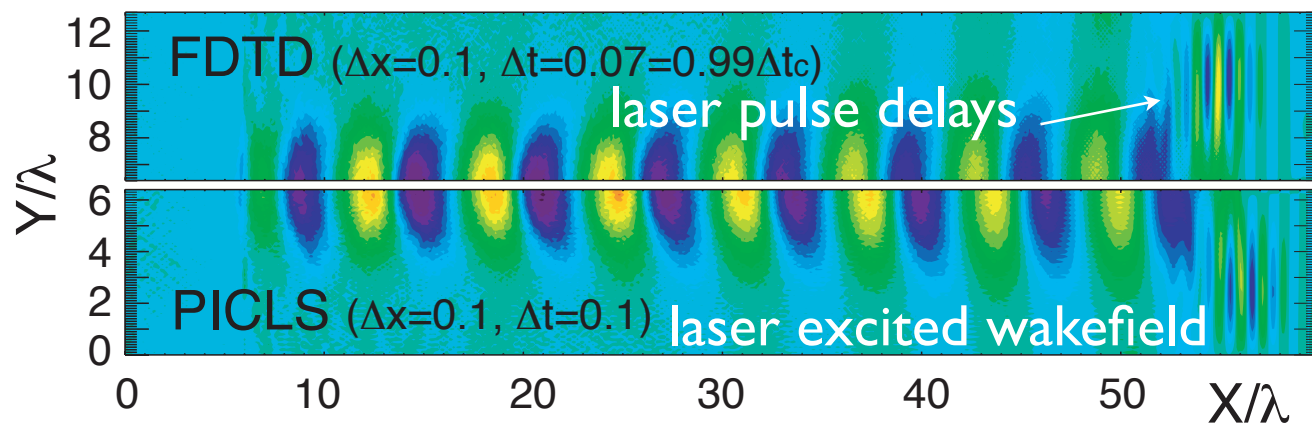
Structure of code



PICLS:

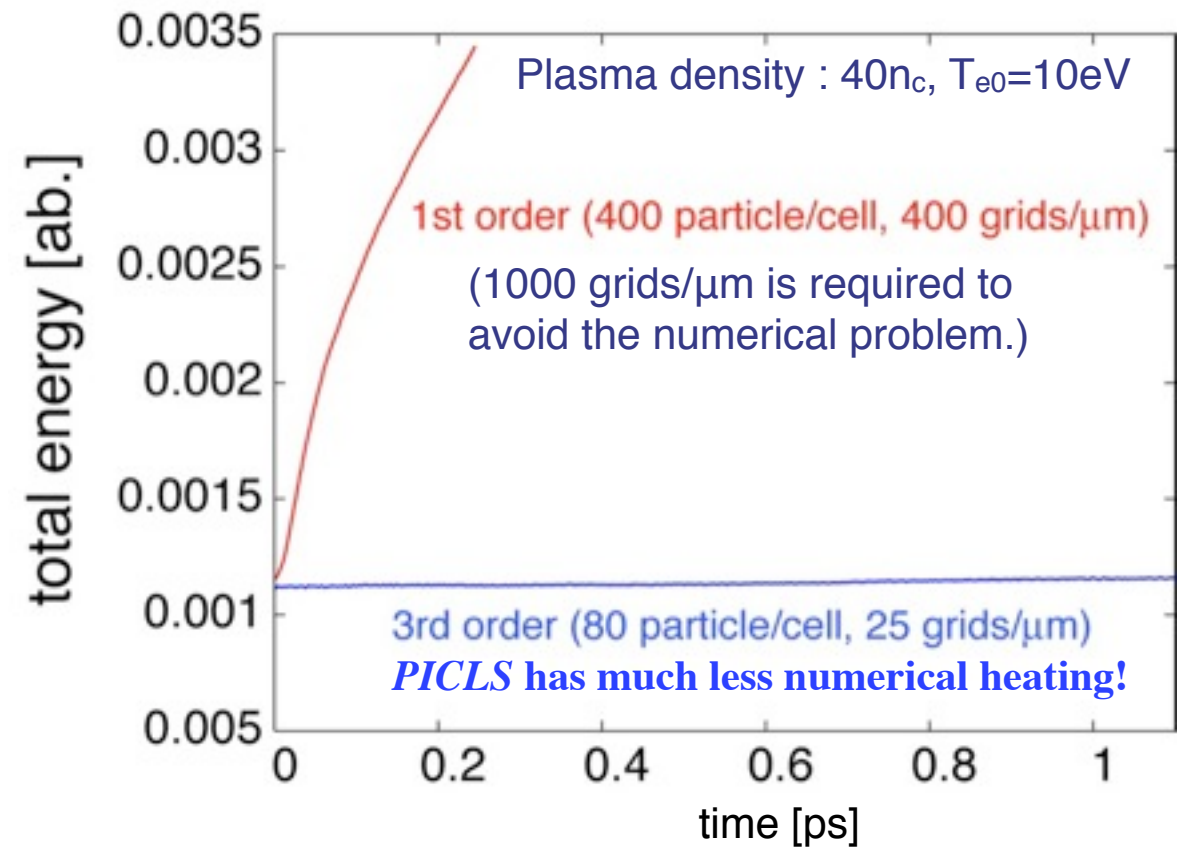
1, 2, & 3D laser plasma simulation code

I. Numerical dispersion free Maxwell solver

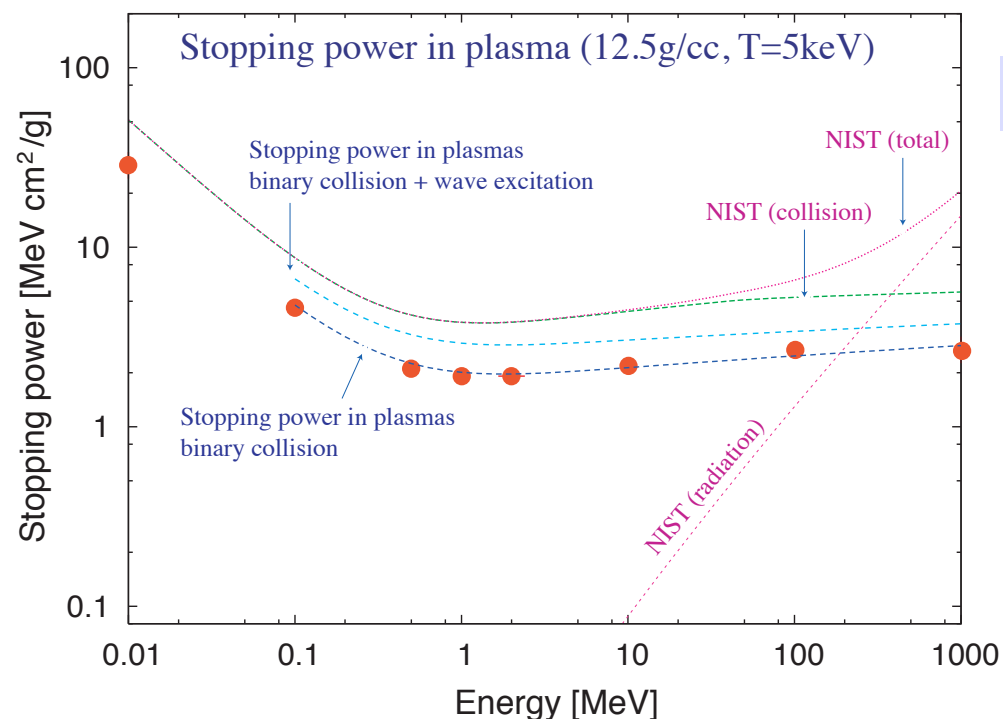


Waves delay due to the numerical diffusion in the standard scheme (FDTD). PICLS can simulate wave propagation correctly with less number of meshes (5 mesh is enough).

II. High order interpolation scheme



Adopting the high order interpolation, PICLS has much less numerical heating with even 40 times larger mesh of Debye length. Drastically reducing PIC cost.



III. Full relativistic collision model for weighted particles

- Based on Takizuka & Abe binary collision model (1977).
- Extended our early work of weakly relativistic model (Sentoku, 1998) to the full relativistic regime.
- Extended the model for weighted particle simulations.
- Verified with the theoretical prediction (stopping power, energy exchange).

Basic equations of PIC simulation

- non-thermal & non-equilibrium plasma -

- Maxwell's equations (PDE: solved on grids)

$$\frac{1}{c} \frac{\partial \mathbf{E}}{\partial t} = \nabla \times \mathbf{B} - \frac{4\pi}{c} \mathbf{J}$$

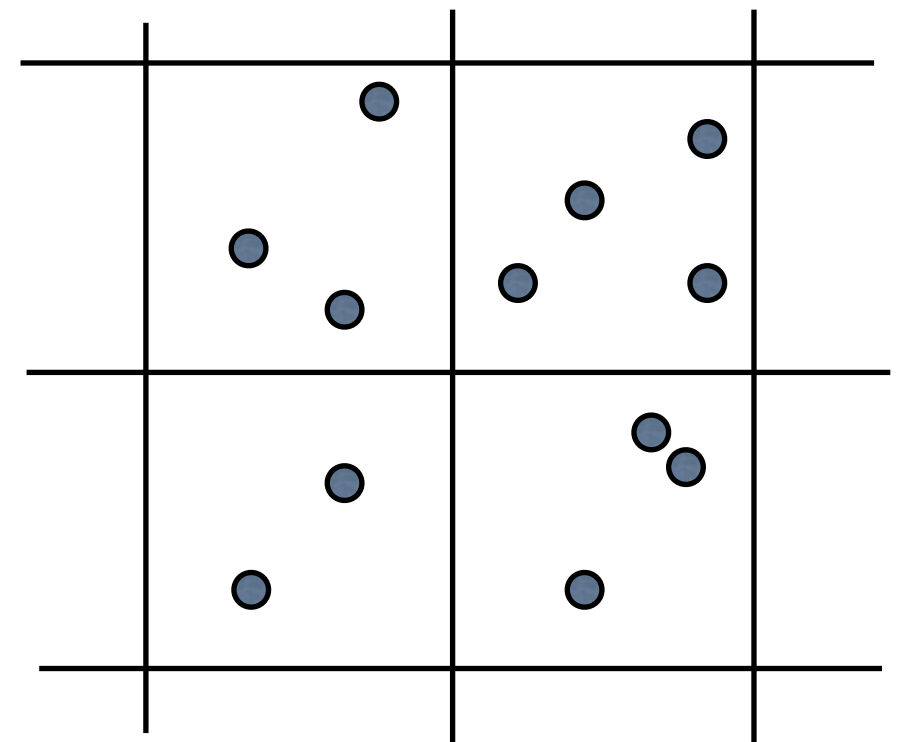
$$\frac{1}{c} \frac{\partial \mathbf{B}}{\partial t} = -\nabla \times \mathbf{E}$$

- Equation of particles (ODE)

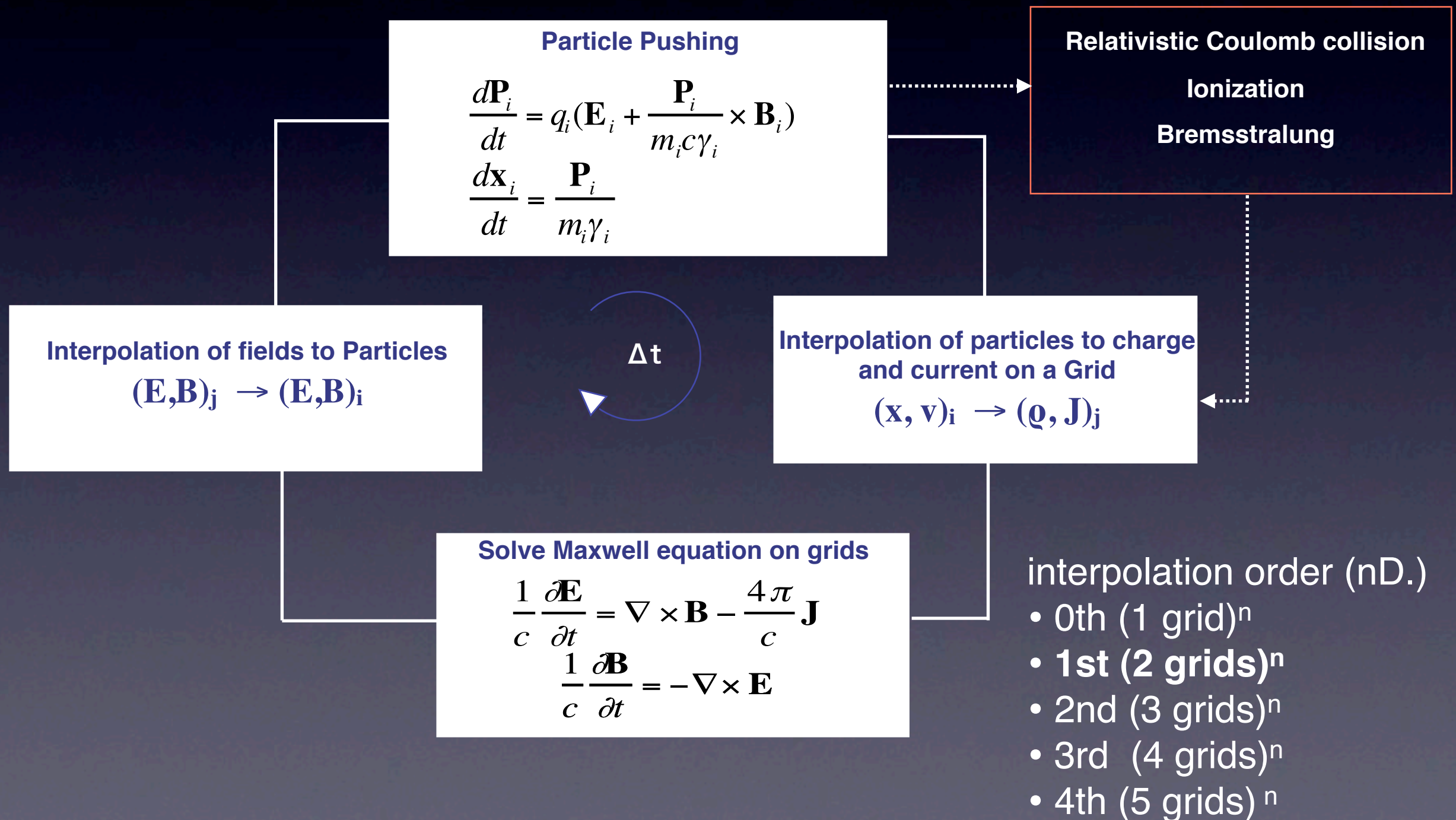
$$\frac{d\mathbf{P}_i}{dt} = q_i \left(\mathbf{E}_i + \frac{\mathbf{P}_i}{m_i c \gamma_i} \times \mathbf{B}_i \right)$$

$$\frac{d\mathbf{x}_i}{dt} = \frac{\mathbf{P}_i}{m_i \gamma_i}$$

γ_i : Lorentz factor



Particle-in-Cell (PIC) simulation with Atomic processes (Monte Carlo models)



Finite Differential Time Domain method (FDTD)

Maxwell equations

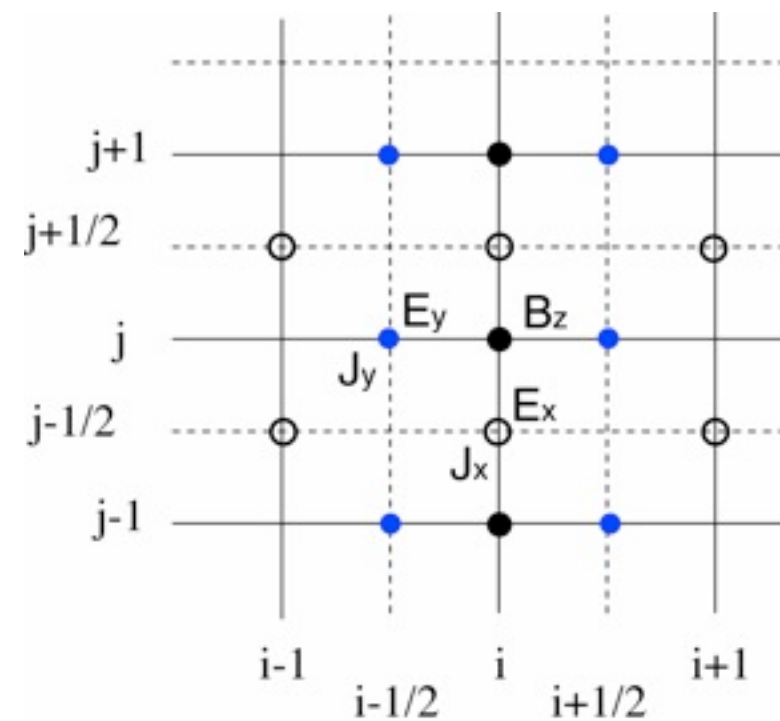
$$\frac{\partial \mathbf{B}}{\partial t} = -c \nabla \times \mathbf{E}$$

$$\frac{\partial \mathbf{E}}{\partial t} = c \nabla \times \mathbf{B} - 4\pi \mathbf{J}$$

Finite differential equations

$$\frac{\mathbf{E}^{n+1} - \mathbf{E}^n}{\Delta t} = c \nabla \times \mathbf{B}^{n+1/2} - 4\pi \mathbf{J}^{n+1/2}$$

$$\frac{\mathbf{B}^{n+1/2} - \mathbf{B}^{n-1/2}}{\Delta t} = -c \nabla \times \mathbf{E}^n$$



Definition of fields on grid

Both the space and time centered differences.

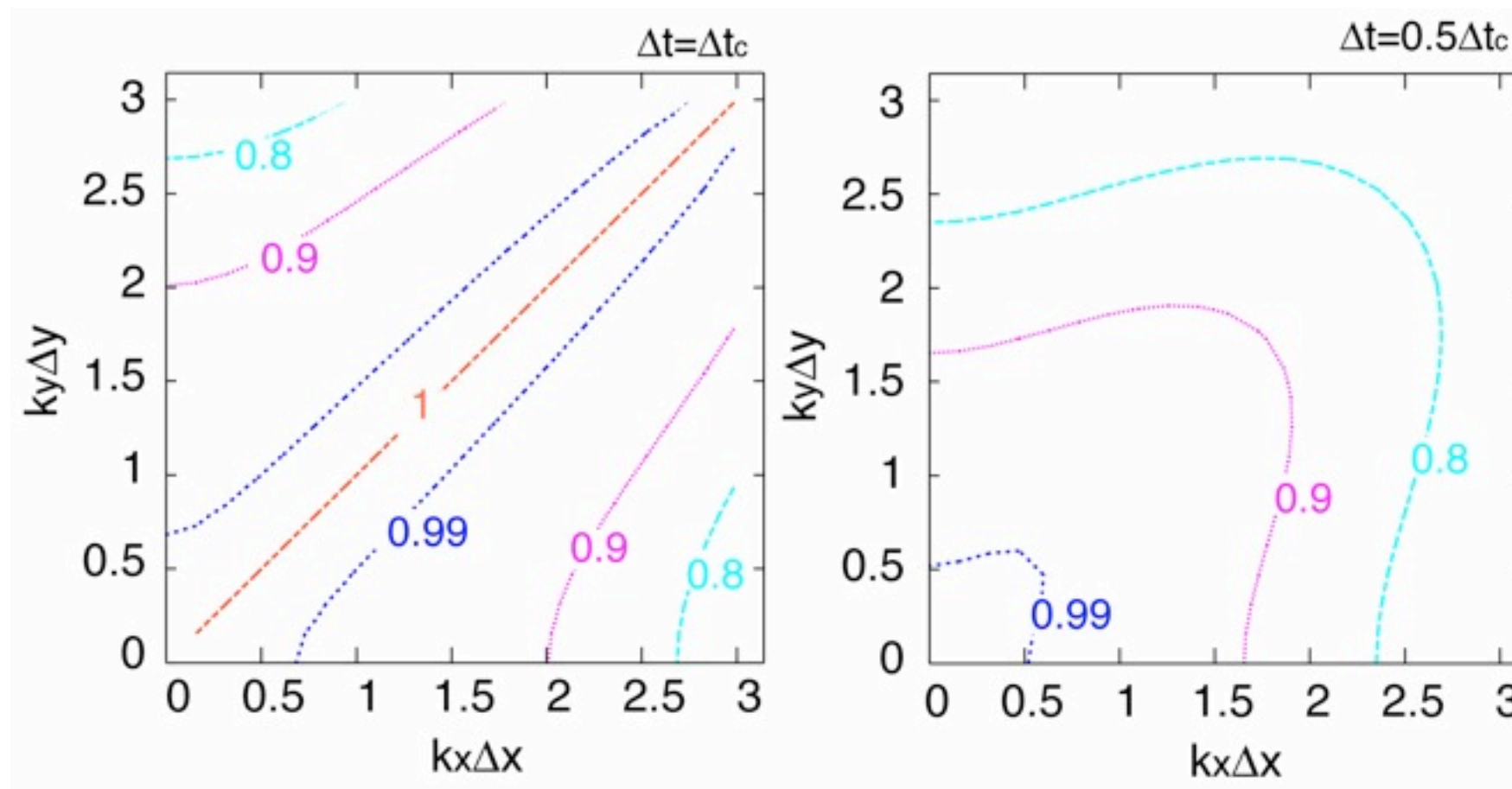
FDTD: Numerical dispersion

by inserting a plane wave $E(\mathbf{x},t) = E_0 \exp[i(\mathbf{k}\cdot\mathbf{x} - \omega t)]$

$$\left(\frac{\sin \omega \Delta t / 2}{c \Delta t}\right)^2 = \left(\frac{\sin k_x \Delta x / 2}{\Delta x}\right)^2 + \left(\frac{\sin k_y \Delta y / 2}{\Delta y}\right)^2$$

Obviously ω is real (stable) when

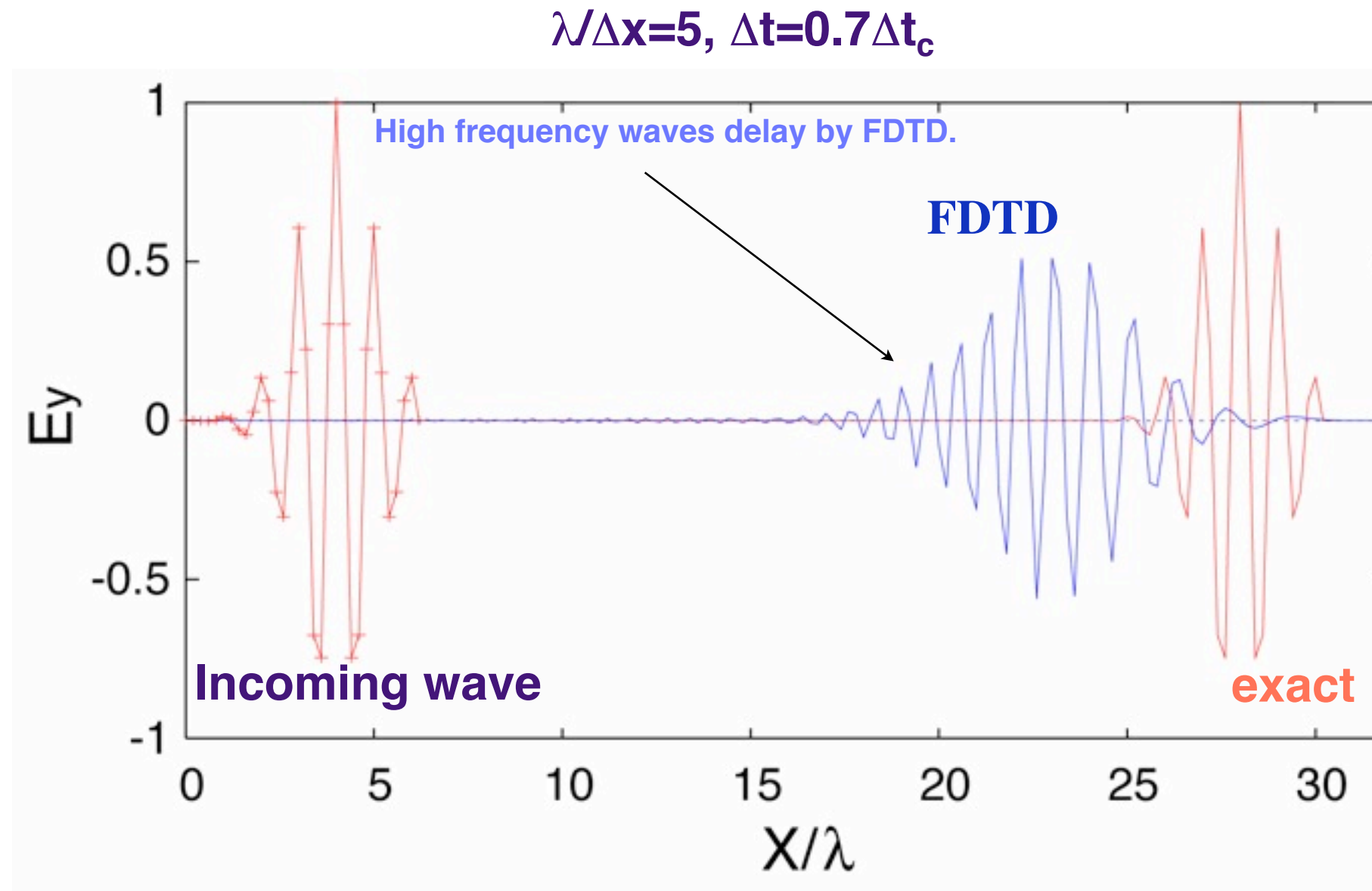
$$c \Delta t < c \Delta t_c \equiv \sqrt{\frac{\Delta x \Delta y}{\Delta x^2 + \Delta y^2}}$$



Map of phase velocity by FDTD

e.g.
 $k_x \Delta x = 0.5$
 $\lambda / \Delta x \sim 12$

FDTD: Wave propagation



Waves delay due to the numerical dispersion, since then a fine resolution (small grid&time-step) is necessary to simulate the laser propagation in a long (cm scale) distance.

Directional splitting (DS) method in PICLS

Maxwell equations

$$\frac{\partial \mathbf{B}}{\partial t} = -c \nabla \times \mathbf{E}$$

$$\frac{\partial \mathbf{E}}{\partial t} = c \nabla \times \mathbf{B} - 4\pi \mathbf{J}$$

P-pol component

$$\frac{\partial}{\partial t} \begin{pmatrix} E_x \\ E_y \\ B_z \end{pmatrix} + \begin{pmatrix} 0 & 0 & 0 \\ 0 & 0 & -c \\ 0 & -c & 0 \end{pmatrix} \frac{\partial}{\partial x} \begin{pmatrix} E_x \\ E_y \\ B_z \end{pmatrix} + \begin{pmatrix} 0 & 0 & c \\ 0 & 0 & 0 \\ c & 0 & 0 \end{pmatrix} \frac{\partial}{\partial y} \begin{pmatrix} E_x \\ E_y \\ B_z \end{pmatrix} = - \begin{pmatrix} J_x \\ J_y \\ 0 \end{pmatrix}$$

Step1: x-direction

$$E_y^\pm = B_z \pm E_y$$

$$\frac{\partial E_y^+}{\partial t} + c \frac{\partial E_y^+}{\partial x} = -\frac{1}{2} J_y$$

$$\frac{\partial E_y^-}{\partial t} - c \frac{\partial E_y^-}{\partial x} = +\frac{1}{2} J_y$$

$$\frac{\partial}{\partial t} \begin{pmatrix} E_x \\ E_y \\ B_z \end{pmatrix} + \begin{pmatrix} 0 & 0 & 0 \\ 0 & 0 & -c \\ 0 & -c & 0 \end{pmatrix} \frac{\partial}{\partial x} \begin{pmatrix} E_x \\ E_y \\ B_z \end{pmatrix} + \begin{pmatrix} 0 & 0 & c \\ 0 & 0 & 0 \\ c & 0 & 0 \end{pmatrix} \frac{\partial}{\partial y} \begin{pmatrix} E_x \\ E_y \\ B_z \end{pmatrix} = - \begin{pmatrix} J_x \\ J_y \\ 0 \end{pmatrix}$$

no d/dy for (Ey, Bz)

Step2: y-direction

$$E_x^\pm = B_z \mp E_x$$

$$\frac{\partial E_x^+}{\partial t} + c \frac{\partial E_x^+}{\partial y} = +\frac{1}{2} J_x$$

$$\frac{\partial E_x^-}{\partial t} - c \frac{\partial E_x^-}{\partial y} = -\frac{1}{2} J_x$$

$$\frac{\partial}{\partial t} \begin{pmatrix} E_x \\ E_y \\ B_z \end{pmatrix} + \begin{pmatrix} 0 & 0 & 0 \\ 0 & 0 & -c \\ 0 & -c & 0 \end{pmatrix} \frac{\partial}{\partial x} \begin{pmatrix} E_x \\ E_y \\ B_z \end{pmatrix} + \begin{pmatrix} 0 & 0 & c \\ 0 & 0 & 0 \\ c & 0 & 0 \end{pmatrix} \frac{\partial}{\partial y} \begin{pmatrix} E_x \\ E_y \\ B_z \end{pmatrix} = - \begin{pmatrix} J_x \\ J_y \\ 0 \end{pmatrix}$$

no d/dx for (Ex, Bz)

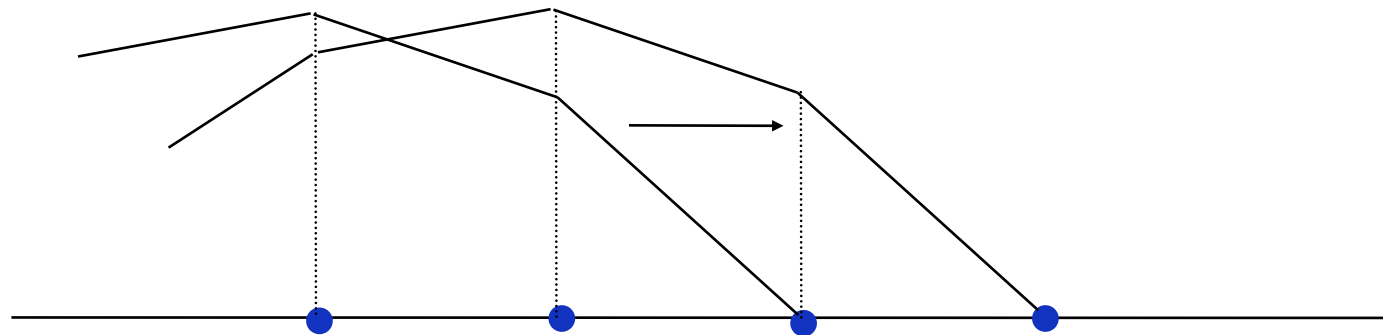
Equation of wave propagation

Equation of wave with constant velocity c ($c > 0$)

$$\frac{\partial f}{\partial t} + c \frac{\partial f}{\partial x} = 0$$

Finite difference equation,

$$f(x_i + \Delta x, t_n + \Delta t) = f(x_i, t_n)$$



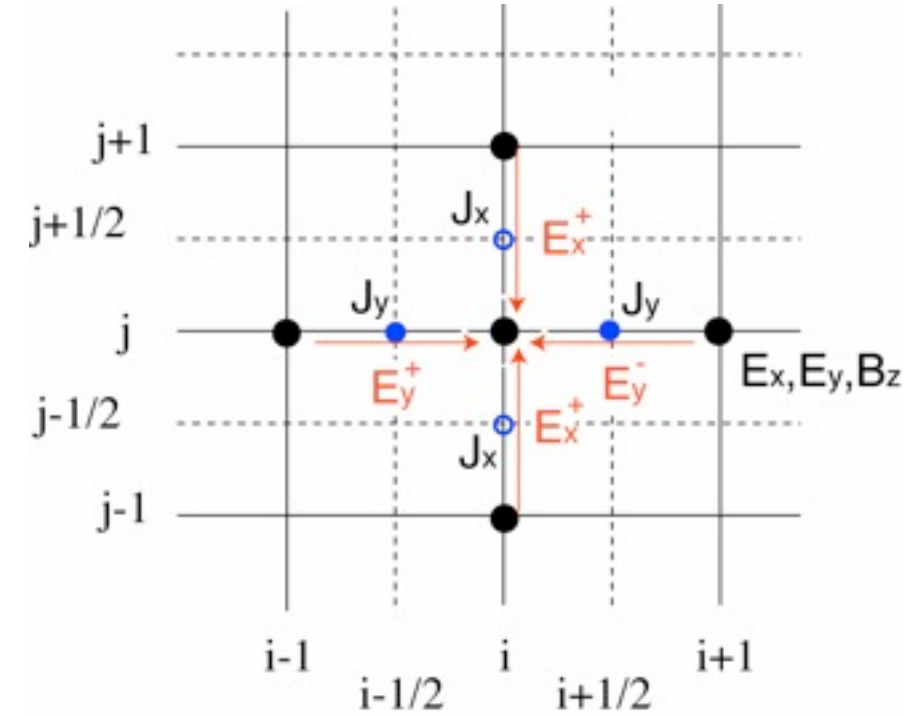
When $\Delta x = c \Delta t$, the numerical solution of this equation is very easy, just copy the grid value to the next grid.

DS: Calculate the numerical dispersion

Step1: x-direction

$$\begin{aligned}
 E_y^{n+1} &= E_{y0} \exp[k_x x_i + k_y y_j - \omega(t_n + \Delta t)] \\
 &= \frac{B_{z0} + E_{y0}}{2} \exp[k_x(x_i - \Delta x) + k_y y_j - \omega(t_n)] - \frac{1}{2} J_{y,i-1/2,j} \\
 &\quad - \frac{B_{z0} - E_{y0}}{2} \exp[k_x(x_i + \Delta x) + k_y y_j - \omega(t_n)] - \frac{1}{2} J_{y,i+1/2,j}
 \end{aligned}$$

$$\begin{aligned}
 B_z^{n*} &= B_{z0} \exp[k_x x_i + k_y y_j - \omega(t_n^*)] \quad \mathbf{t_n^*: \text{transient time}} \\
 &= \frac{B_{z0} + E_{y0}}{2} \exp[k_x(x_i - \Delta x) + k_y y_j - \omega(t_n)] - \frac{1}{2} J_{y,i-1/2,j} \\
 &\quad + \frac{B_{z0} - E_{y0}}{2} \exp[k_x(x_i + \Delta x) + k_y y_j - \omega(t_n)] + \frac{1}{2} J_{y,i+1/2,j}
 \end{aligned}$$



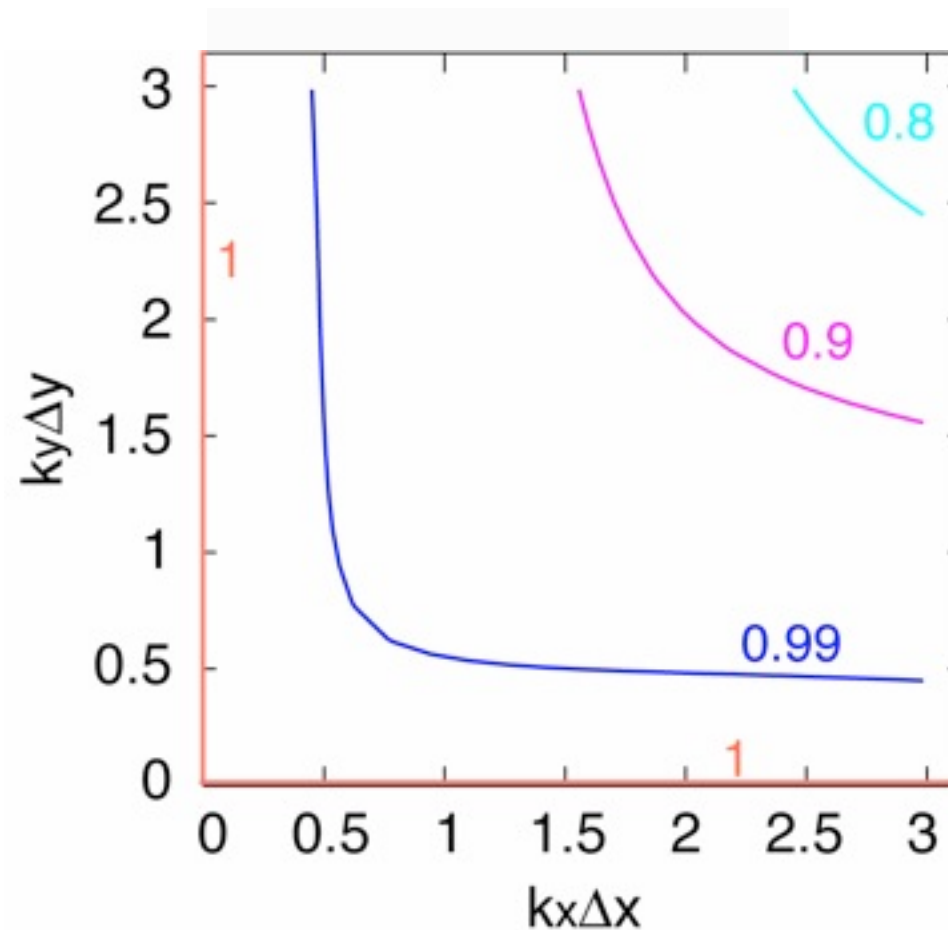
Step2: y-direction

$$\begin{aligned}
 E_x^{n+1} &= E_{x0} \exp[k_x x_i + k_y y_j - \omega(t_n + \Delta t)] \\
 &= -\frac{B_{z0}}{2} \exp[k_x x_i + k_y(y_j - \Delta y) - \omega(t_n^*)] + \frac{E_{x0}}{2} \exp[k_x x_i + k_y(y_j - \Delta y) - \omega(t_n)] - \frac{1}{2} J_{x,i,j-1/2} \\
 &\quad + \frac{B_{z0}}{2} \exp[k_x x_i + k_y(y_j + \Delta y) - \omega(t_n^*)] + \frac{E_{x0}}{2} \exp[k_x x_i + k_y(y_j + \Delta y) - \omega(t_n)] - \frac{1}{2} J_{x,i,j+1/2}
 \end{aligned}$$

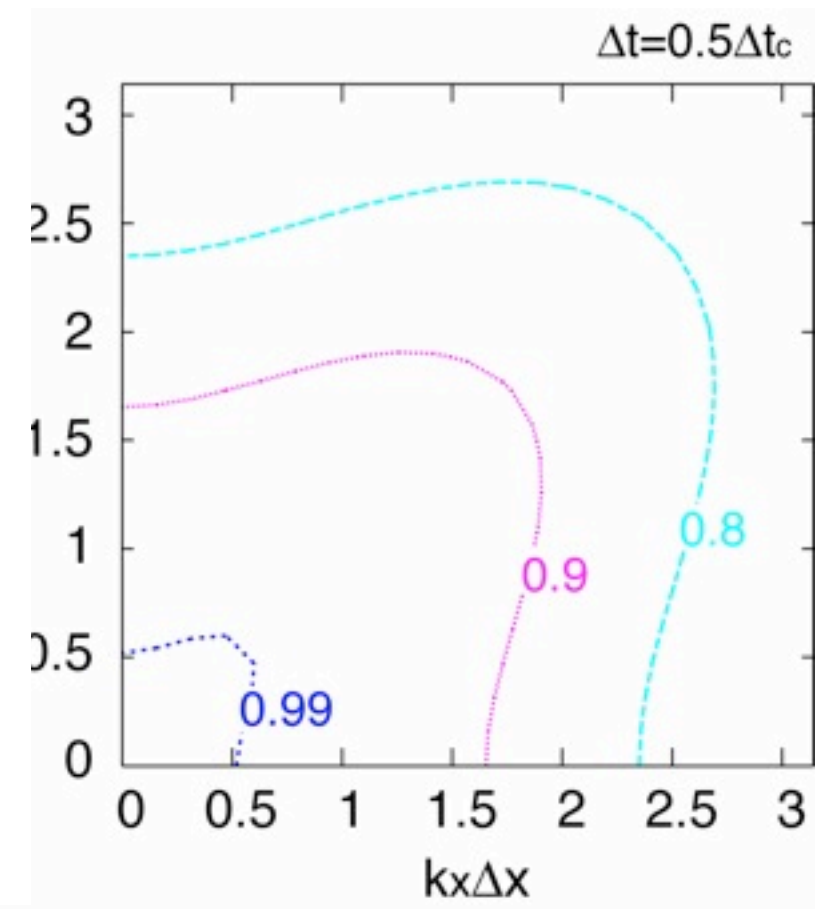
$$\begin{aligned}
 B_z^{n+1} &= B_{z0} \exp[k_x x_i + k_y y_j - \omega(t_n + \Delta t)] \\
 &= \frac{B_{z0}}{2} \exp[k_x x_i + k_y(y_j - \Delta y) - \omega(t_n^*)] - \frac{E_{x0}}{2} \exp[k_x x_i + k_y(y_j - \Delta y) - \omega(t_n)] + \frac{1}{2} J_{x,i,j-1/2} \\
 &\quad + \frac{B_{z0}}{2} \exp[k_x x_i + k_y(y_j + \Delta y) - \omega(t_n^*)] + \frac{E_{x0}}{2} \exp[k_x x_i + k_y(y_j + \Delta y) - \omega(t_n)] - \frac{1}{2} J_{x,i,j+1/2}
 \end{aligned}$$

DS: Numerical dispersion

$$\cos \omega \Delta t = \frac{1}{2} \left(-1 + \cos k_x \Delta x \cos k_y \Delta y + \cos k_x \Delta x + \cos k_y \Delta y \right)$$



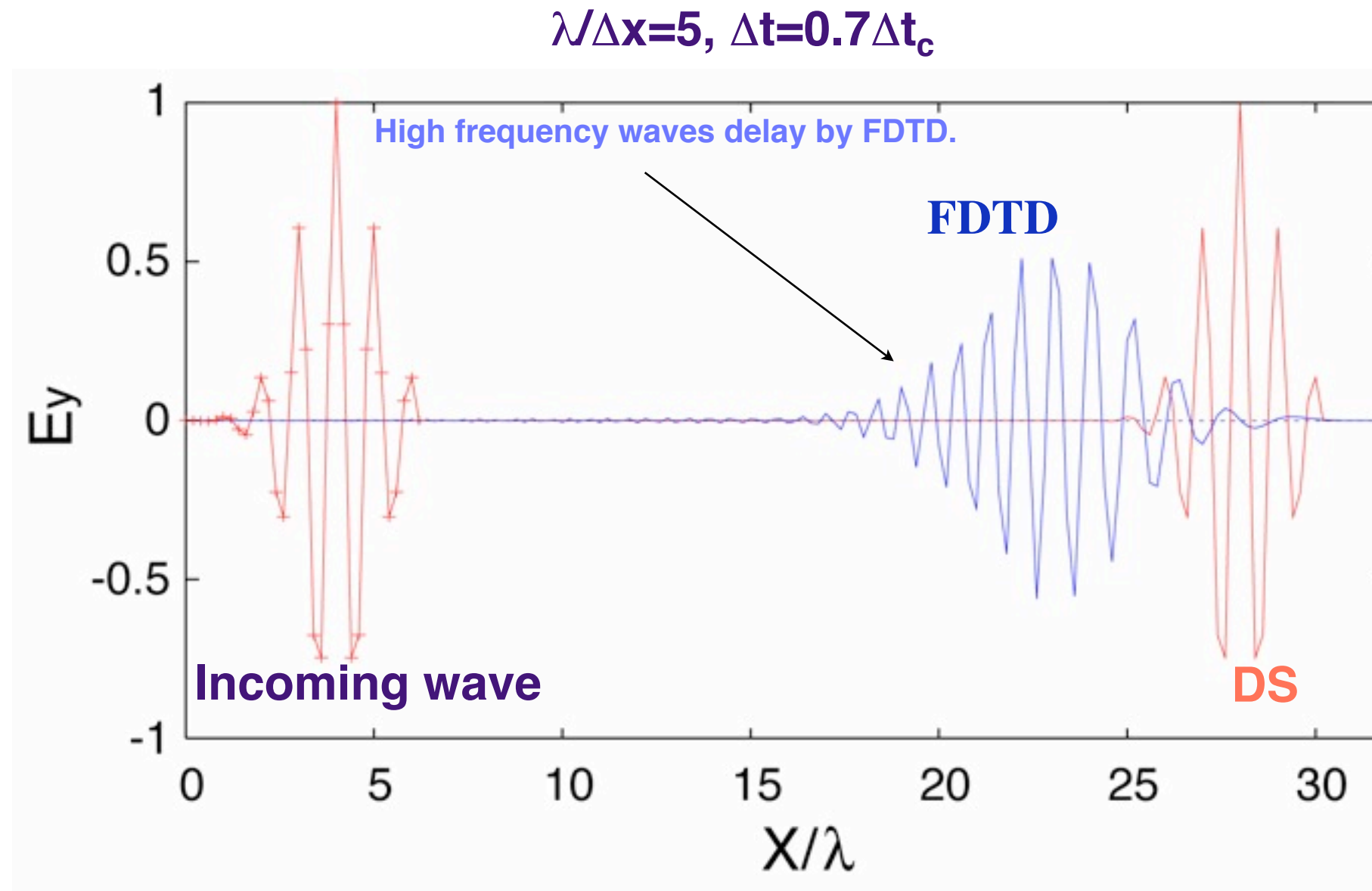
Map of phase velocity by DS



Map of phase velocity by FDTD

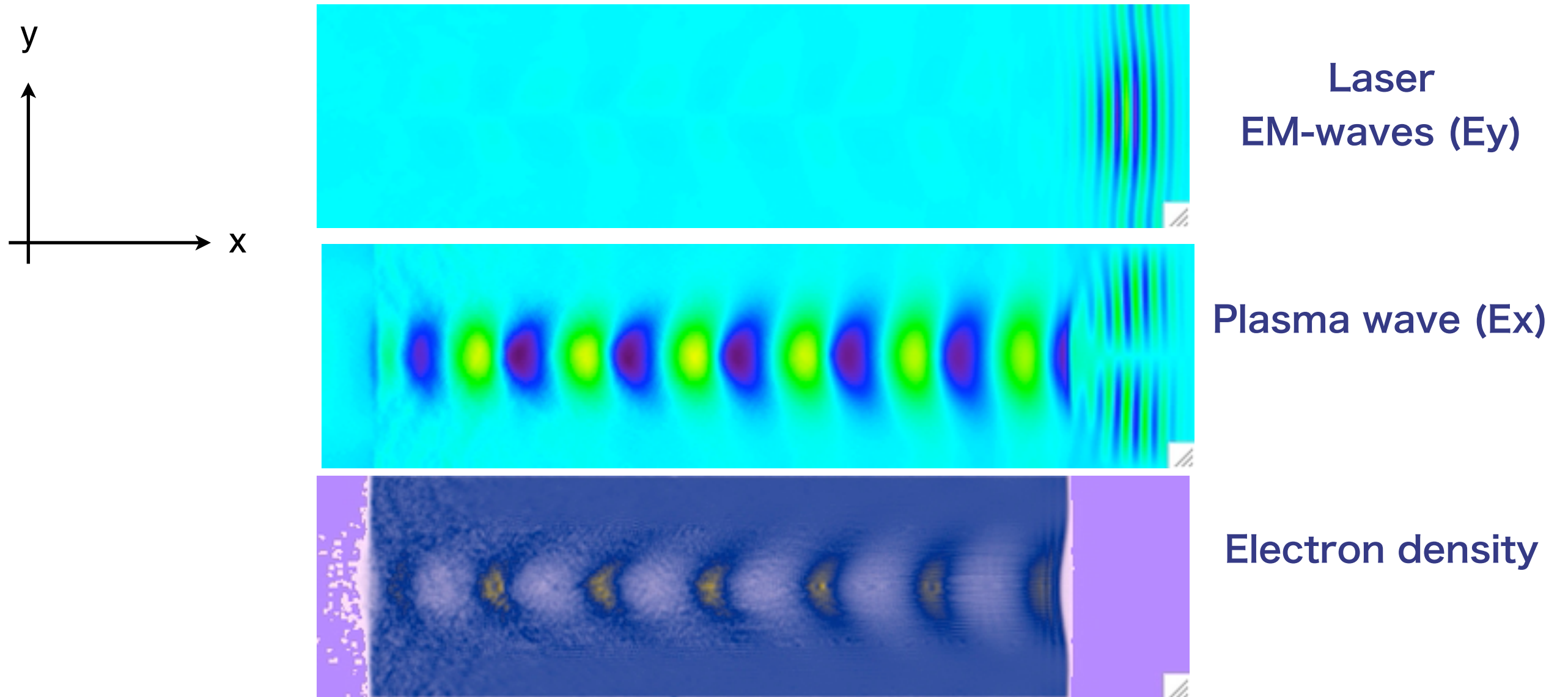
NO numerical dispersion along the grids.

FDTD: Wave propagation



Waves delay due to the numerical dispersion, since then a fine resolution (small grid&time-step) is necessary to simulate the laser propagation in a long (cm scale) distance.

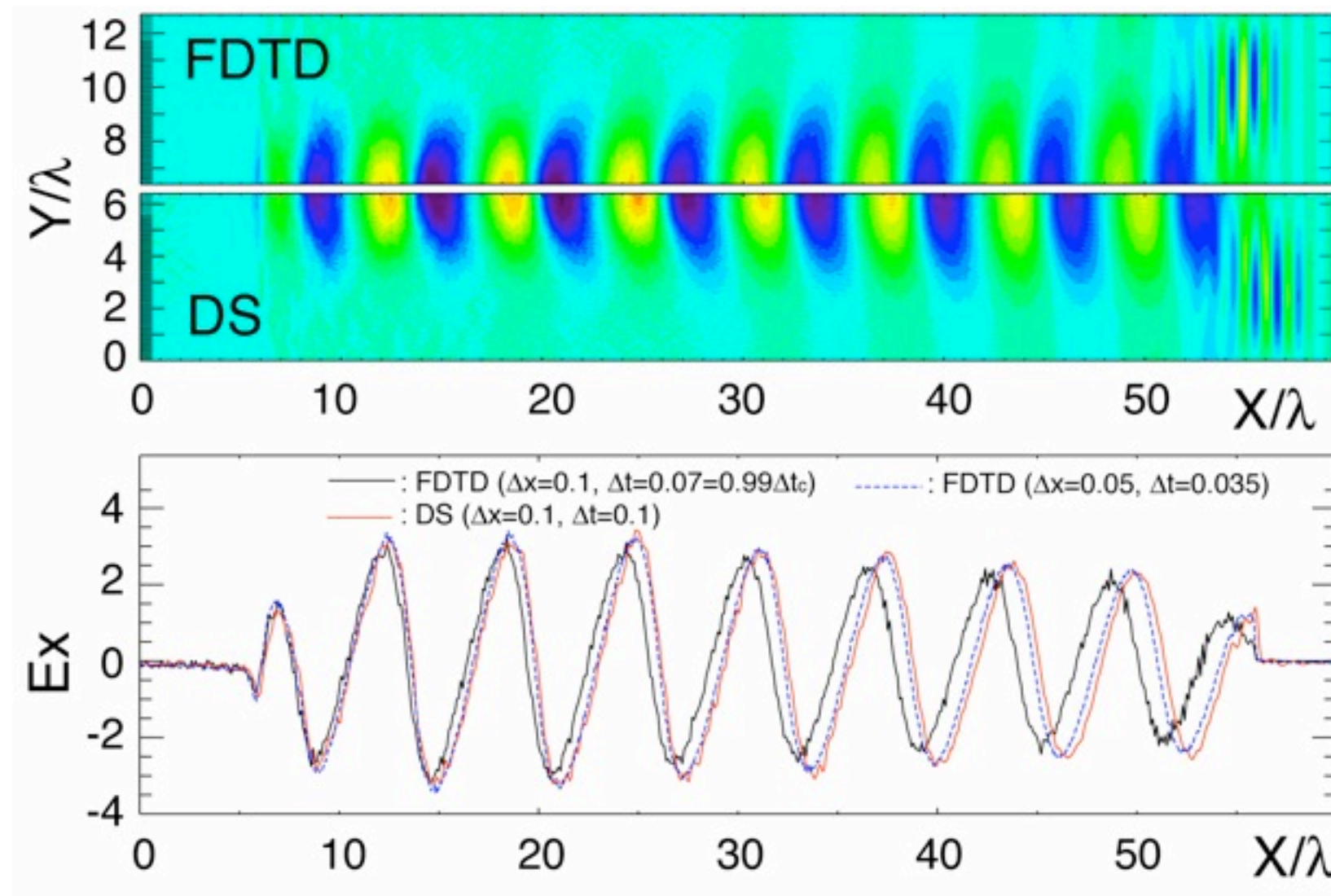
Wakefield simulation by PIC



PIC solves the Maxwell equations and kinetic equations of charged particles.

Test II: Wake fields

Laser: $a = 1$, pulse length = 5λ



DS:
300x128 mesh

10 mesh is quite enough for one laser wavelength with the DS scheme. The FDTD needs two times more meshes in one direction.

numerical modeling of hot dense plasma is challenging due to large scale both in time and space

- e.g. • fast ignition in inertial confinement fusion (ICF)
time scale \sim ps, spatial scale \sim 100 μ m

time step $\sim 1/\omega_p \sim 0.01$ fs \rightarrow simulation time scale \sim ps
mesh size $\propto T_e^{1/2}/\omega_p \sim 0.001$ μ m \rightarrow simulation scale 100 μ m

time step will be $>10^5$
number of mesh will be $\sim 10^{5 \times N_D}$
impossible by current computers!!

**Can we extend grid size greater than
debye length without having numerical
heating?**

**High order interpolation to extend grid size ~
plasma skin length \gg Debye length**

Extend grid size beyond Debye length

- reduce numerical heating by high order interpolation -

Time evolution of system energy of thermal plasma

demonstration (1d)

- *internal energy evolution* -

Plasma: solid density ($40n_c$),

$T_{e0}=10\text{eV}$ (without a laser pulse)

To resolve the above plasma with
standard PIC simulation,
1000 grids/ μm resolution
is required to suppress
the numerical heating!

Extend grid size beyond Debye length

- reduce numerical heating by high order interpolation -

demonstration (1d)

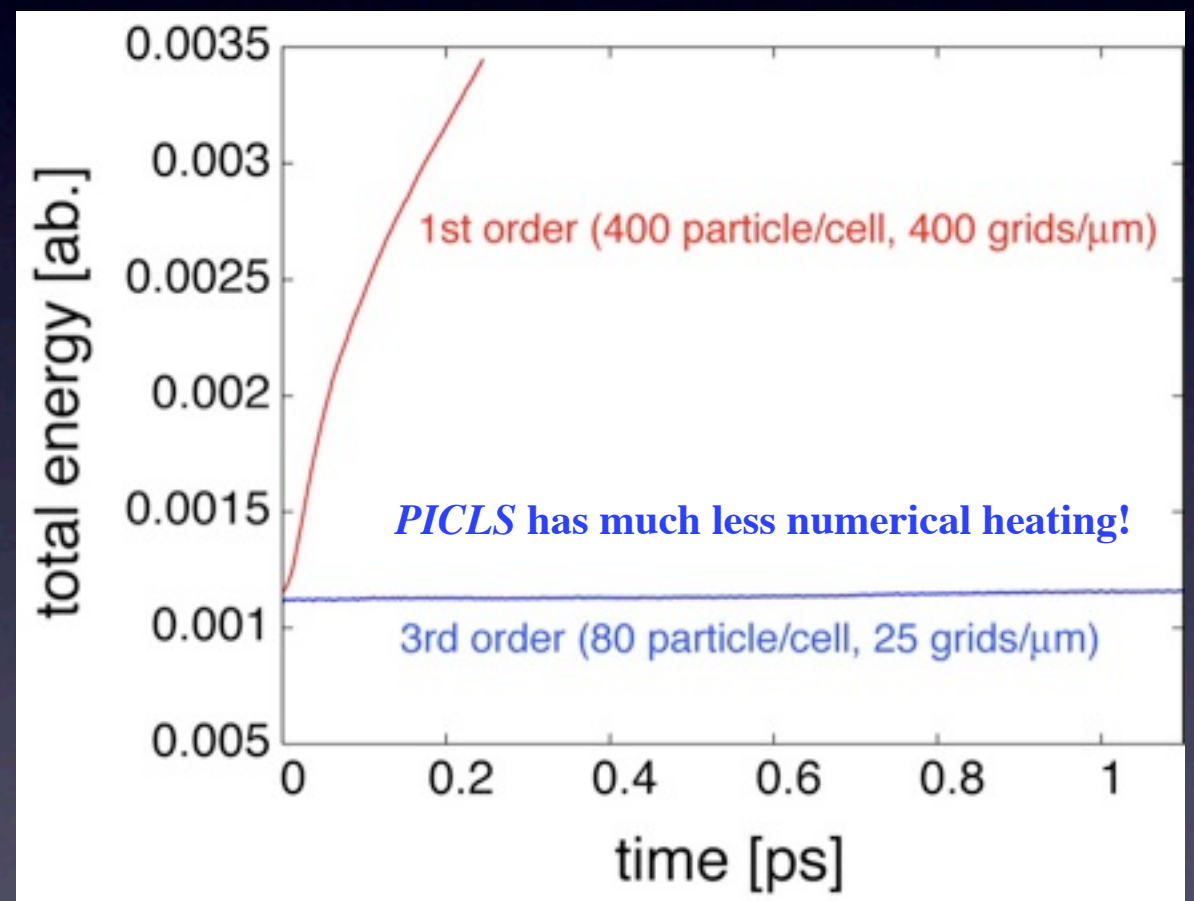
- *internal energy evolution* -

Plasma: solid density ($40n_c$),

$T_{e0}=10\text{eV}$ (without a laser pulse)

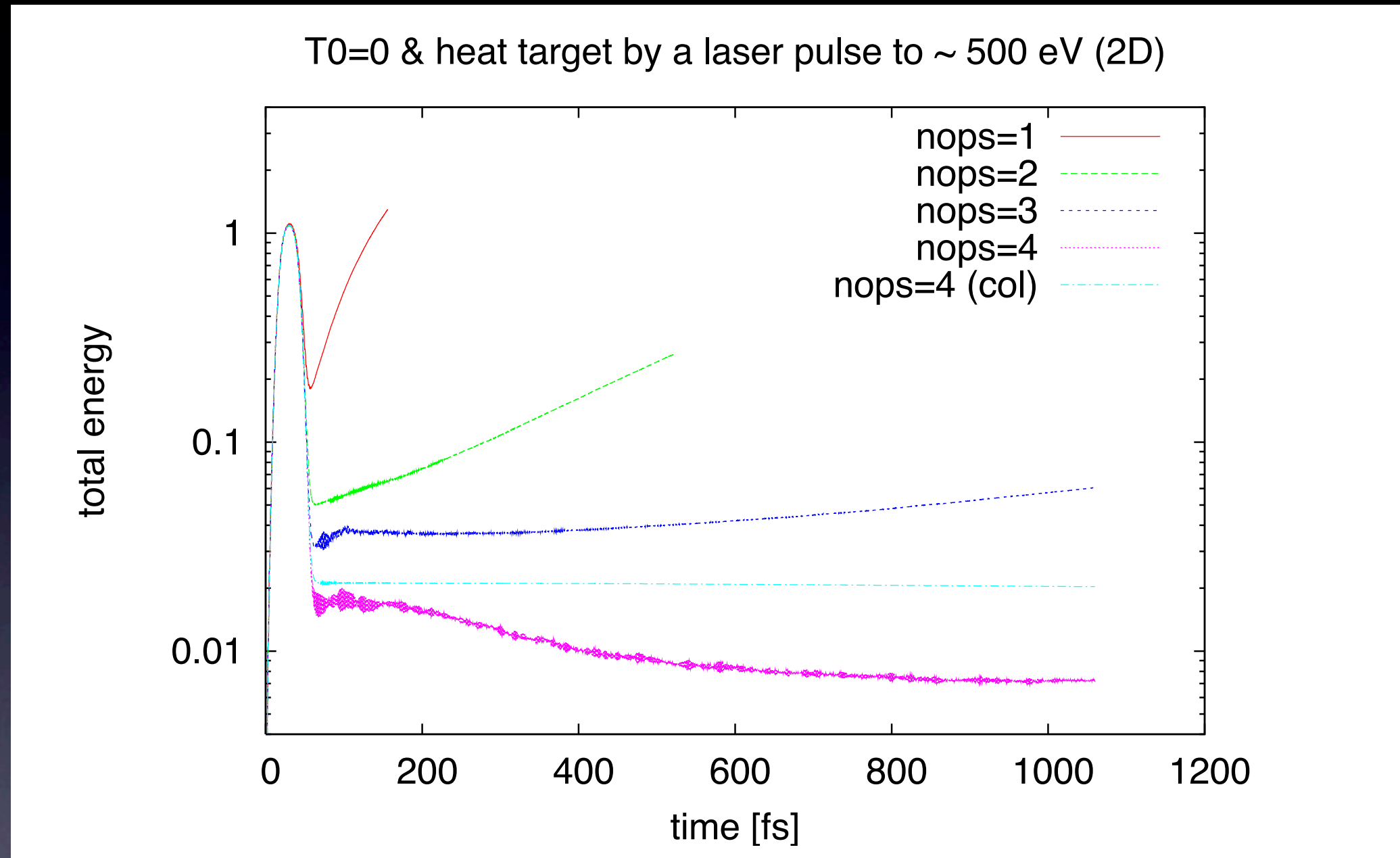
To resolve the above plasma with standard PIC simulation, 1000 grids/ μm resolution is required to suppress the numerical heating!

Time evolution of system energy of thermal plasma



4 order magnitude less computational cost in 2D!!

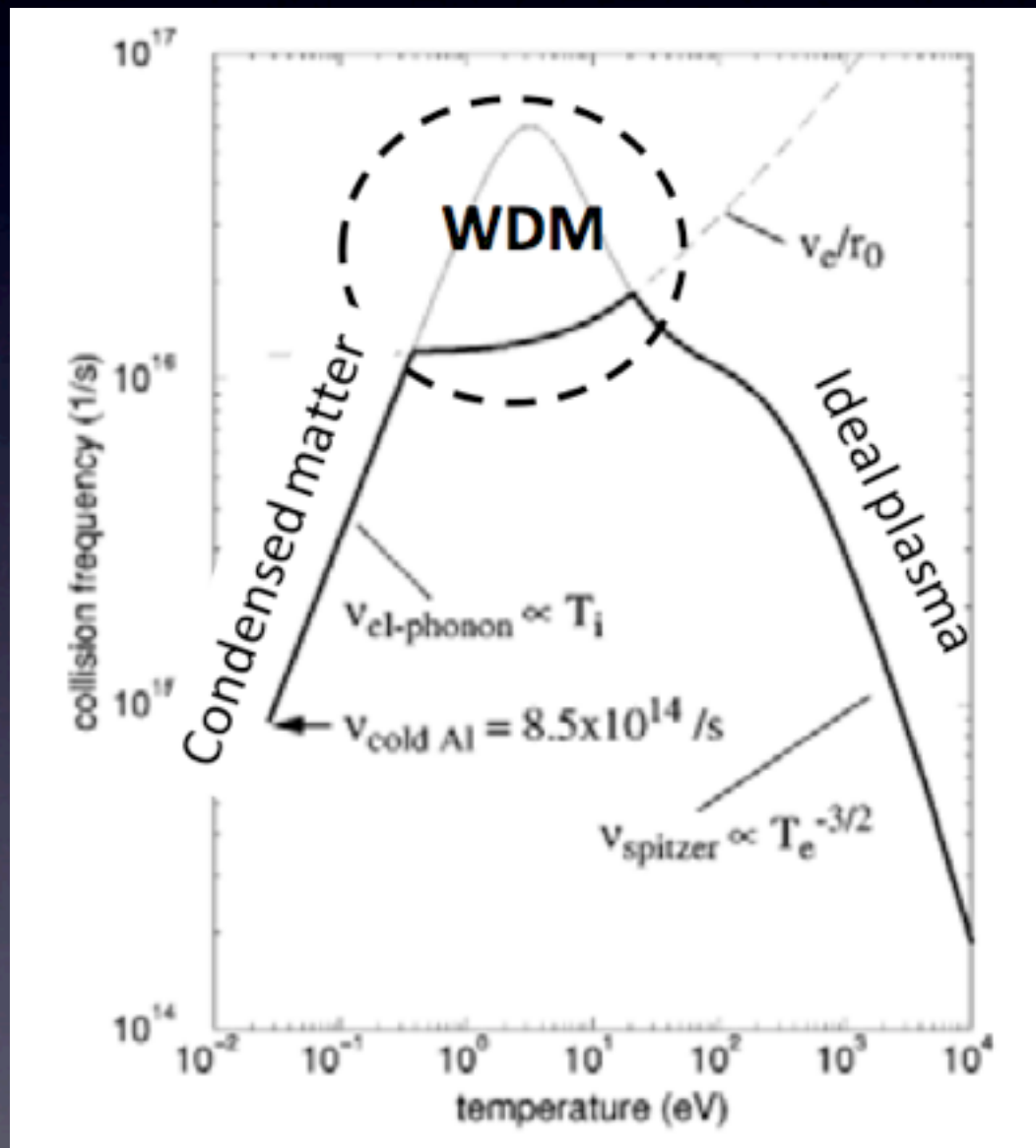
Long time stability with high order interpolation - demonstration by 2D PIC -



Time evolution of thin plasma after short pulse irradiation

target $40n_c$, thickness $2 \mu\text{m}$, box: $10\mu\text{m} \times 6\mu\text{m}$
 $a=2$, 30 fs , $np=10$, $\Delta x=1\mu\text{m}/25$

Relativistic collision model for weighted particles



$$\nu_{\alpha\beta} = \frac{4\pi(e_{\alpha}e_{\beta})^2 n_1 L}{p_{\text{rel}}^2 v_{\text{rel}}}$$

Collision frequency in Spitzer regime

$$\frac{T_0}{m_e c^2} = \left(\frac{\sqrt{2}\pi^{3/2} \hbar^3 n_h}{m_e^{3/2}} \right)^{2/3}$$

T_0 : transition temperature from Spitzer regime to degenerate regime

$$\nu_{\alpha\beta} = \frac{4m_e Z e^4 L}{3\pi \hbar^3}$$

Collision frequency in degenerate regime

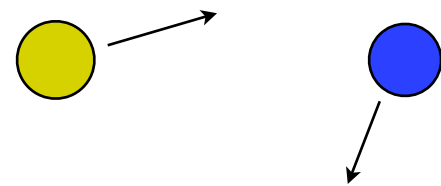
Y.T. Lee, R.M. More, Phys. Fluids 27 (1984) 1273.

Y. Sentoku and A. J. Kemp, J. Comp. Phys. 227, 6846 (2008).

Full relativistic kinematic of energy transfer in collision

Binary collision model (Takizuka & Abe, J. Comp. Phys., 1977)

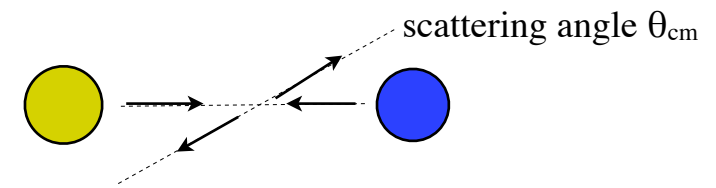
Weakly relativistic collision model (Sentoku et al., J. Phys. Soc. Jpn, 1998)



laboratory frame



Lorentz transform



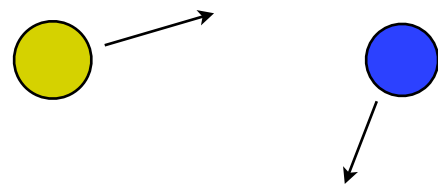
center of mass frame, γ_{cm}

Perfect energy and momentum conservation!

Full relativistic kinematic of energy transfer in collision

Binary collision model (Takizuka & Abe, J. Comp. Phys., 1977)

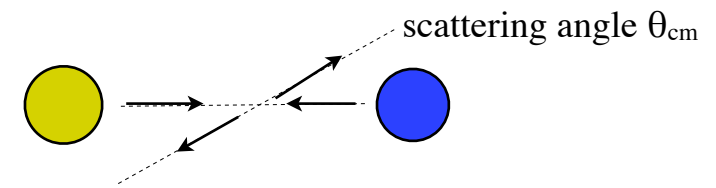
Weakly relativistic collision model (Sentoku et al., J. Phys. Soc. Jpn, 1998)



laboratory frame

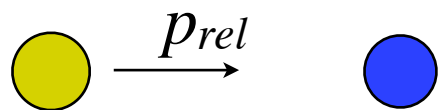


Lorentz transform



center of mass frame, γ_{cm}

evaluate the collision frequency on the one particle at rest frame.



one particle at rest frame

$$v_{\alpha\beta} = \frac{4\pi(e_{\alpha}e_{\beta})^2 n_l L}{p_{rel}^2 v_{rel}}$$

$$L = \ln(\lambda_D p_{rel} / \hbar)$$

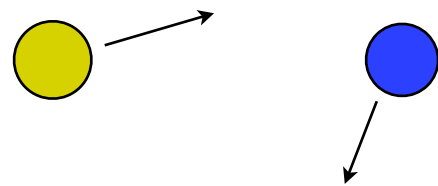
$$\langle \tan^2 \theta_L / 2 \rangle = v_{\alpha\beta} \Delta t$$

Perfect energy and momentum conservation!

Full relativistic kinematic of energy transfer in collision

Binary collision model (Takizuka & Abe, J. Comp. Phys., 1977)

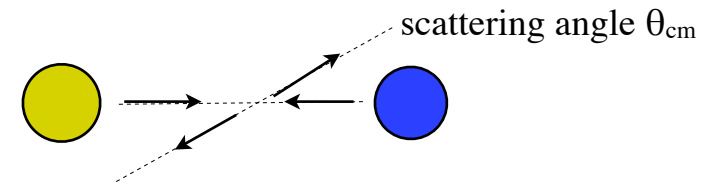
Weakly relativistic collision model (Sentoku et al., J. Phys. Soc. Jpn, 1998)



laboratory frame

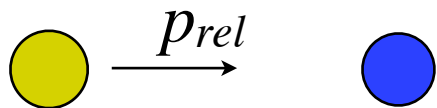


Lorentz transform



center of mass frame, γ_{cm}

evaluate the collision frequency on the one particle at rest frame.



one particle at rest frame

$$v_{\alpha\beta} = \frac{4\pi(e_\alpha e_\beta)^2 n_l L}{p_{rel}^2 v_{rel}}$$

$$L = \ln(\lambda_D p_{rel} / \hbar)$$

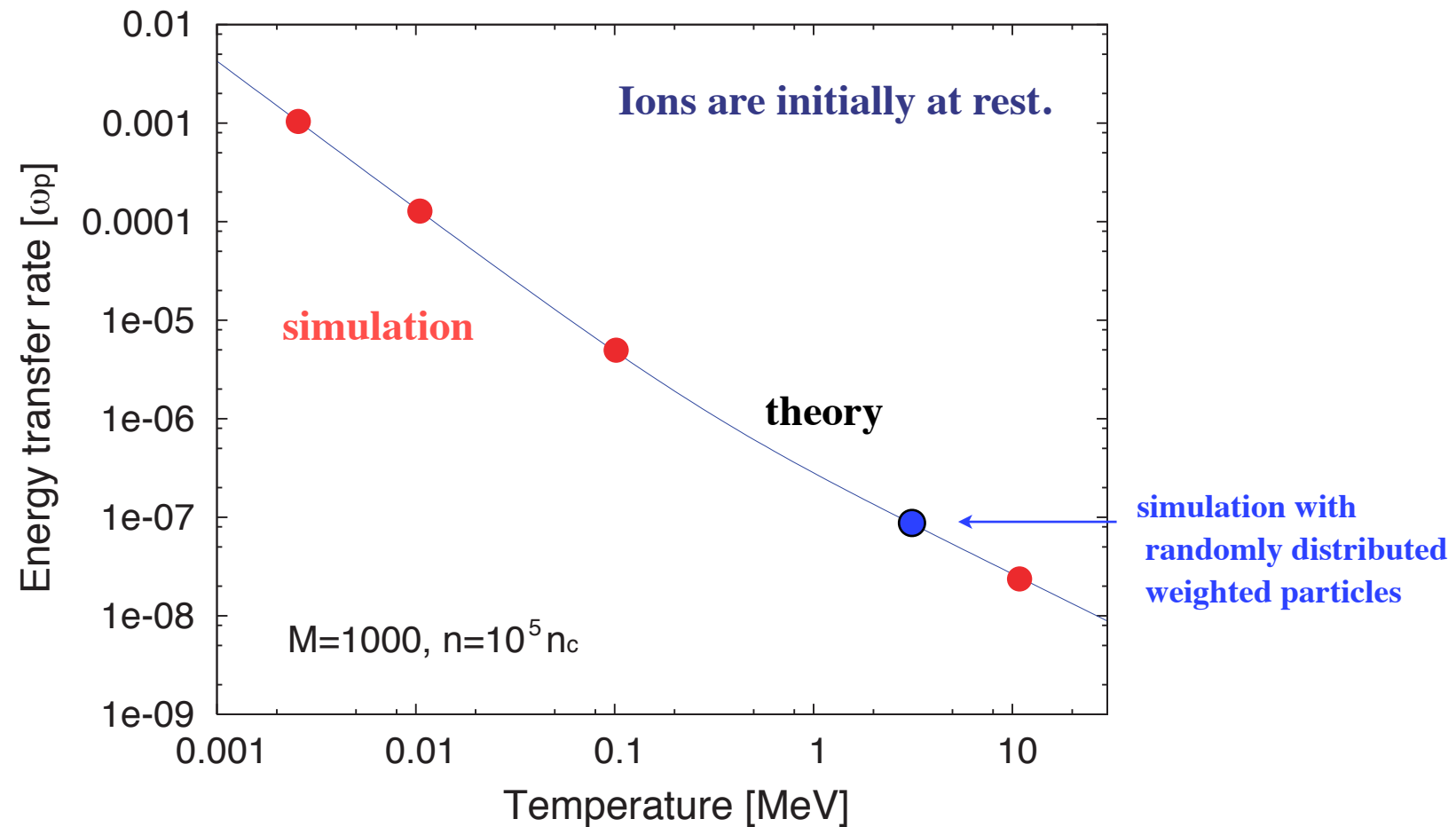
$$\langle \tan^2 \theta_L / 2 \rangle = v_{\alpha\beta} \Delta t$$

$$\tan \theta_{cm} = \frac{\sin \theta_L}{\gamma_{cm} (\cos \theta_L - \beta_{cm} / \beta)}$$

Lorentz transform

Perfect energy and momentum conservation!

Energy transfer rate from hot electrons to ions - test simulation of relativistic collision model -

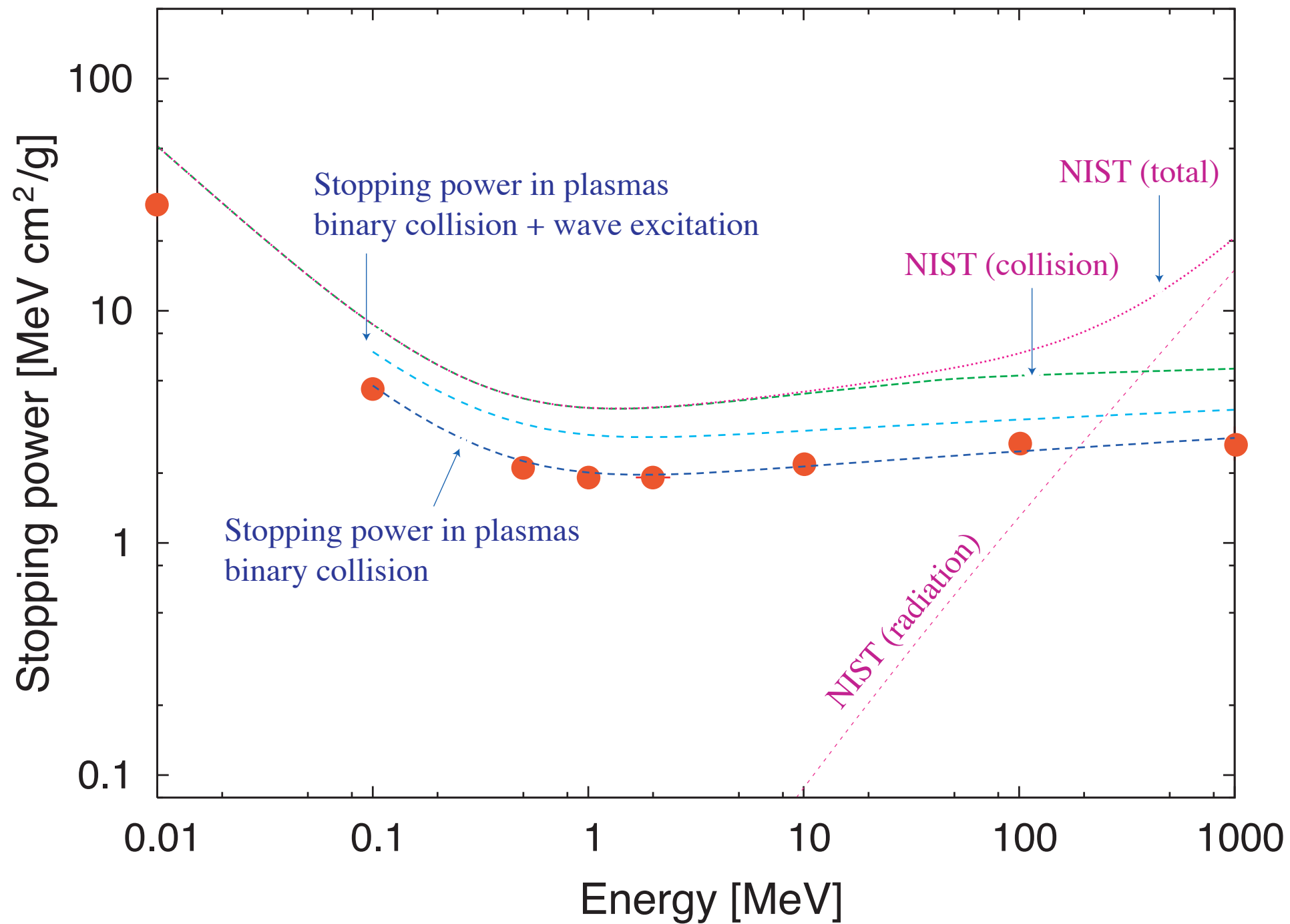


theory
(Lifshitz, 1981)

$$\frac{d(E_i / E_e)}{dt} = \frac{8\pi z^2 e^4 nL}{Mm_e c^3 (\gamma - 1)}$$

Electron stopping power in hydrogen plasma

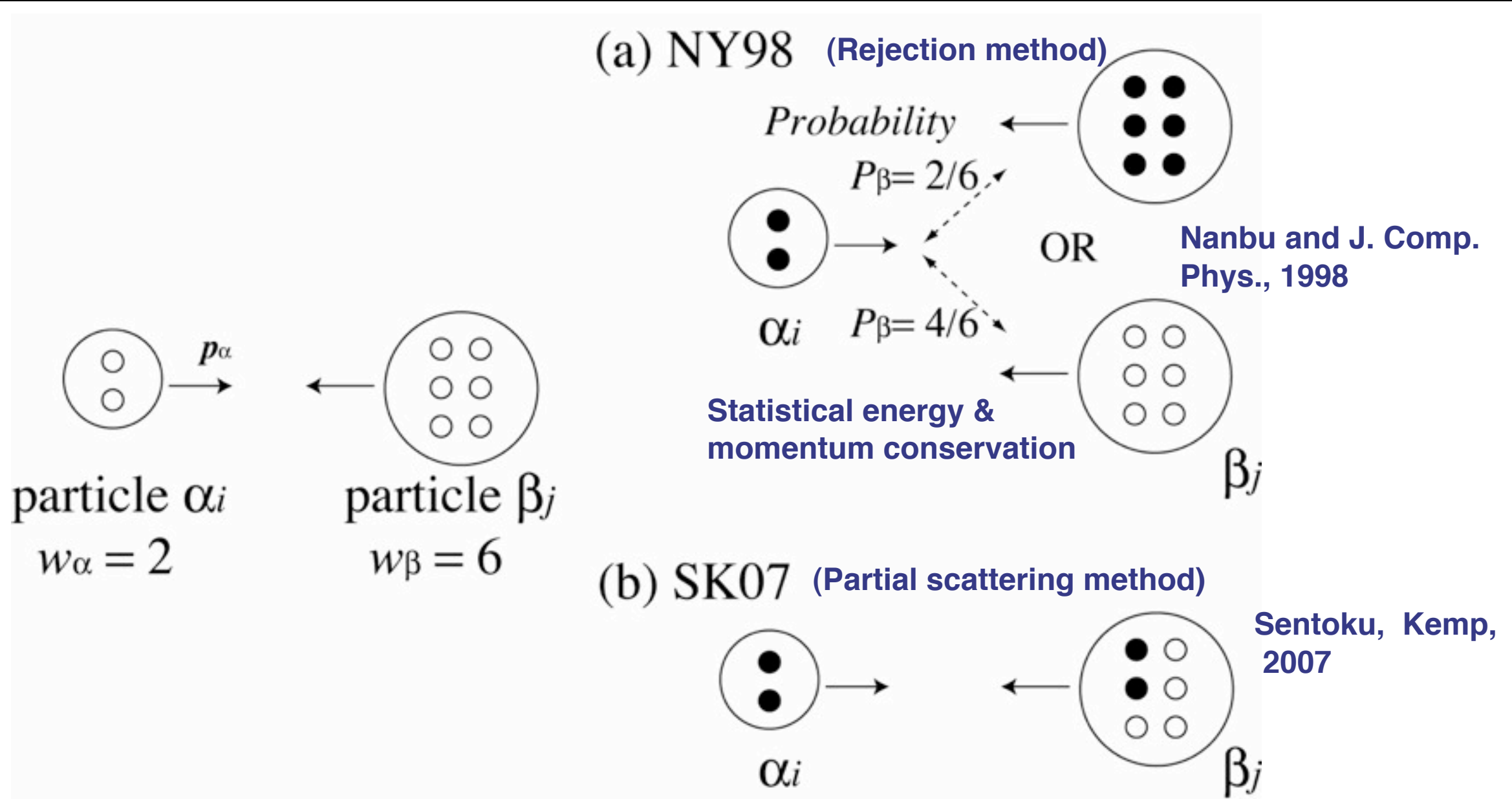
- test simulation of e-e collision -



NIST database: electron stopping power in hydrogen gas

Collision model of weighted particles in PICLS

- Rejection method & Partial scattering method -



particle β energy

$$\epsilon_{\beta}^{\text{after}} = \epsilon_{\beta}^{\text{before}} \cdot (1 - P_{\beta}) + \epsilon_{\beta}^{\text{scattered}} \cdot P_{\beta},$$

particle β momentum

$$\mathbf{p}_{\beta}^{\text{after}} = \mathbf{p}_{\beta}^{\text{before}} \cdot (1 - P_{\beta}) + \mathbf{p}_{\beta}^{\text{scattered}} \cdot P_{\beta}.$$

$$\mathbf{p}_{\beta}^{\text{final}} = \mathbf{p}_{\beta}^{\text{after}} + \Delta \mathbf{p}_{\beta \perp}. \quad \Delta \mathbf{p}_{\beta \perp}: \text{random vector}$$

Scale up momentum to conserve energy by adding a random vector.
Perfect energy conservation & statistical momentum conservation

Beam relaxation: benchmark of weighted particle collision model

Bulk e- 90%

Beam e- 10% with $p_{\text{drift}}=0.7m_e c$

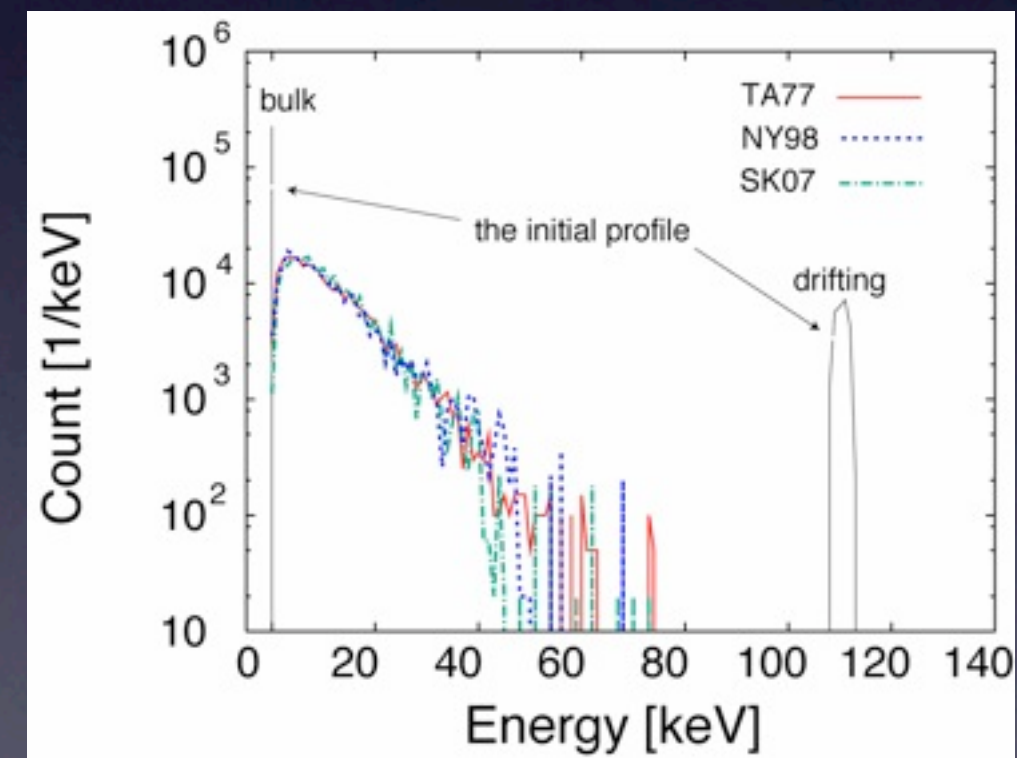
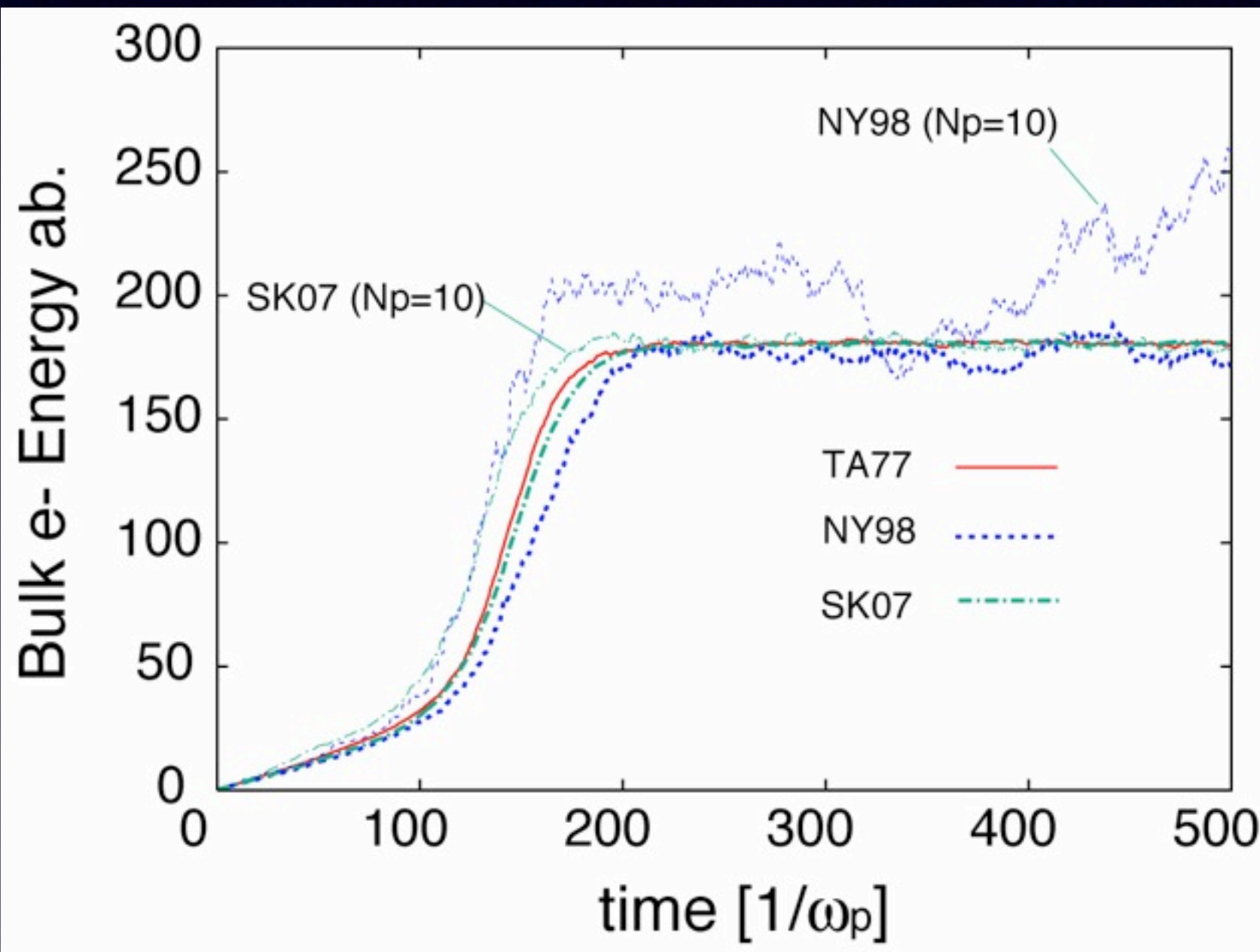
$n=10^{25} \text{ 1/cm}^3$

e-e collision

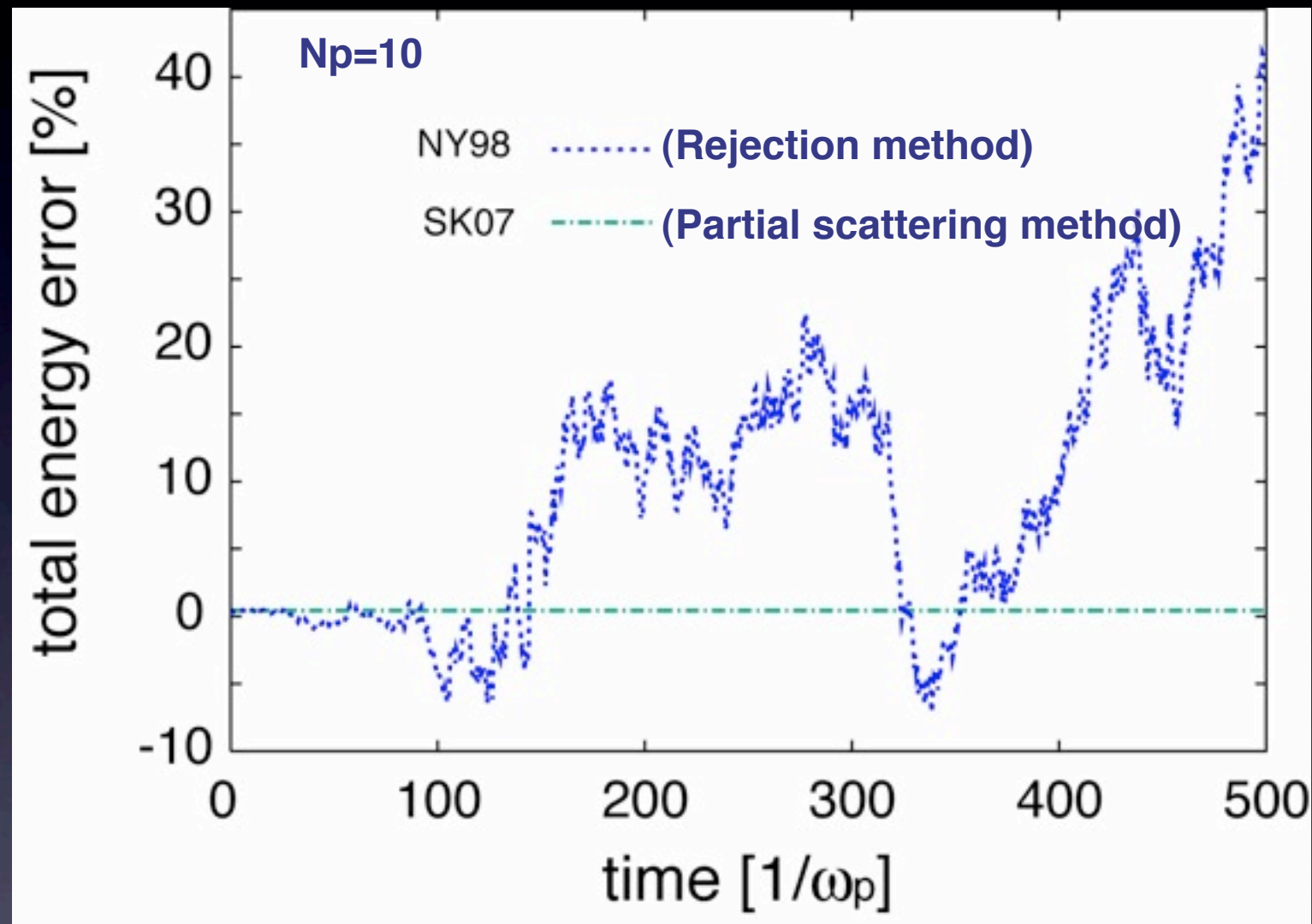
case A (TA77): uniform weighted particle, 500/cell (bulk 450, beam 50)

case B (NY98): weighted 250/cell (bulk 125, beam 125)

case C (SK07): weighted 250/cell (bulk 125, beam 125)



Rejection method has serious energy violation with small number of particle



Partial scattering method has a perfect energy conservation with small particles.

ionization

Field ionization

Collisional ionization (equilibrium model)

Collision for partially ionized plasmas

Field ionization in PICLS

- Tunneling ionization model -

Ionization Rate

(Landau and Lifshitz, Quantum Mechanics)

$$W[E(t)] = 4\omega_a \left(\frac{\varepsilon_i}{\varepsilon_h} \right)^{5/2} \frac{E_a}{E(t)} \exp \left[-\frac{2}{3} \left(\frac{\varepsilon_i}{\varepsilon_h} \right)^{3/2} \frac{E_a}{E(t)} \right]$$

ε_i : ionization potential

ε_h : potential of hydrogen (13.6eV)

$$\omega_a = \frac{m_e e^4}{\hbar^3} \quad E_a = \frac{m^2 e^5}{\hbar^4}$$

- We use the ADK formula to calculate the ionization rate $W(E)$. Ionization probability $R=1-\exp[-W(E)\Delta t]$, E is the electric field.
- Condition of ionization: $R >$ random number [0-1].
- The new electron has the same weight and position as the ionized ion. It is created with no momentum.

— [

Field calculation

— [

Field ionization and calculation of the ionization current

— [

Particle movement

— [

Current calculation

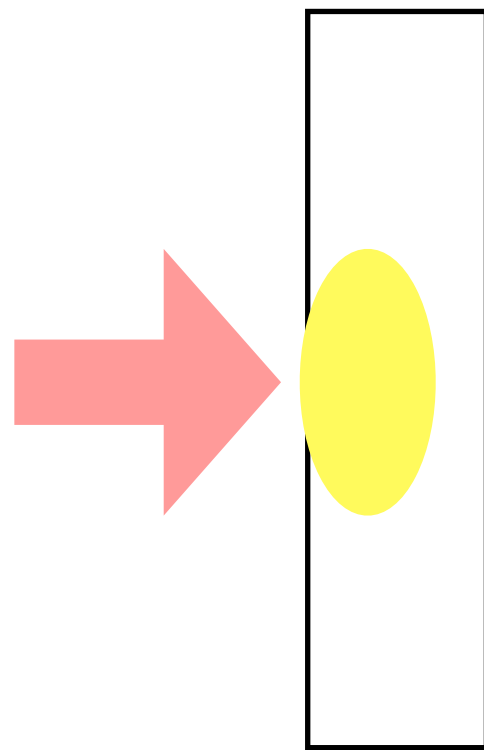
$$j_{ion}^{(i)} = \frac{U_p^{eV}}{|E_{norm}|^2 \Delta t} E^{(i)}$$

Ionization current

S. Kato, Y. Kishimoto, and J. Koga, Phys. Plasmas 5, 292 (1998).

Ionization model in PICLS

- Thomas Fermi model (equilibrium model) -

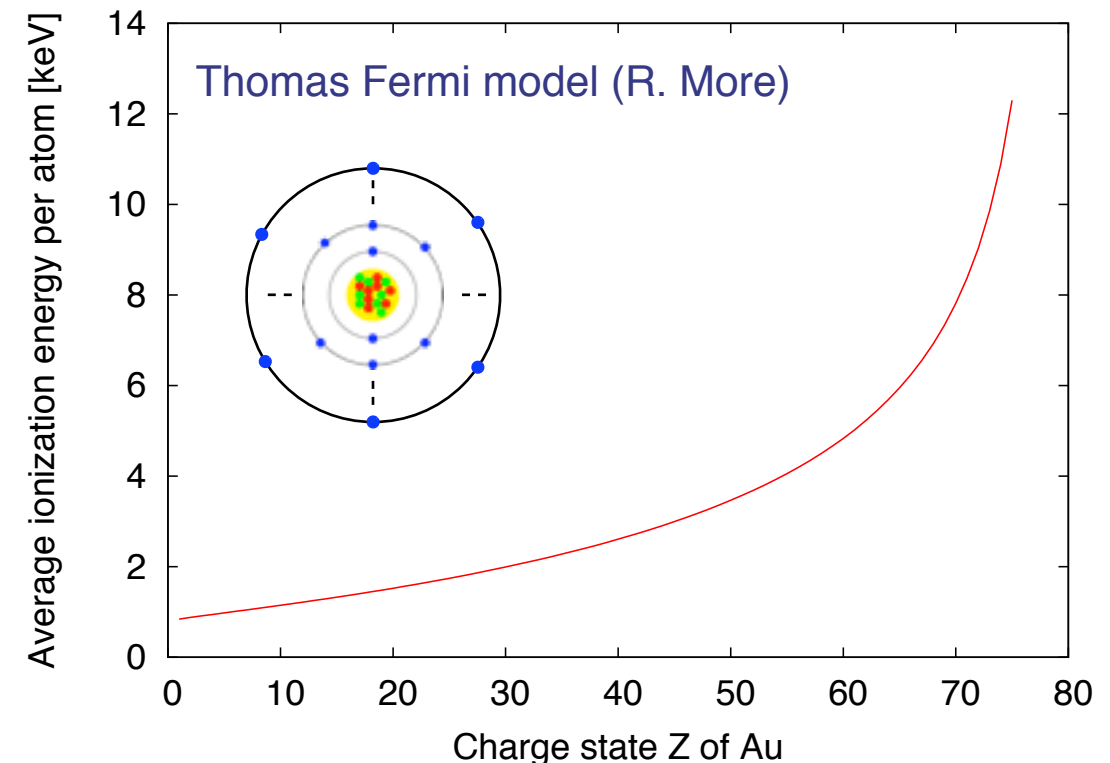
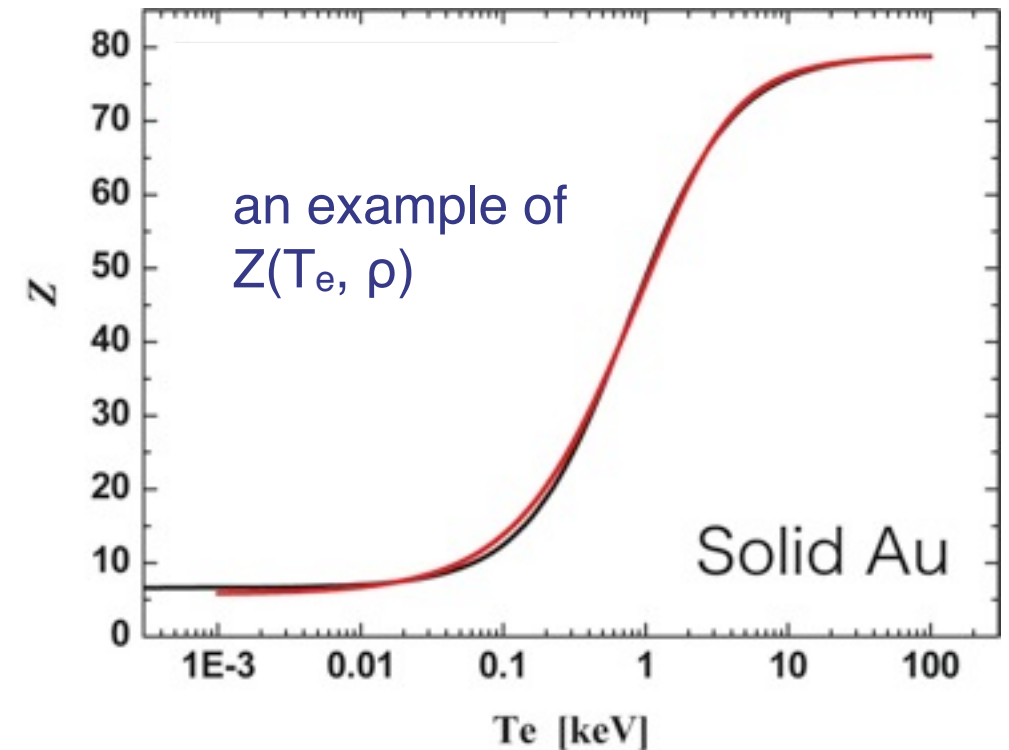


Bulk electrons are heated up by hot electrons via collisional or collective processes.

The heating is calculated by the collisional PIC.

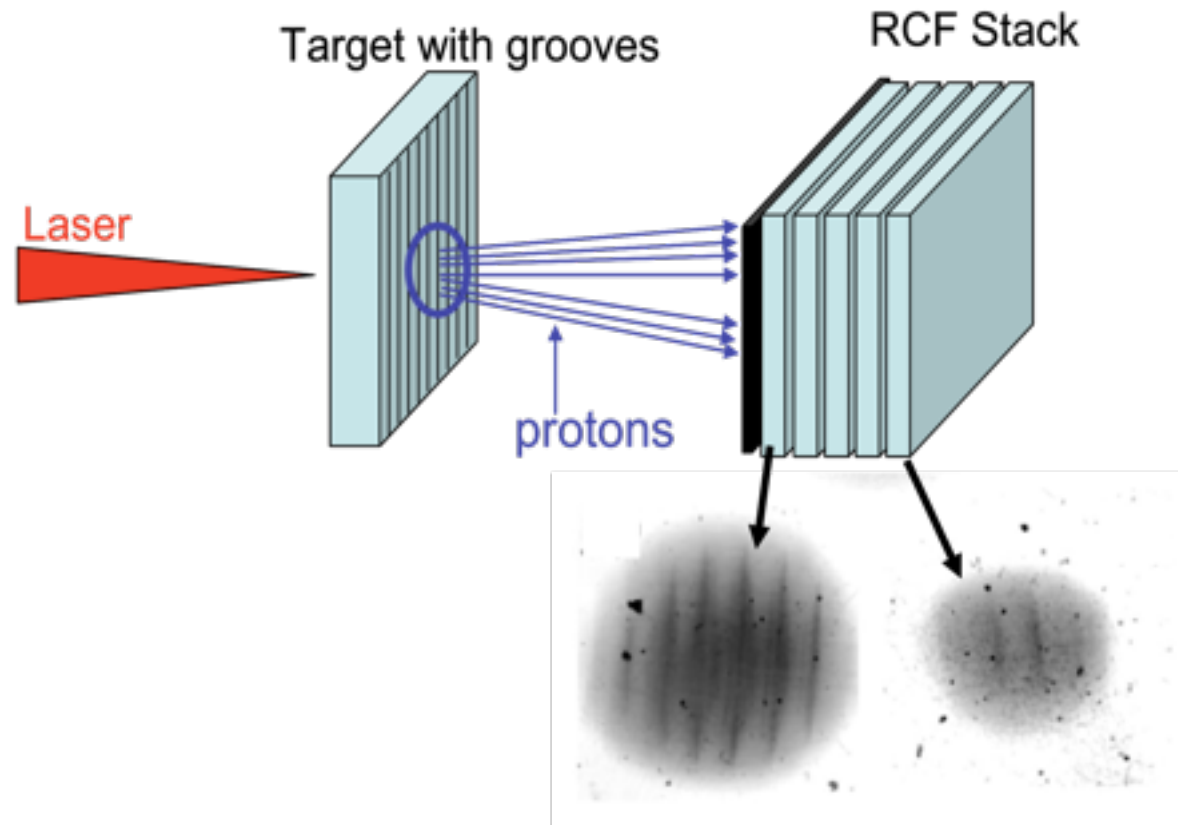
1) Average charge state is calculated as function of bulk electron temperature T_e and local mass density ρ . The function $Z(T_e, \rho)$ is obtained by fitting the EOS database.

2) After the ionization is done, new electrons are born, and the bulk electrons will lose the ionization energy (by shrinking momenta to conserve energy).



The field ionization is also implemented for the insulator target.

Proton Image as result of MA current transport in Al, Cu, and Au targets



- What makes a modulated transport?**
- 1. instabilities at the interface?**
 - 2. modulation inside target?**
 - 3. instabilities at the vacuum interface**

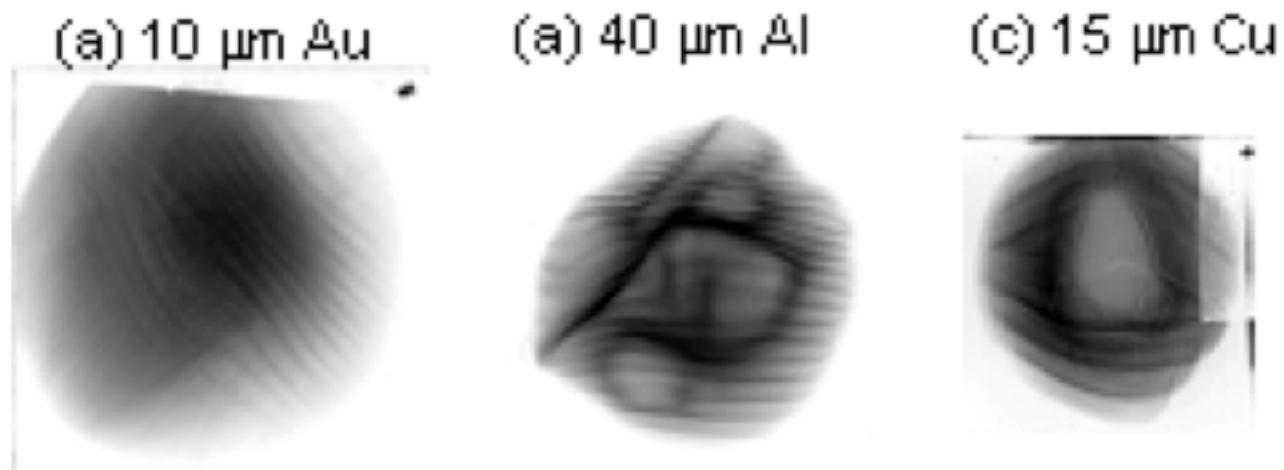
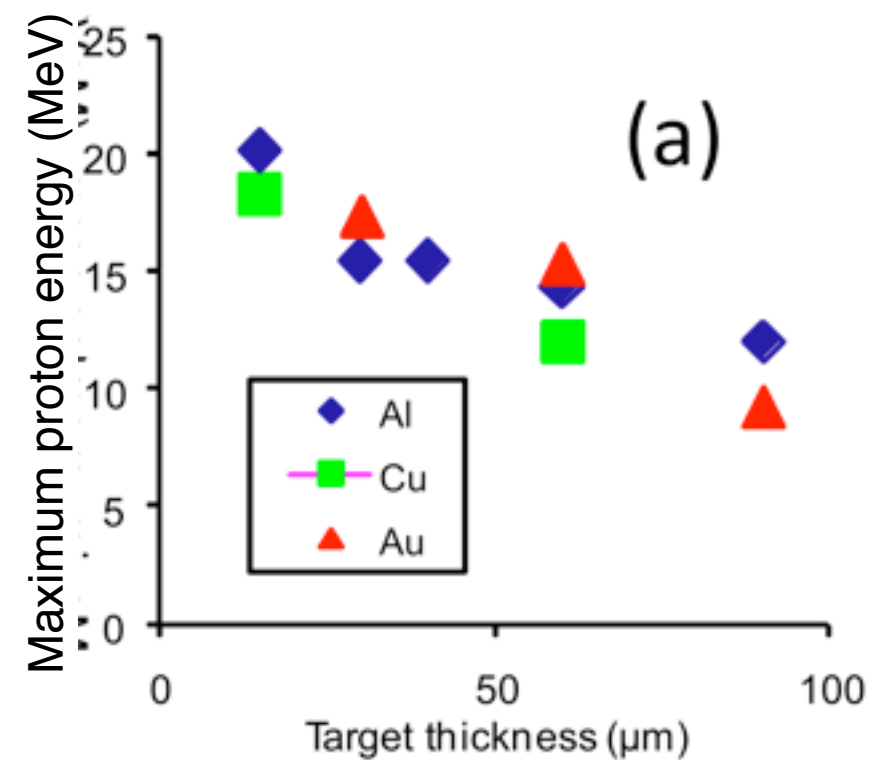
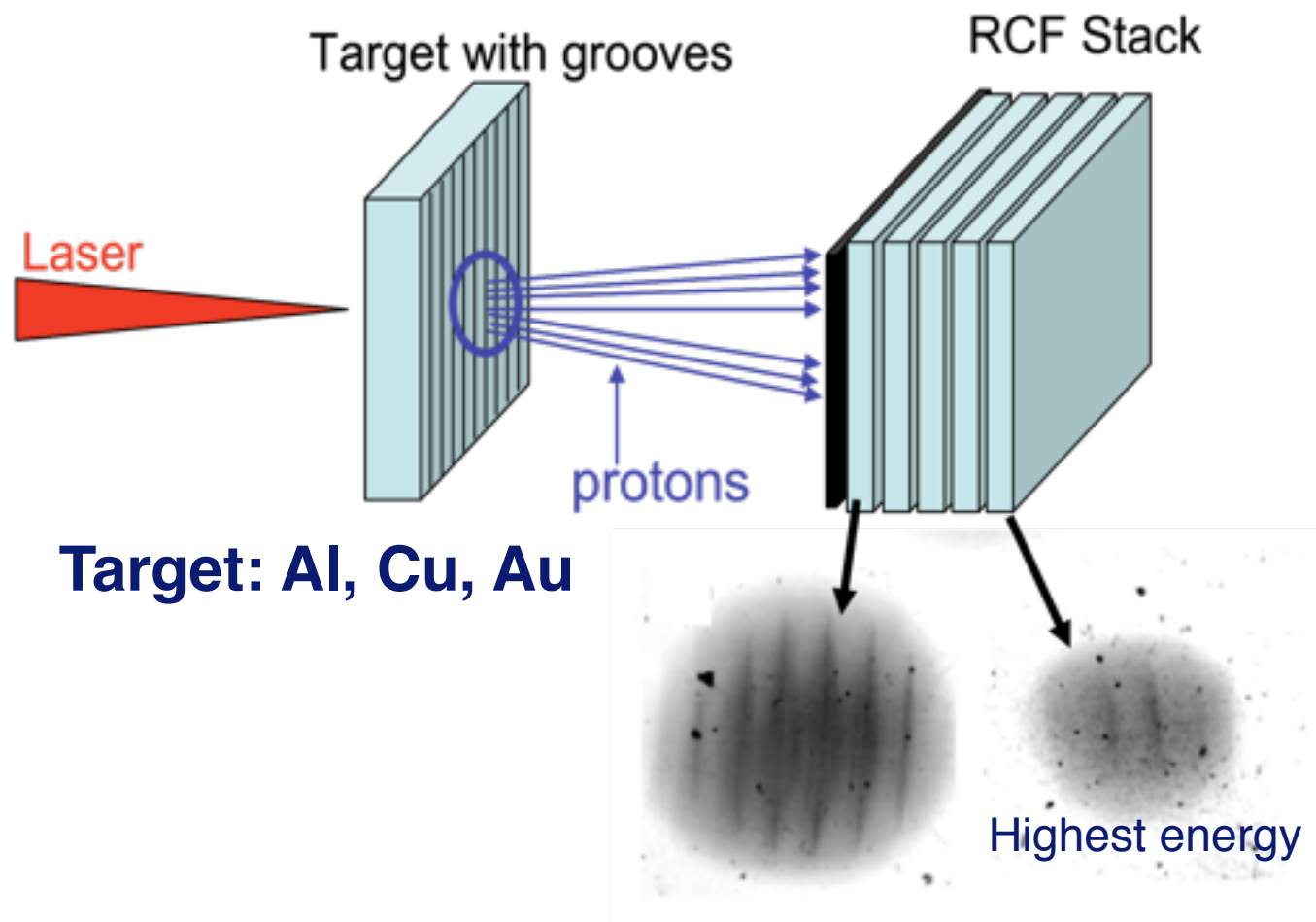


Figure:
Proton angular distributions at 6 MeV
for different target materials, Au, Al Cu.
by J. Fuchs, LULI

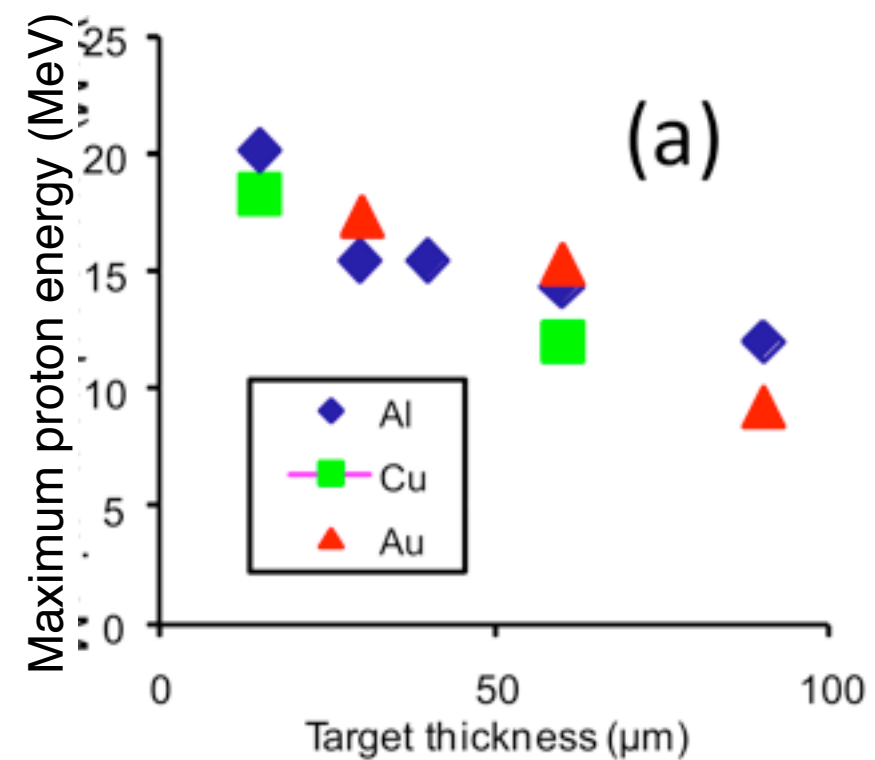
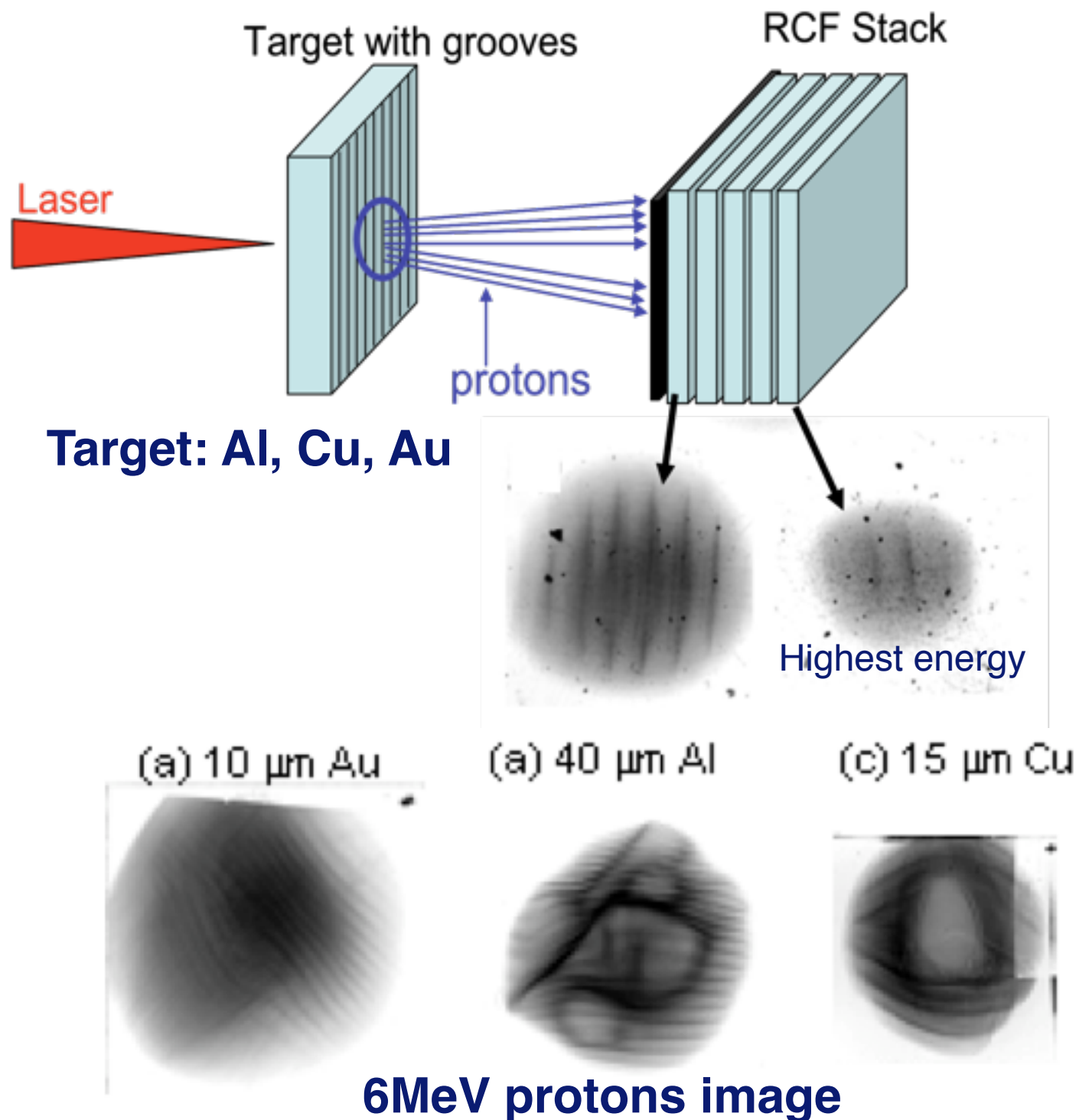
LULI Experiment

Laser: $I=6 \times 10^{19} \text{ W/cm}^2$
 duration=350fs, spot=8 μm



LULI Experiment

Laser: $I=6 \times 10^{19} \text{ W/cm}^2$
 duration=350fs, spot=8 μm



Benchmark 2D Code with Collision&Ionization

- MA current transport in Al, Cu, and Au targets-



PICLS2d

Ionization: Thomas-Fermi model

Collision : Relativistic binary collision

Laser: $I=6 \times 10^{19} \text{ W/cm}^2$ (P-pol, $\lambda=1 \mu\text{m}$)
 duration=350fs, spot=8 μm **LULI Laser**

Target:

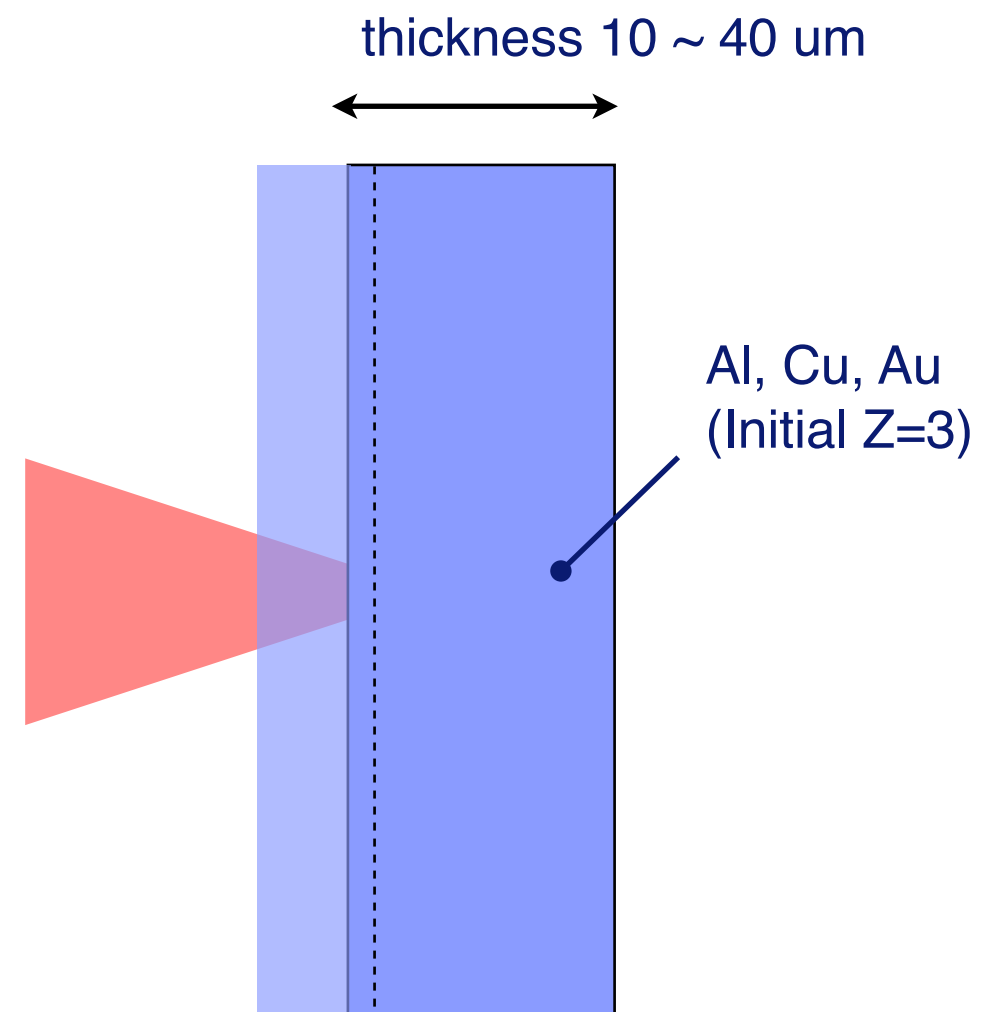
Al, Cu, Au thin foil (Initial $Z=3$)
 + small pre-plasma

	mass,	Z	ion dens.	e- dens.
Au:	197 M_p	79	50 n_c	3950 n_c
Cu:	64 M_p	29	50 n_c	1450 n_c
Al :	27 M_p	13	50 n_c	650 n_c

n_c : critical density of 1 μm laser (10^{21} 1/cm^3)

Time step $\Delta t = \tau/50$, Grid size $\Delta x = \lambda/50$

Same parameters with the LULI experiment.



Resistive magnetic fields has two source terms



Resistive field

$$\frac{\partial \mathbf{B}}{\partial t} = -\nabla \times \mathbf{E}$$

$$\mathbf{E} = \eta \mathbf{J}$$

η : resistivity

$$\eta \propto \frac{Ze^2}{T^{3/2}}$$

$$\frac{\partial \mathbf{B}}{\partial t} = - \left(\underbrace{\eta \nabla \times \mathbf{J}}_{\text{Current term}} + \underbrace{\nabla \eta \times \mathbf{J}}_{\text{Resistivity term}} \right)$$

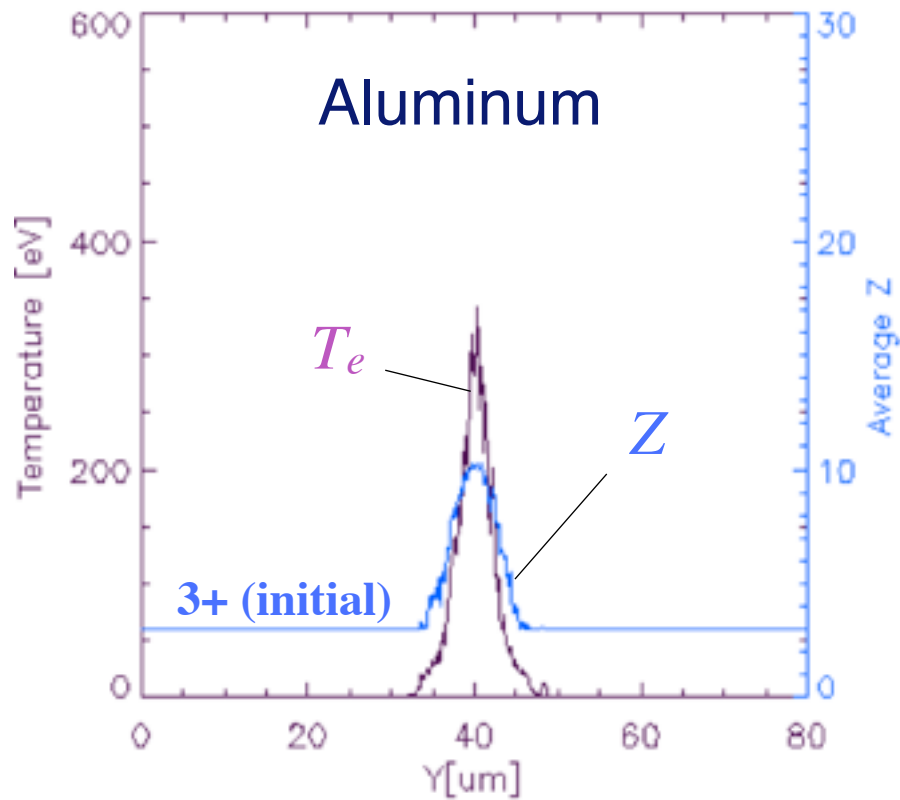
Current term

Resistivity term

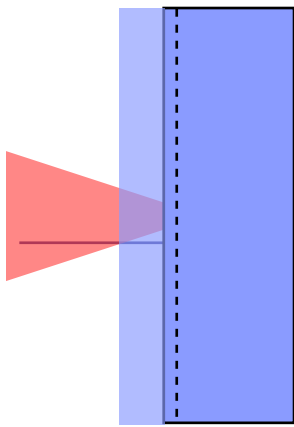
Resistivity term is a minor term in fixed Z case.

Resistivity evolution in ionizing target - competition between heating and cooling -

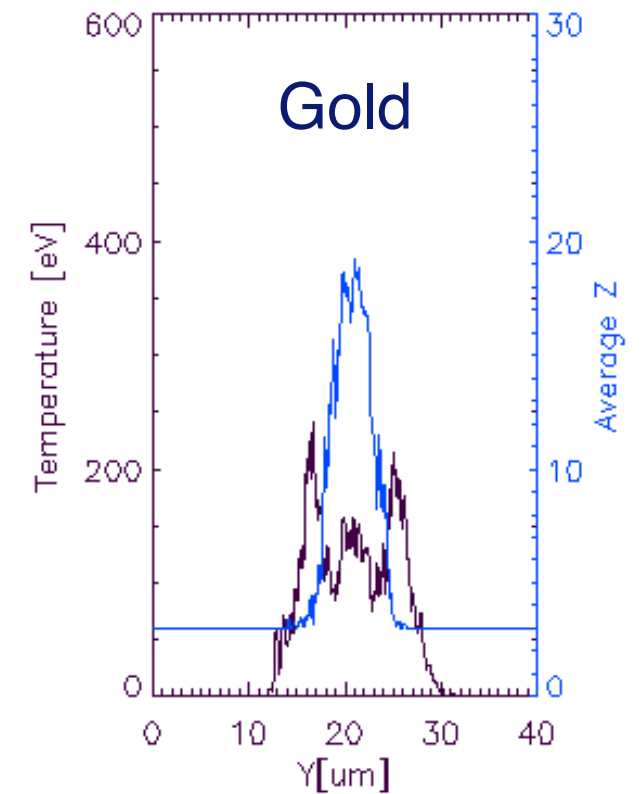
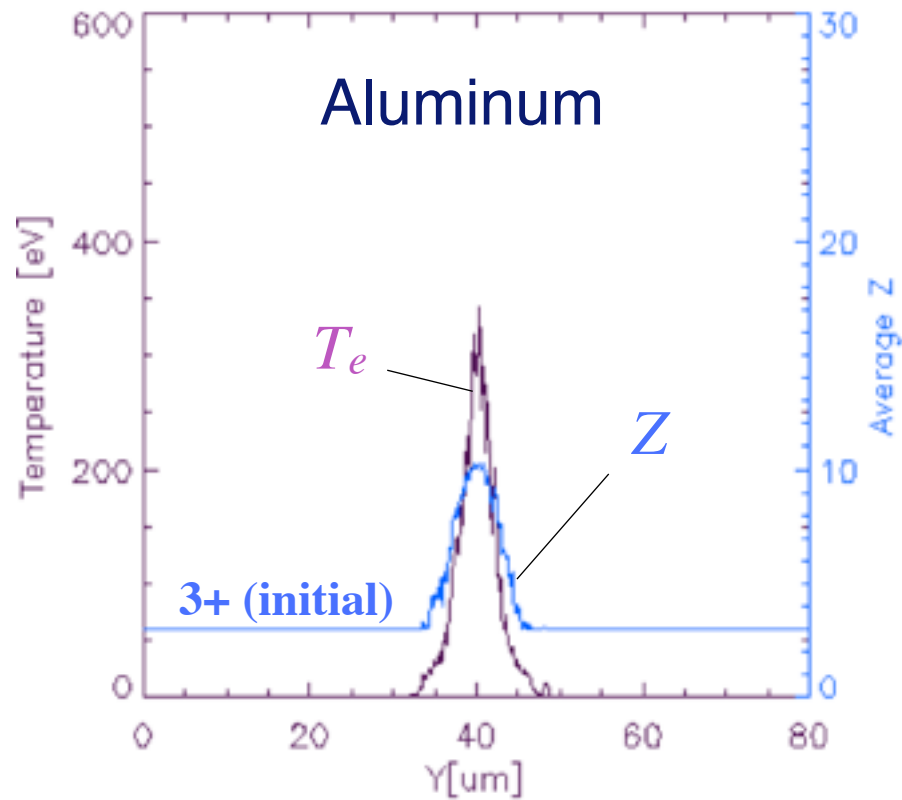
Temperature and average Z distribution inside 1um at t=80fs



Resistivity evolution in ionizing target - competition between heating and cooling -



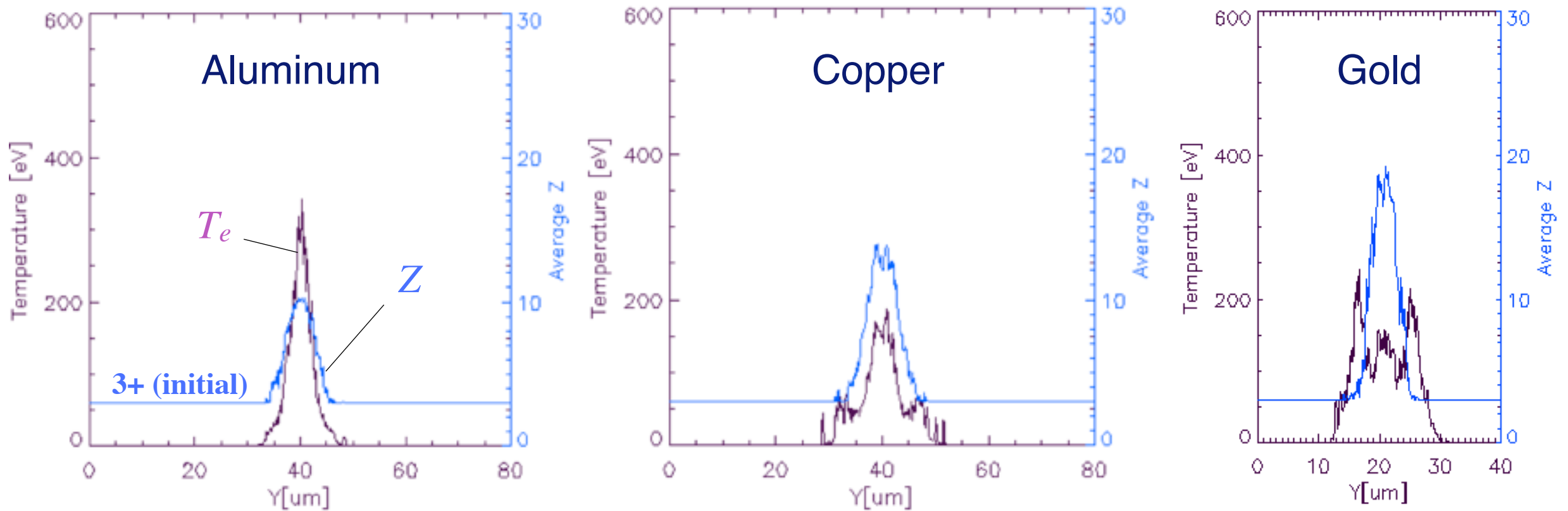
Temperature and average Z distribution inside 1um at t=80fs



ionization consumes
local energy

Resistivity evolution in ionizing target - competition between heating and cooling -

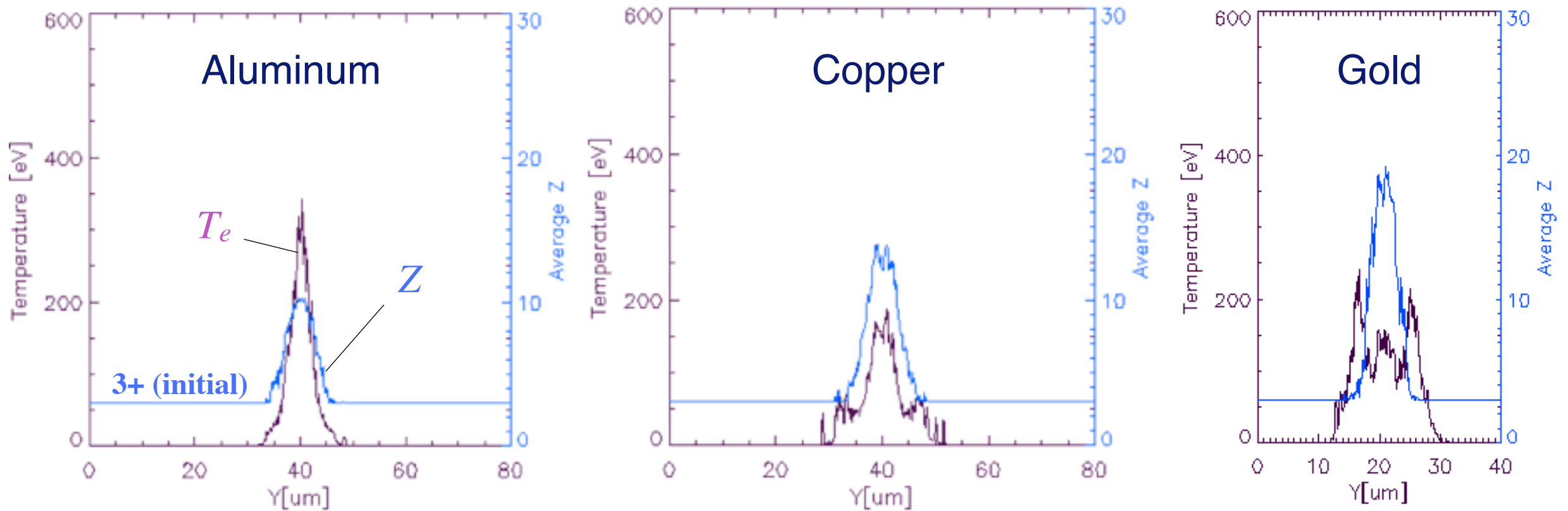
Temperature and average Z distribution inside 1 μ m at t=80fs



ionization consumes
local energy

Resistivity evolution in ionizing target - competition between heating and cooling -

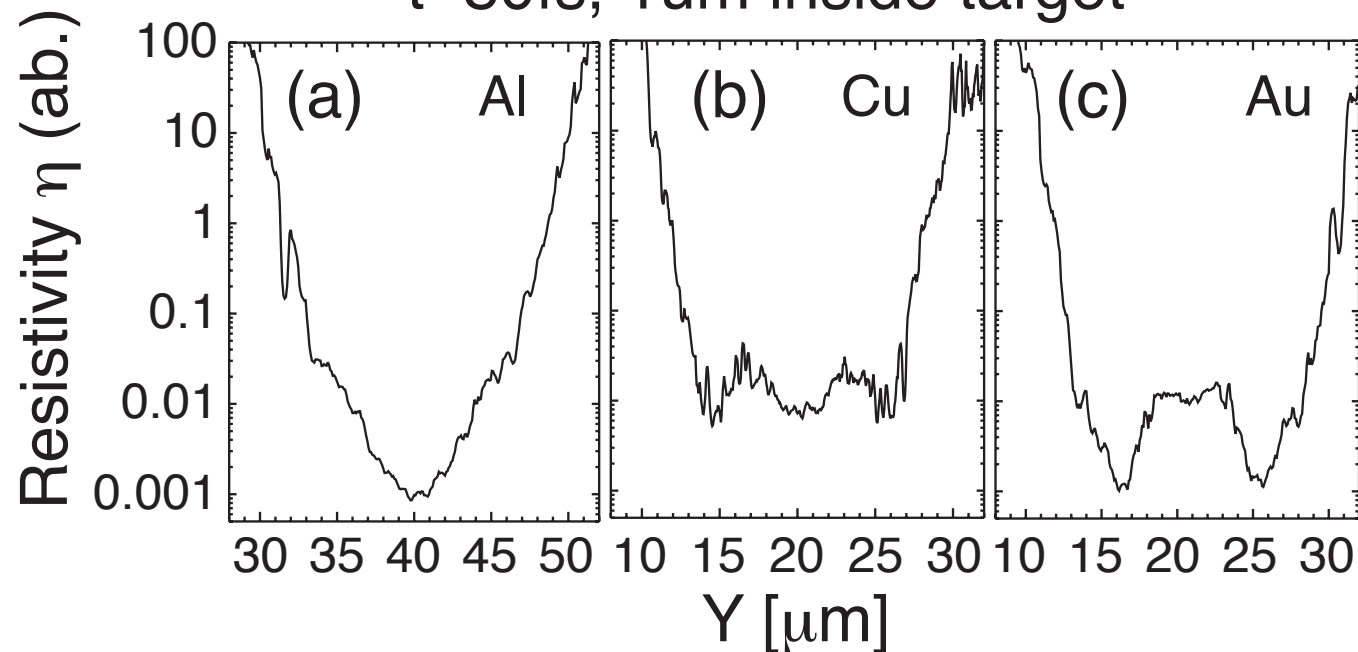
Temperature and average Z distribution inside 1μm at t=80fs



t~80fs, 1μm inside target

ionization consumes local energy

$$\eta \propto \frac{Ze^2}{T^{3/2}}$$



Resistive magnetic fields evolution in high Z target - competition between heating and cooling (ionization) -



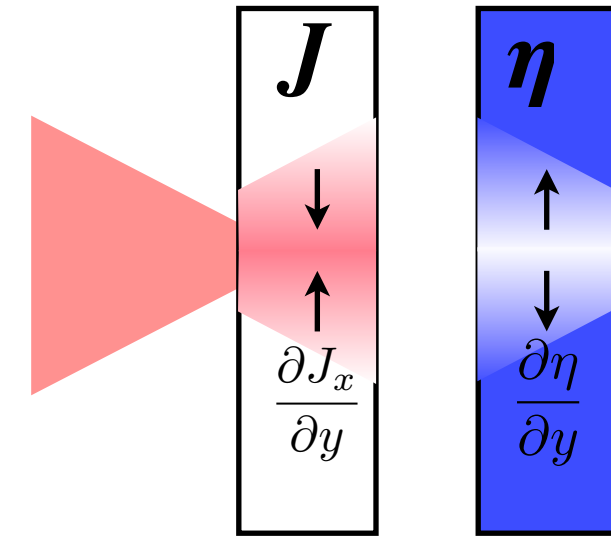
Resistive B-field (B_z)

$$\frac{\partial B_z}{\partial t} = \left(\eta \frac{\partial J_x}{\partial y} + \frac{\partial \eta}{\partial y} J_x \right)$$

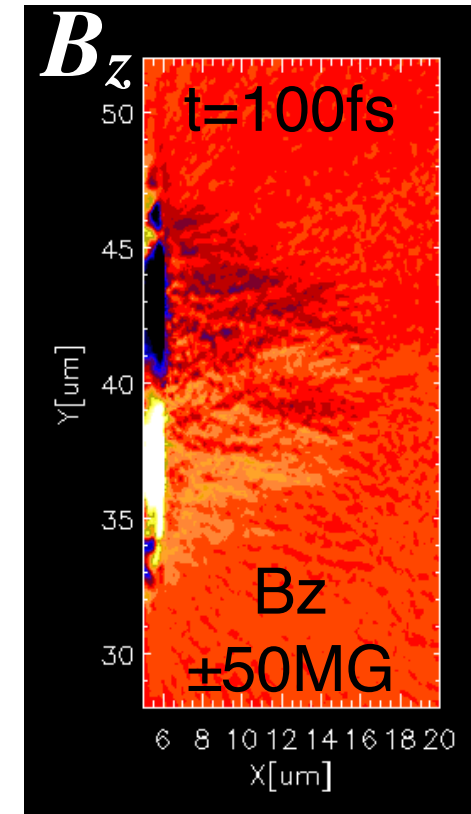
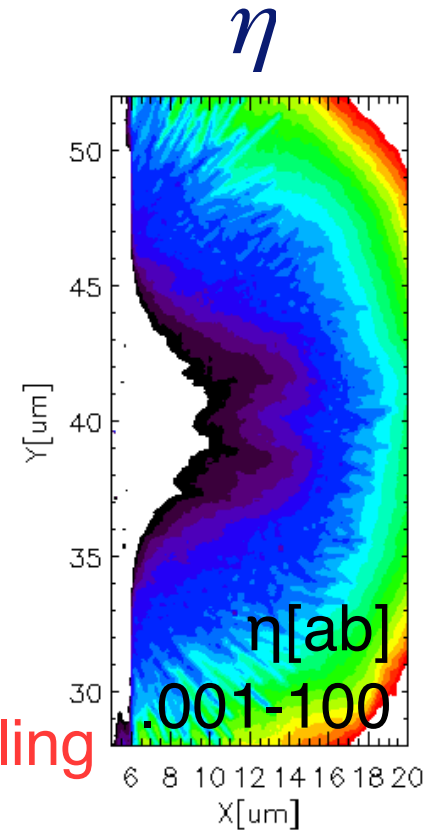
Aluminum

Resistivity

$$\eta \propto \frac{Ze^2}{T^{3/2}}$$



heating > ionization cooling



Current term
 $\nabla \times J$ dominant
(1st term)

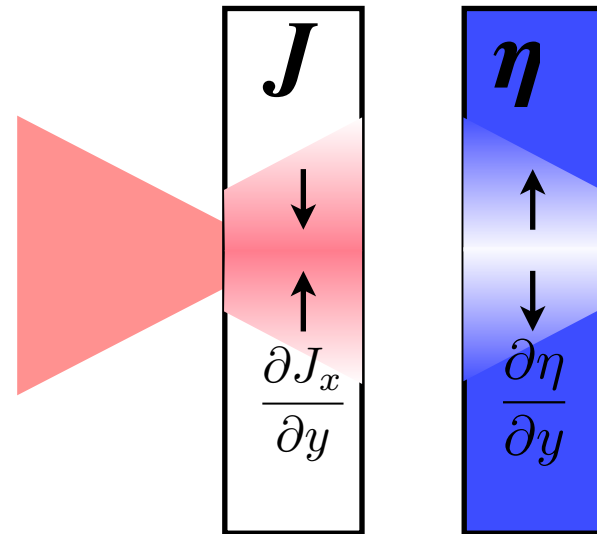
Resistive magnetic fields evolution in high Z target - competition between heating and cooling (ionization) -



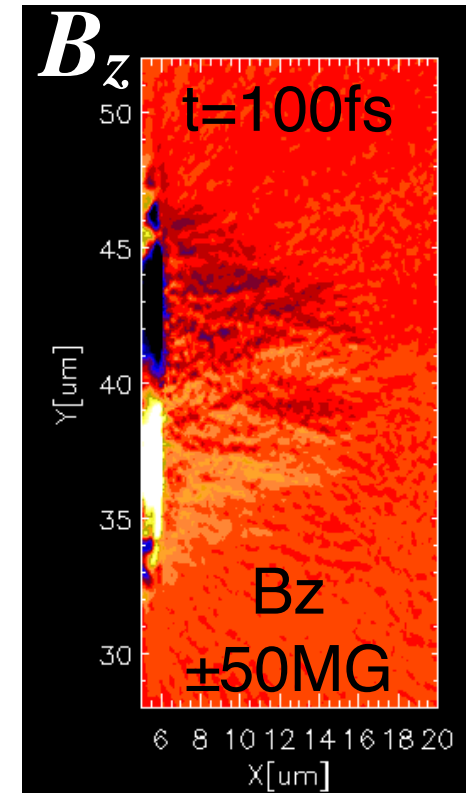
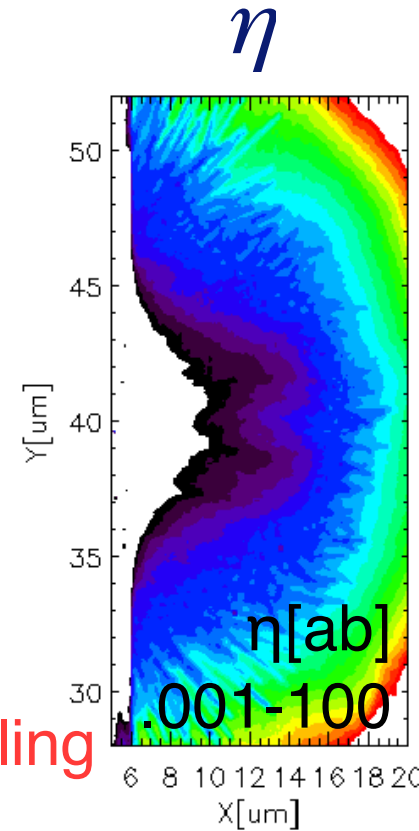
Resistive B-field (B_z)

$$\frac{\partial B_z}{\partial t} = \left(\eta \frac{\partial J_x}{\partial y} + \frac{\partial \eta}{\partial y} J_x \right)$$

Aluminum



heating > ionization cooling

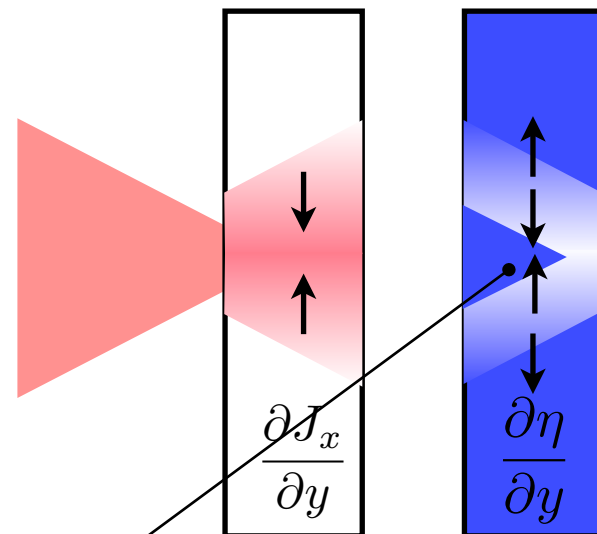


Current term
 $\nabla \times J$ dominant
(1st term)

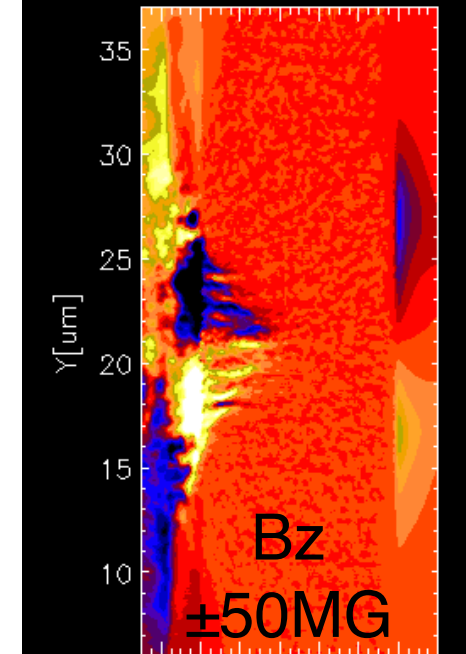
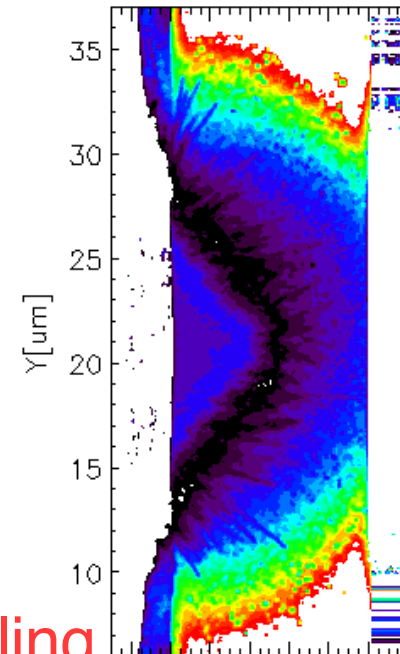
Resistivity

$$\eta \propto \frac{Ze^2}{T^{3/2}}$$

Gold



heating < ionization cooling



Resistivity term
 $\nabla \eta$ dominant
(2nd term)

Resistivity η drops by bulk heating, however η recovers in high Z target due to local cooling via ionization. Strong B fields grow in the ionization wave (slower than fast e-).

Ionization affects the resistivity inside target and excites 100MG resistive magnetic fields in Au & Cu

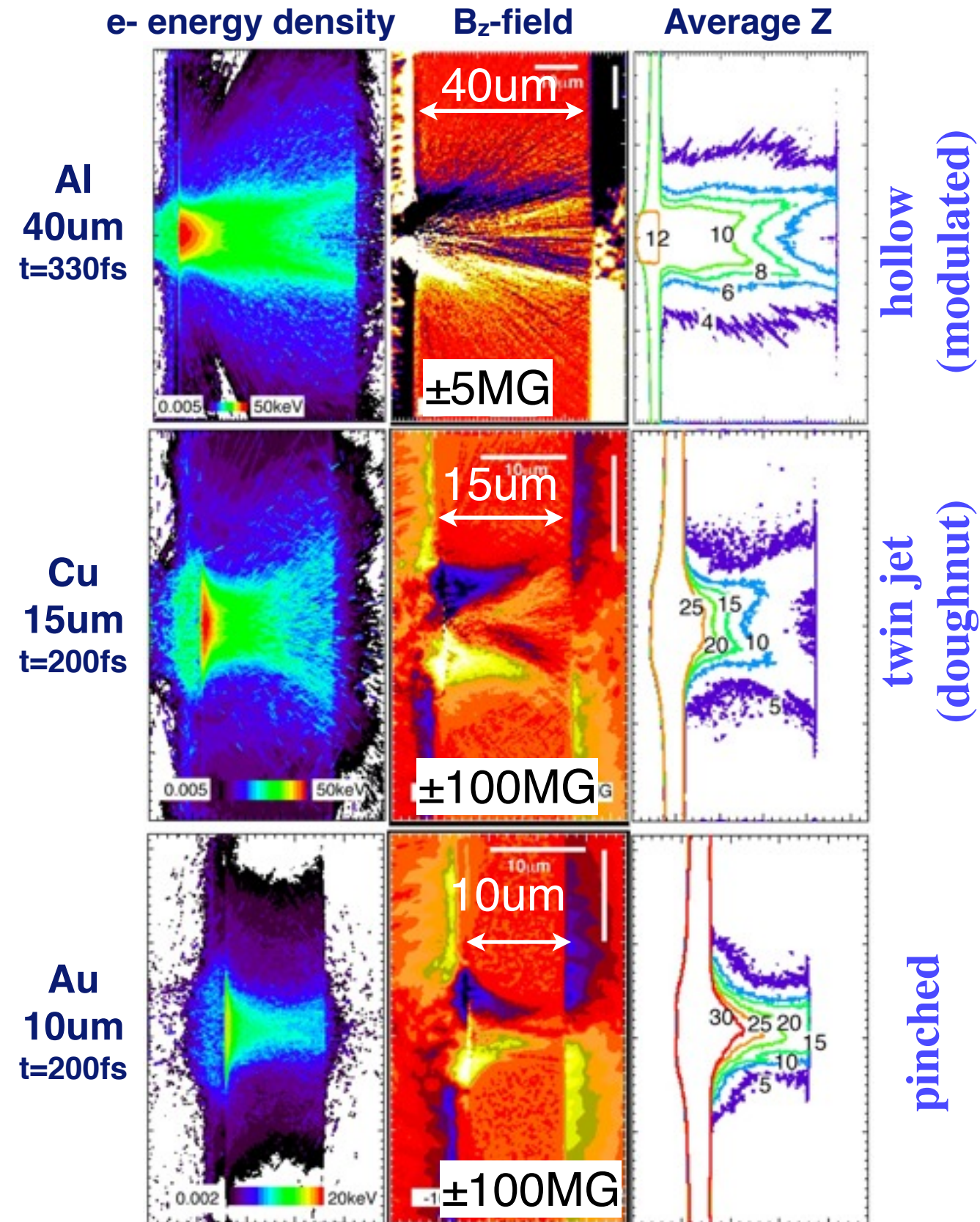


Resistive B-field

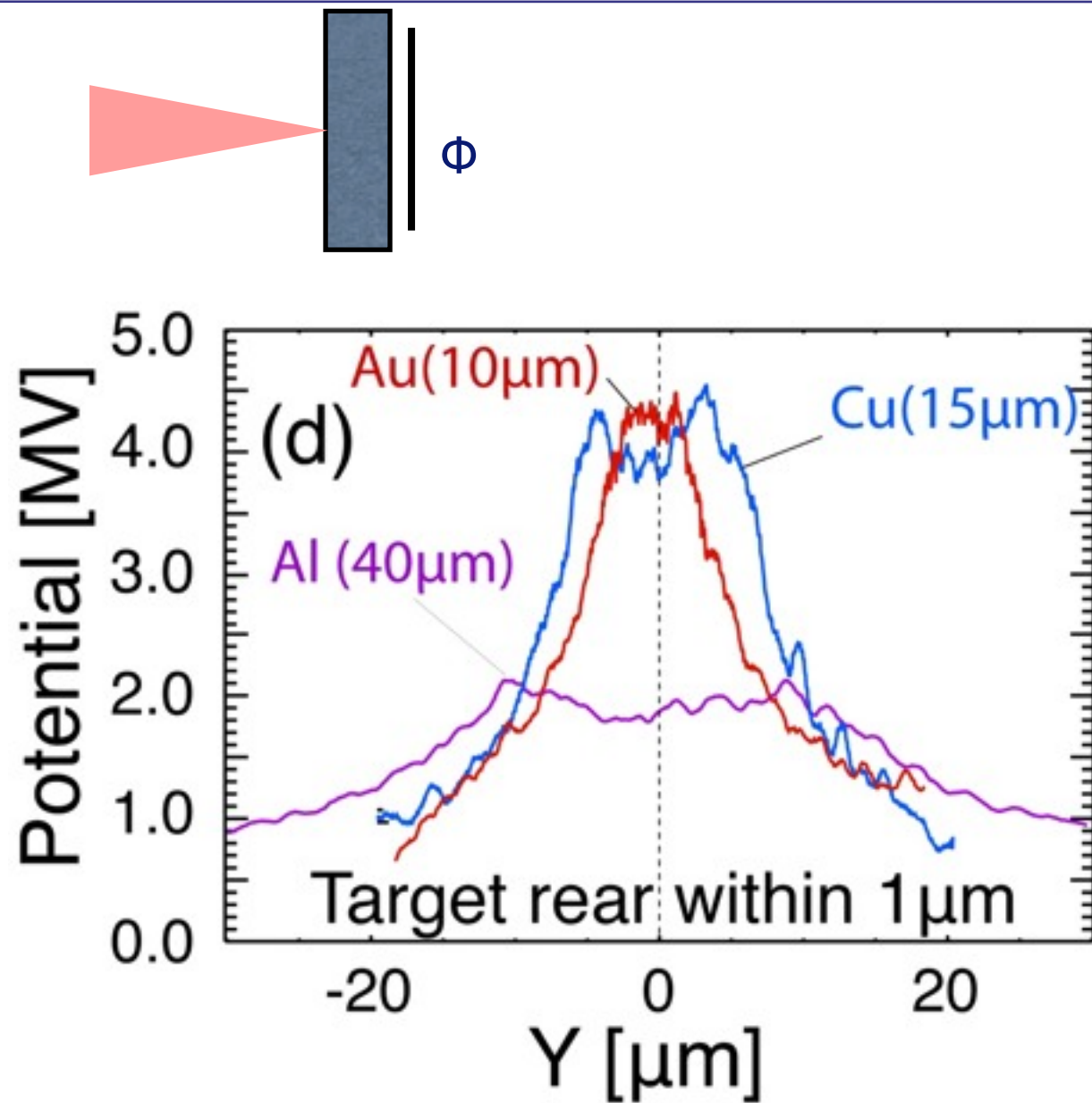
$$\frac{\partial \mathbf{B}}{\partial t} = -(\eta \nabla \times \mathbf{J} + \nabla \eta \times \mathbf{J})$$

- Al target: $\nabla \times \mathbf{J}$ term is dominant. Resistive magnetic fields is $\sim 5\text{MG}$. Modulated.
- Au target: $\nabla \eta$ term is dominant. Strong resistive magnetic fields $\sim 100\text{MG}$. Single channel.
- Cu target: η has a twin peak distribution. Strong resistive fields like gold, but twin channel (2D), would be hollow (3D) pattern.

The cyclotron frequency will become $\sim \omega_0$ (laser frequency) under 100MG B-field. The fine resolution of sub-micron, sub-femtosecond is required!



Pattern of sheath is consistent with the proton image observed in different material, Al, Cu, and Au in LULI exp.



Laser: $I=6 \times 10^{19} \text{ W/cm}^2$ (P-pol)
duration=350fs, spot=8 μm

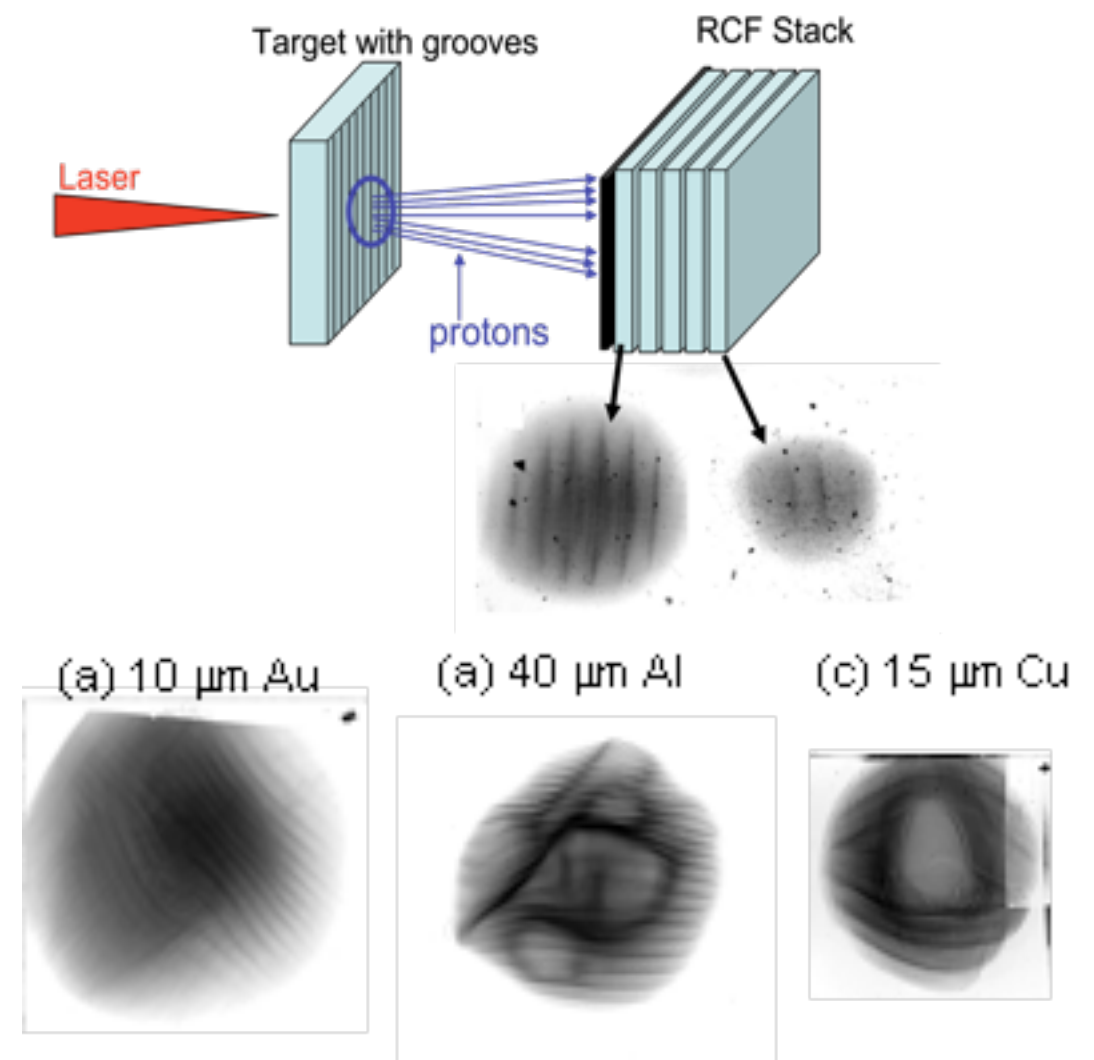


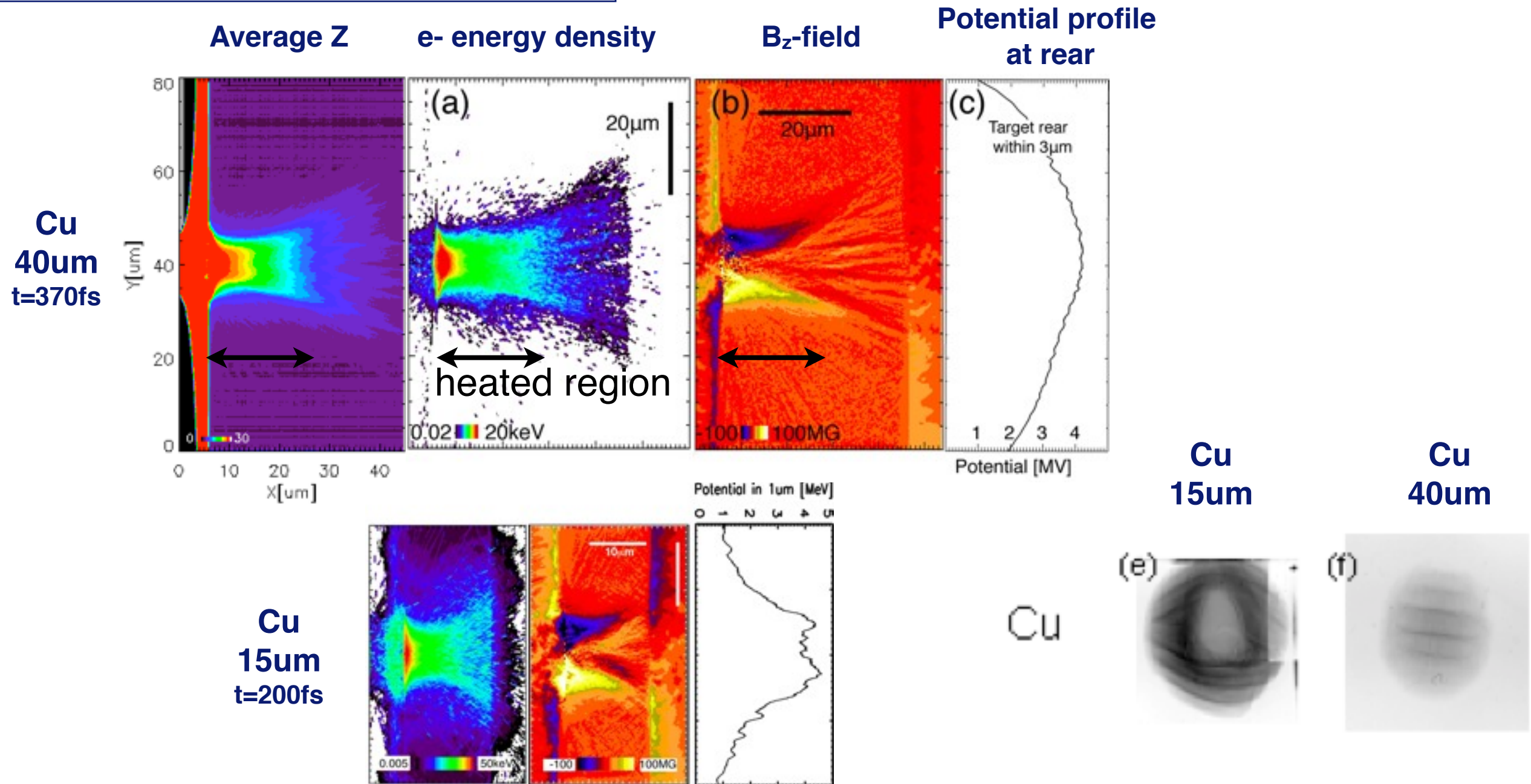
Fig. Electrostatic potential at the target rear in $1\mu\text{m}$. Plots observed at the time when the sheath potential has the maximum, and time-averaged during 100 fs.

Fig. 6MeV proton images from different material target.

Proton has a smooth image from thicker Cu target



**Laser: $I=6 \times 10^{19}$ W/cm² (P-pol)
duration=350fs, spot=8 μ m**



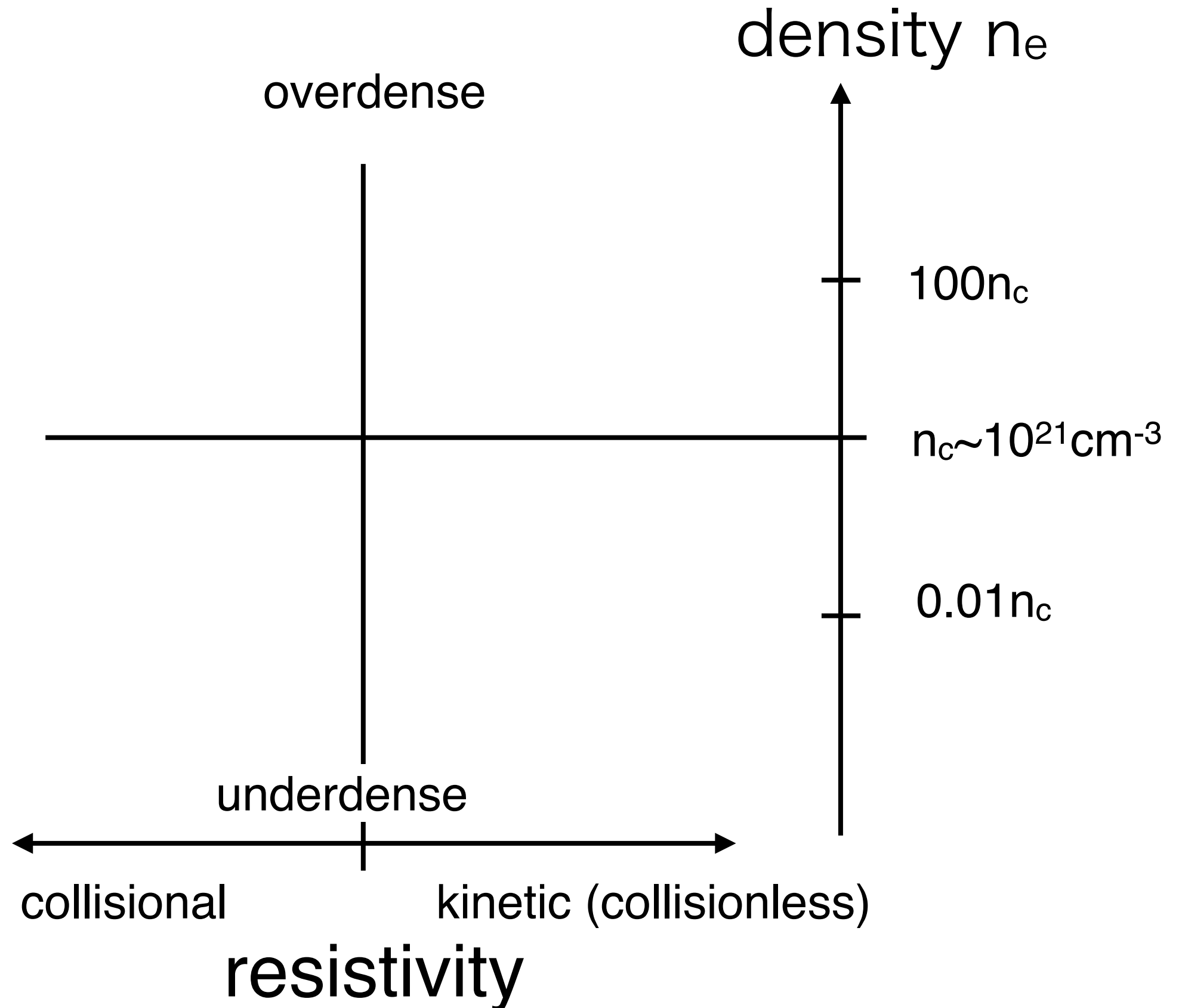
Ionization driven resistive magnetic fields extend only in the heated region (propagation speed $\sim 0.15c$, heat diffusion velocity). MeV electrons, which go beyond the strong B fields, are spraying and make a smooth potential at the target rear.

Summary

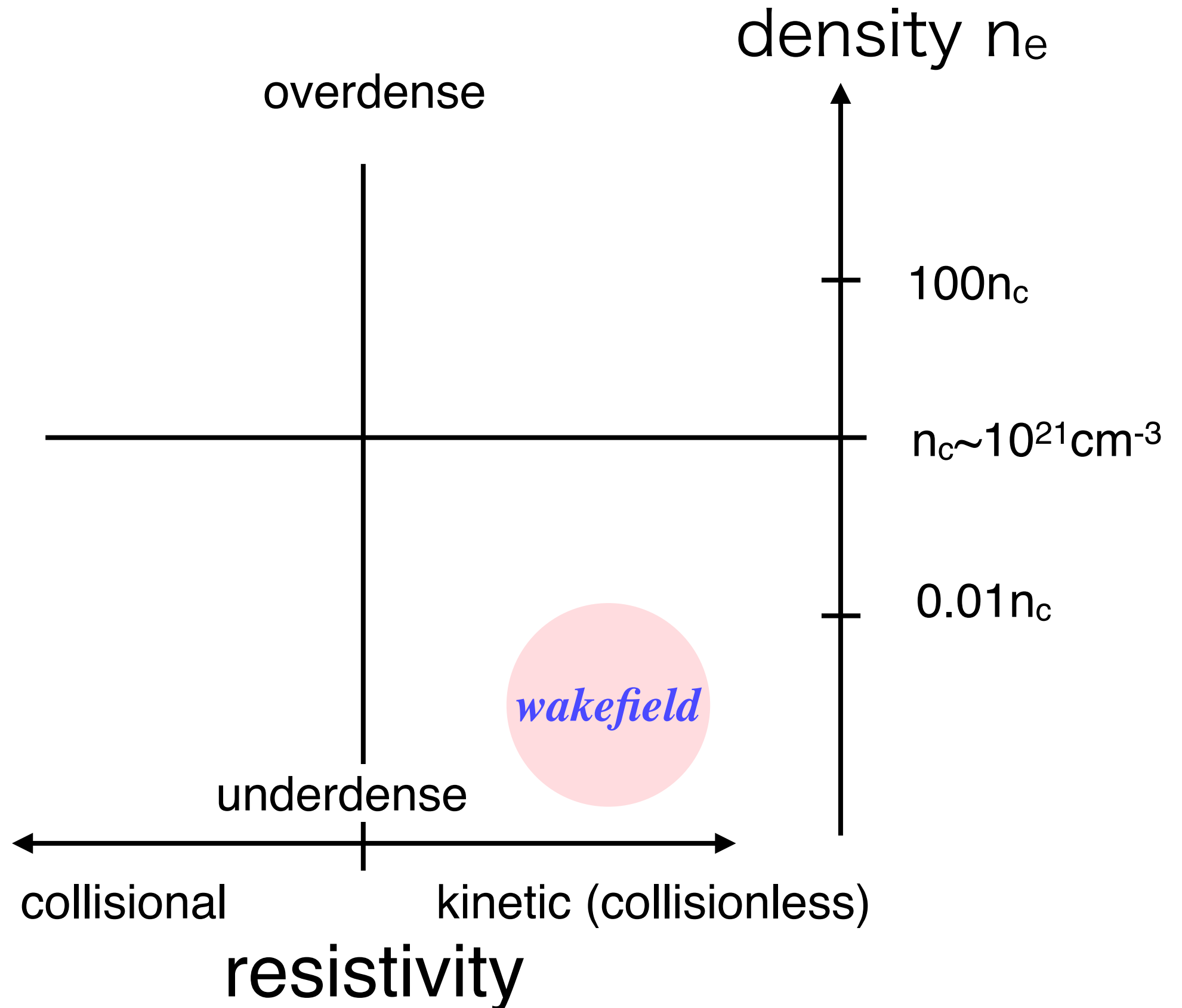


- We had studied the MA current transport in high conductive target by collisional/ionization PICLS code.
- We found that the current term ($\nabla \times \mathbf{J}$) is dominant in low Z target (Al) as a source term of resistive magnetic fields. While the resistivity term ($\nabla \eta$) plays an important role, and produces extremely strong B-fields (~ 0.1 gigagauss) in high Z target (Cu, Au). Important to include ionization in Cu&Au targets.
- The resistive magnetic field structure depends on the resistivity evolution in the heated region. The Cu target has a twin jets (hollow) structure, and the Au has a single channel under the current experiment/simulation conditions.
- Hot electron transport is affected by the strong resistive B fields, and it makes modulation in the sheath potential at target rear, which is recorded in the MeV proton image. PICLS shows a consistent potential profile with the proton images for Al, Cu, and Au targets.

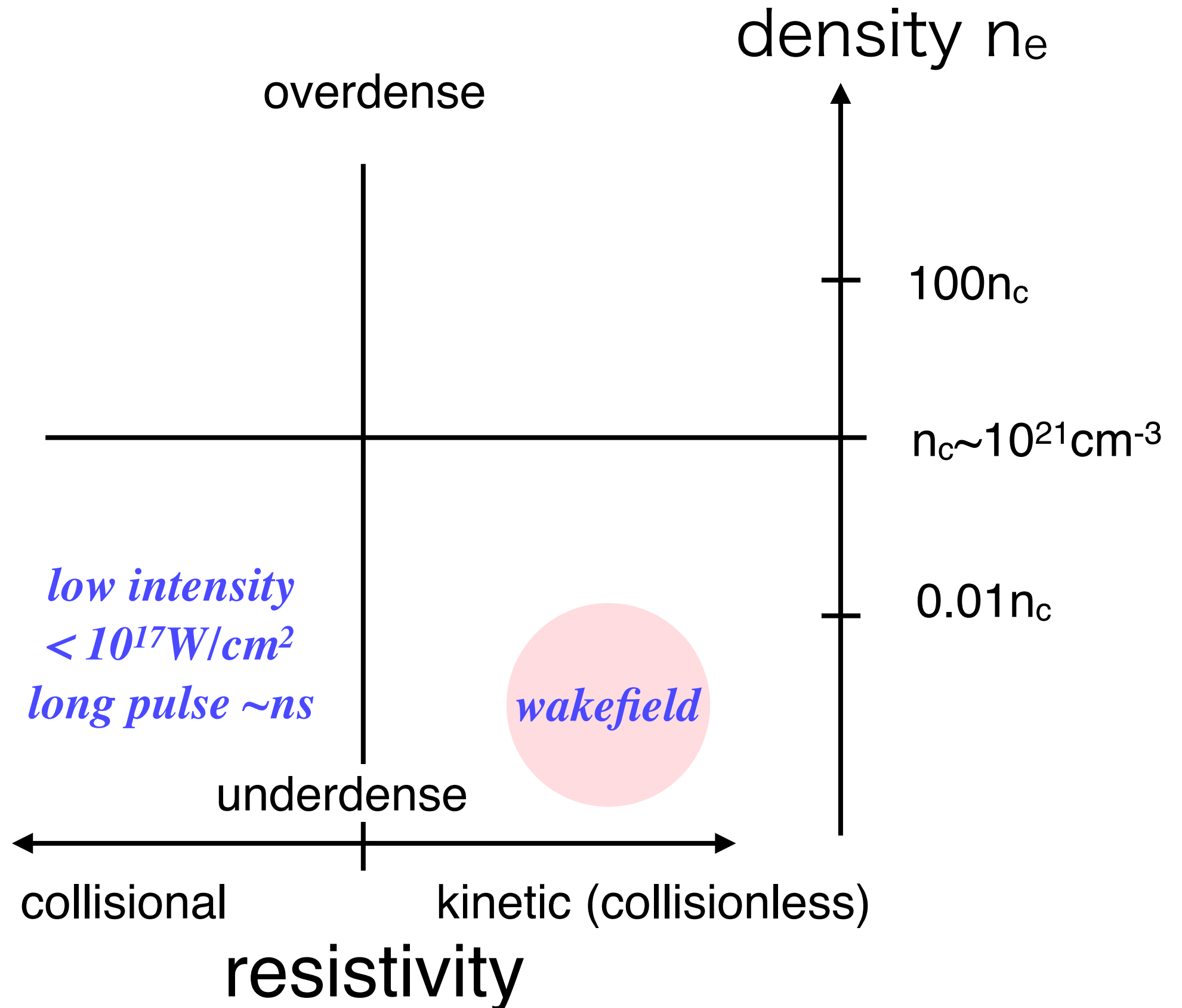
Is your plasma kinetic or collisional?



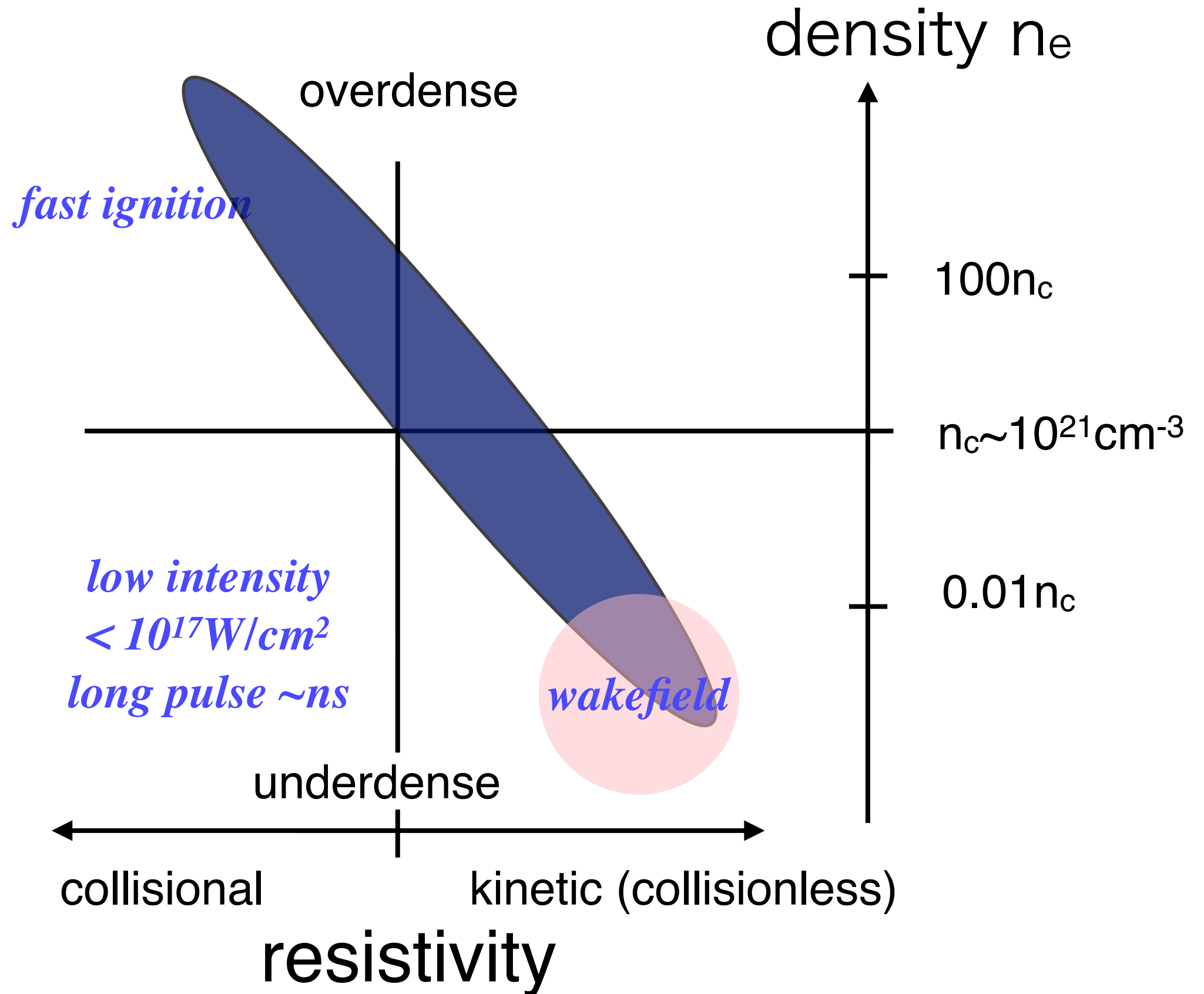
Is your plasma kinetic or collisional?



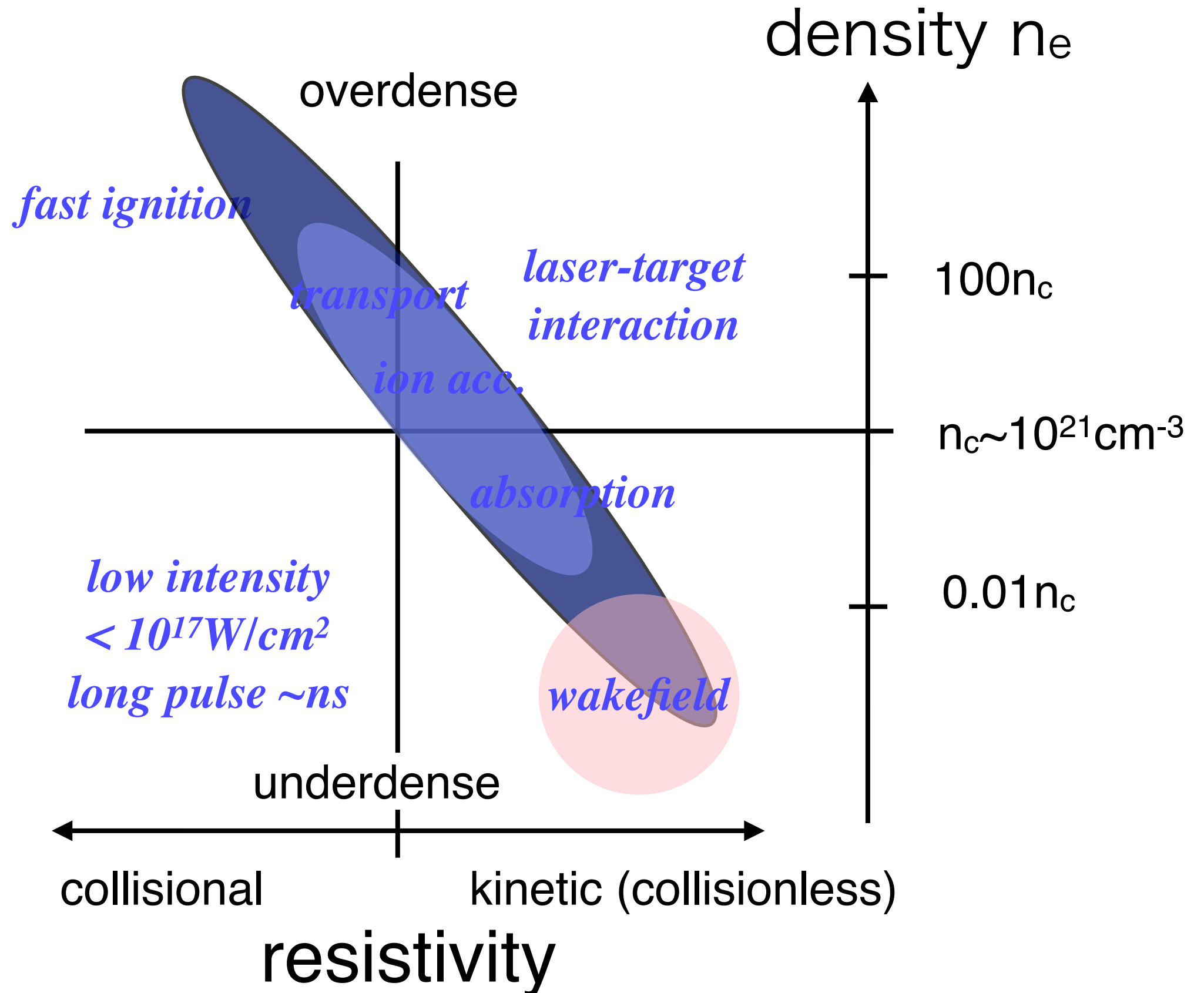
Is your plasma kinetic or collisional?



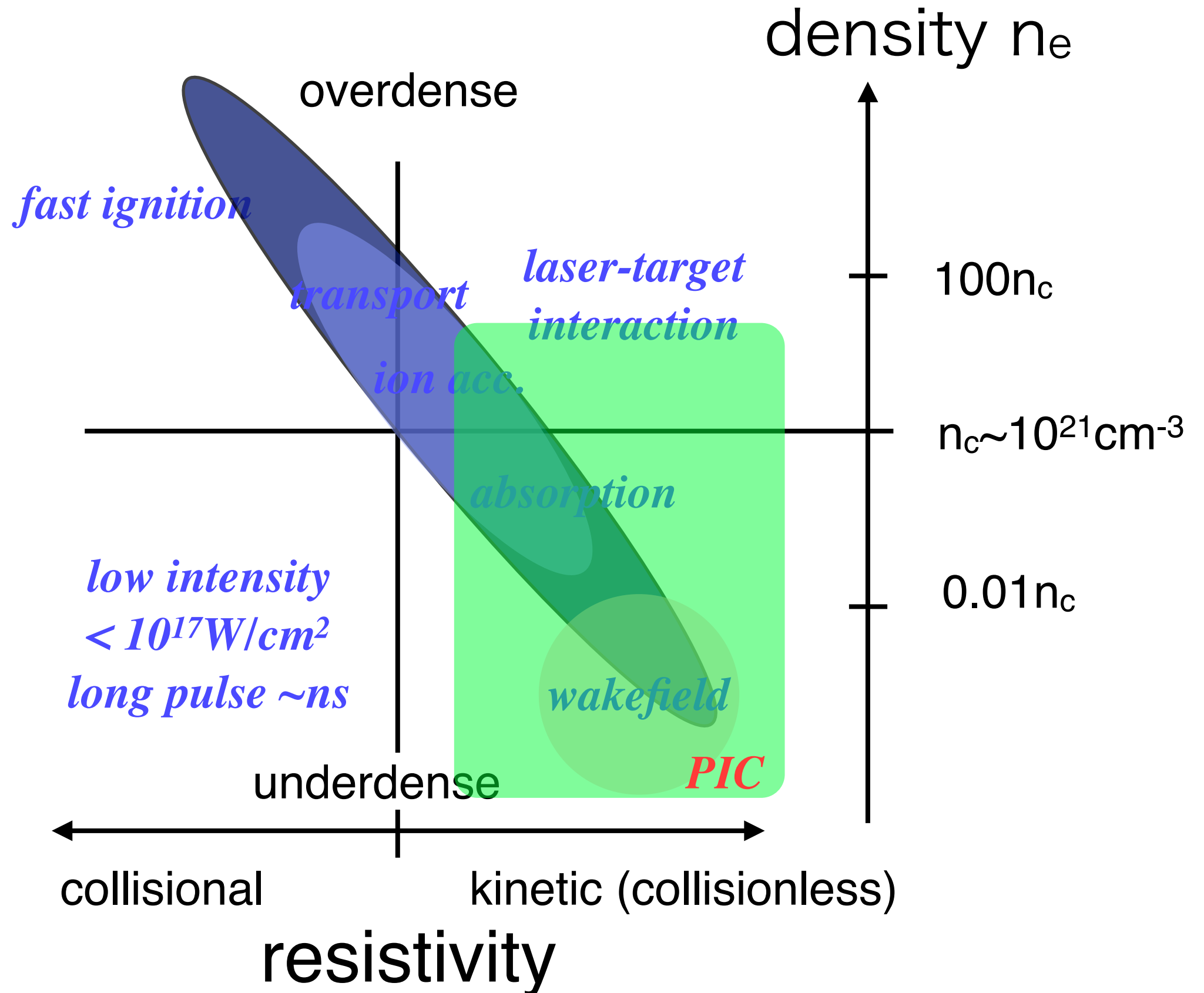
Is your plasma kinetic or collisional?



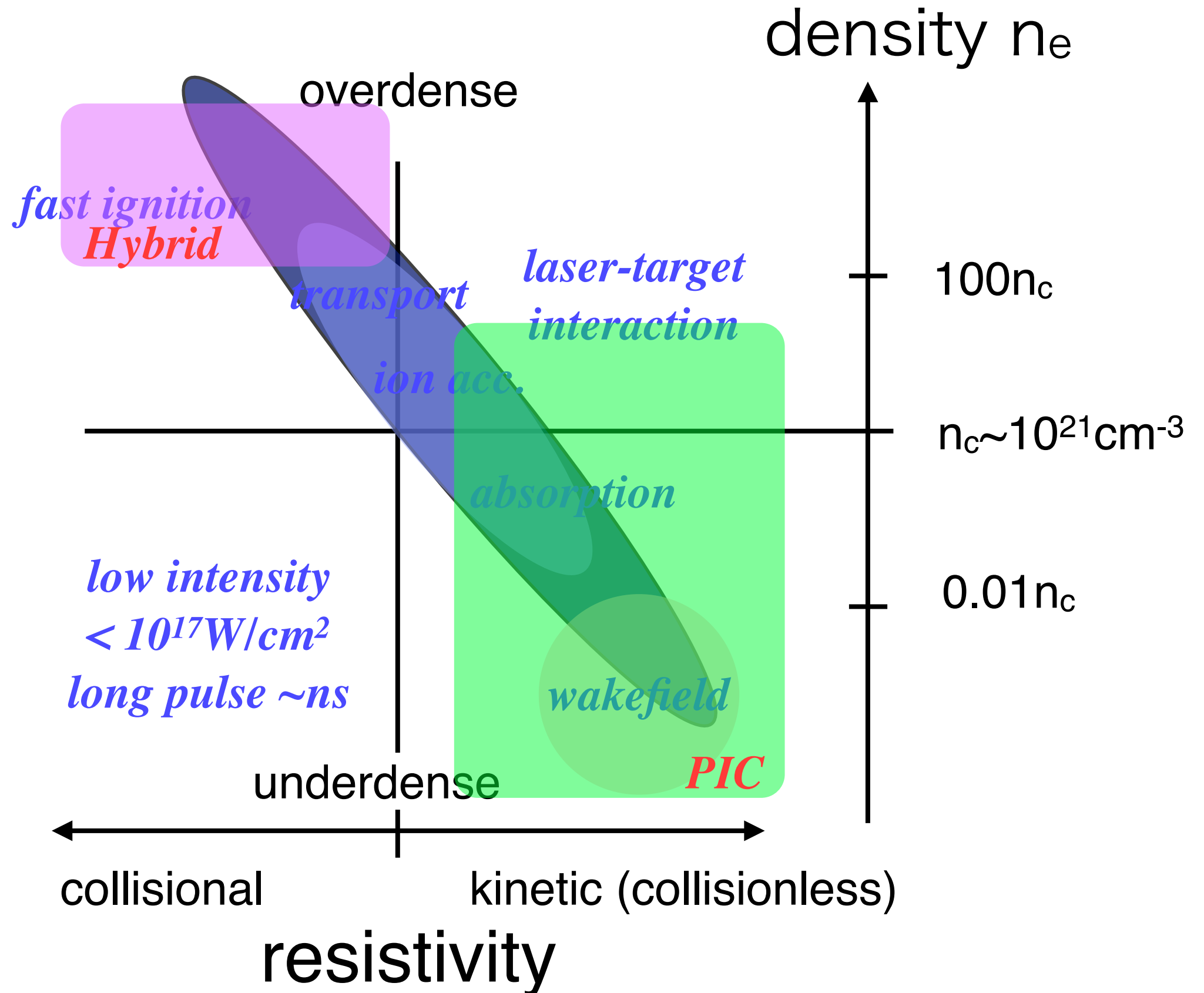
Is your plasma kinetic or collisional?



Is your plasma kinetic or collisional?



Is your plasma kinetic or collisional?



Is your plasma kinetic or collisional?

